Supporting Information

Post-Assembly Modification of Phosphine Cages Controls Host-Guest Behavior

*Charlie T. McTernan, Tanya K. Ronson, Jonathan R. Nitschke**

Contents

S2. Materials and methods

Unless otherwise specified, all reagents were purchased from commercial sources and used as received without further purification. Flash column chromatography was performed using Silica Gel high purity grade (pore size 60 Å, 230-400 mesh particle size, Sigma-Aldrich). TLC analyses were performed on Merck TLC Silica Gel 60 F254 Glass plates. Product spots were visualized under UV light (λ_{max} = 254 nm). Phosphine oxide trianiline **S2** was synthesised in two steps according to modified literature procedures.[1] Nickel(II) triflimide was synthesised according to literature procedures.[2]

S2.1 Nuclear Magnetic Resonance (NMR)

NMR spectra were recorded using a 400 MHz Avance III HD Smart Probe (routine ^{1}H and 2D NMR experiments), DCH 500 MHz dual cryoprobe (high-resolution ^{1}H and ^{13}C NMR and 2D NMR experiments) and DPX S5 500 MHz BB ATM (variable temperature NMR) NMR spectrometers. Coupling constants (*J*) are reported in hertz (Hz). The following abbreviations are used to describe signal multiplicity ^{1}H, ^{13}C and ^{19}F NMR spectra: s: singlet, d: doublet, t: triplet, dd: doublet of doublets; dt: doublet of triplets; m: multiplet, br: broad. DOSY NMR experiments were performed on a 400 MHz Avance III HD Smart Probe NMR spectrometer. Maximum gradient strength was 6.57 G/cm A. The standard Bruker pulse program, ledbpgp2s, employing a stimulated echo and longitudinal eddy-current delay (LED) using bipolar gradient pulses for diffusion using 2 spoil gradients was utilised. Rectangular gradients were used with a total duration of 1.5 ms. Gradient recovery delays were 875-1400 µs. Individual rows of the S4 quasi-2D diffusion databases were phased and baseline corrected.

S2.2 Mass spectrometry (MS)

Low resolution electrospray ionisation (LR-ESI) mass spectrometry was undertaken on a Micromass Quattro LC mass spectrometer (cone voltage 5-30 eV; desolvation temp. 313 K; ionisation temp. 313 K) infused from a Harvard syringe pump at a rate of 10 µL min^{-1}. High-resolution mass spectra were acquired using a Thermofisher LTQ Orbitrap XL or performed by the EPSRC facility at Swansea.

S3. *in situ* Functionalization Studies

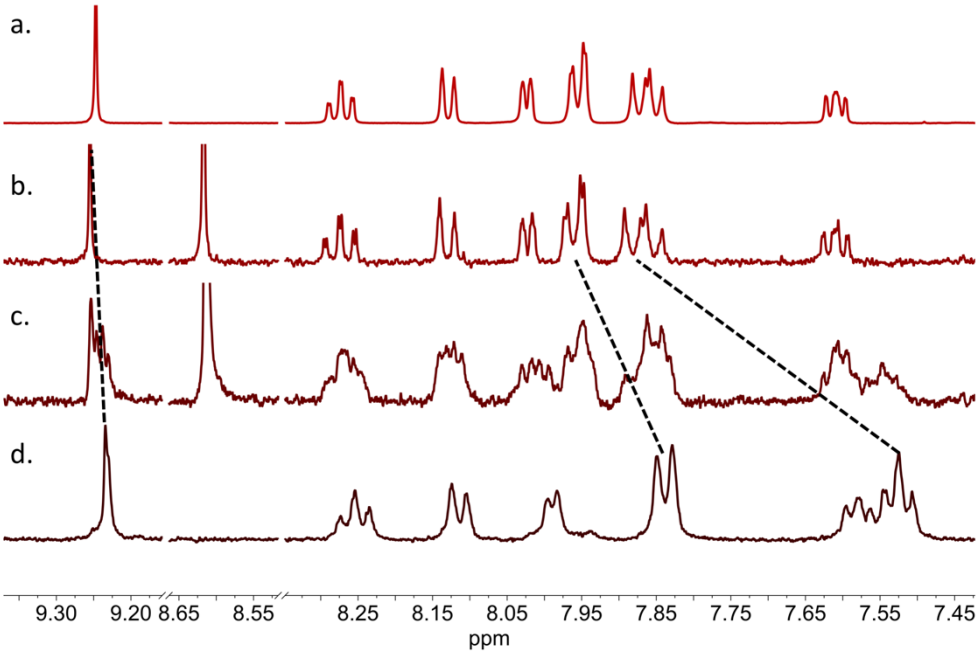

Figure S1: *in situ* oxidation of phosphine cage **2** to phosphine oxide cage **3**. a) Phosphine oxide cage **3** formed from phosphine oxide ligand **S1**. b) Phosphine oxide cage **3** formed *in situ* from the oxidation of phosphine cage **1** after 16 hours ar r.t.. c) Intermediate state during oxidation reaction, 10 minutes after addition of 16 eq. of H_2O_2. Multiple triazole peaks were observed indicative of cages with varying ratios of **2**:**S1** incorporated. d) Phosphine cage **2** prior to oxidation.

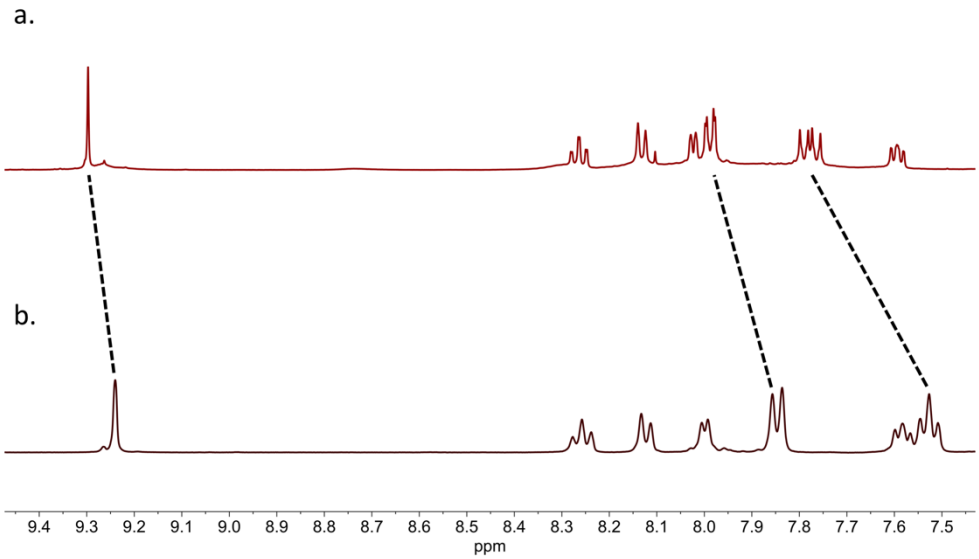

Figure S2: *in situ* Auration of phosphine cage **2**. a) Aurated cage **5** formed from phosphine cage **2** *in situ* after heating to 70 °C for 16 hours. b) Phosphine cage **2** prior to addition of (DMS)AuCl (6.8 mg) to a solution of cage **2** (3.8 mg) in MeCN-d_3 (500 µL).

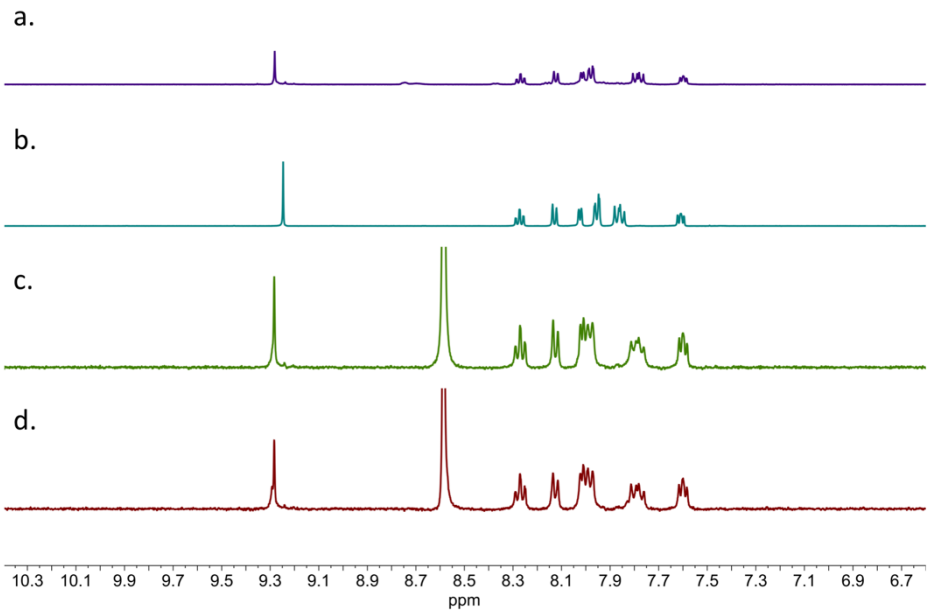

Figure S3: Addition of H_2O_2 to Aurated cage **5**. a) Aurated Cage **5** before addition of H_2O_2. b) Phosphine oxide cage **3**. c) Aurated cage **5** 10 minutes after addition of H_2O_2. d) Aurated cage **5** 16 hours after addition of 16 eq. H_2O_2.

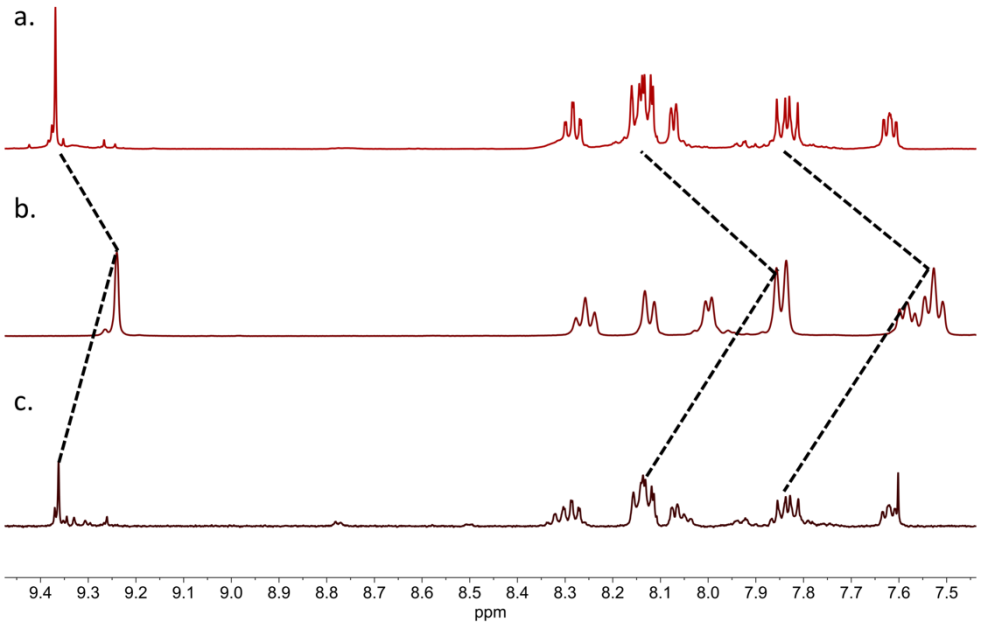

Figure S4: *in situ* Methylation of phosphine cage **2**. a) Phosphonium salt cage **4** formed from isolated ligand **S4**. b) Phosphine cage **2** prior to addition of MeI. c) Phosphonium salt cage **4** formed from *in situ* methylation. To phosphine cage **1** (3.8 mg) and $LiNTf_2$ (5 mg) in MeCN-d_3 (500 µL), MeI (10 µL) was added, and the reaction heated to 70 °C for 1 hour.

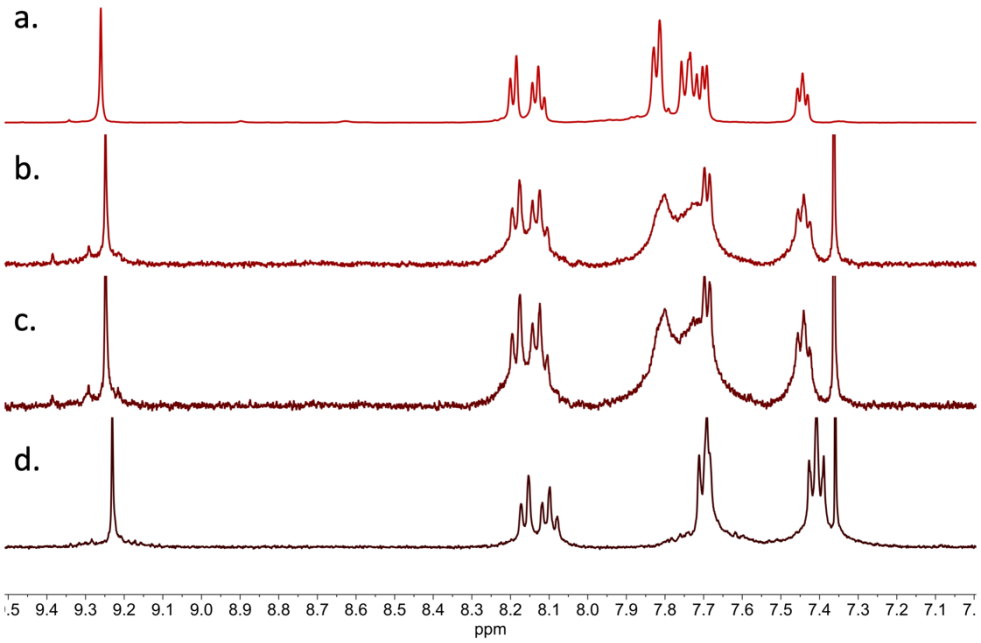

Figure S5: *in situ* oxidation of Iron phosphine cage **6** to Iron phosphine oxide cage **7**. a) Phosphine oxide cage **7** formed from phosphine oxide ligand **S1**. b) Phosphine oxide cage **7** formed *in situ* from the oxidation of phosphine cage **6** after 16 hours ar r.t. c) 10 minutes after addition of 6 eq. of H_2O_2. d) Phosphine cage **6** prior to oxidation.

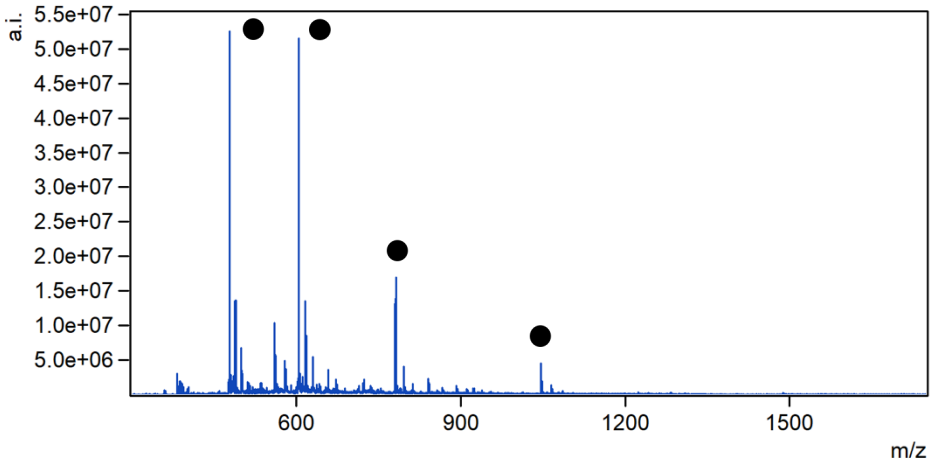

Figure S6: *in situ* oxidation of Iron phosphine cage **6** to Iron phosphine oxide cage **7**. LRMS of sample after oxidation, showing Iron phosphine oxide cage **7**.

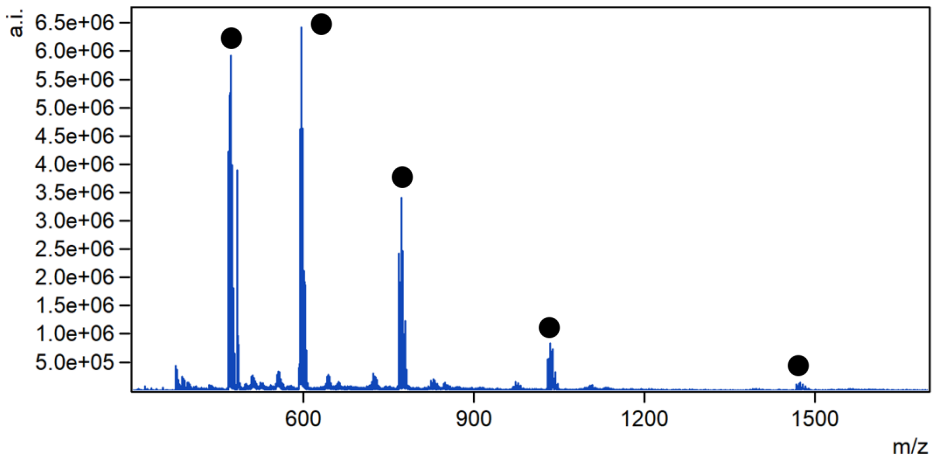

Figure S7: LRMS of Iron phosphine cage **6**, prior to oxidation, for comparison.

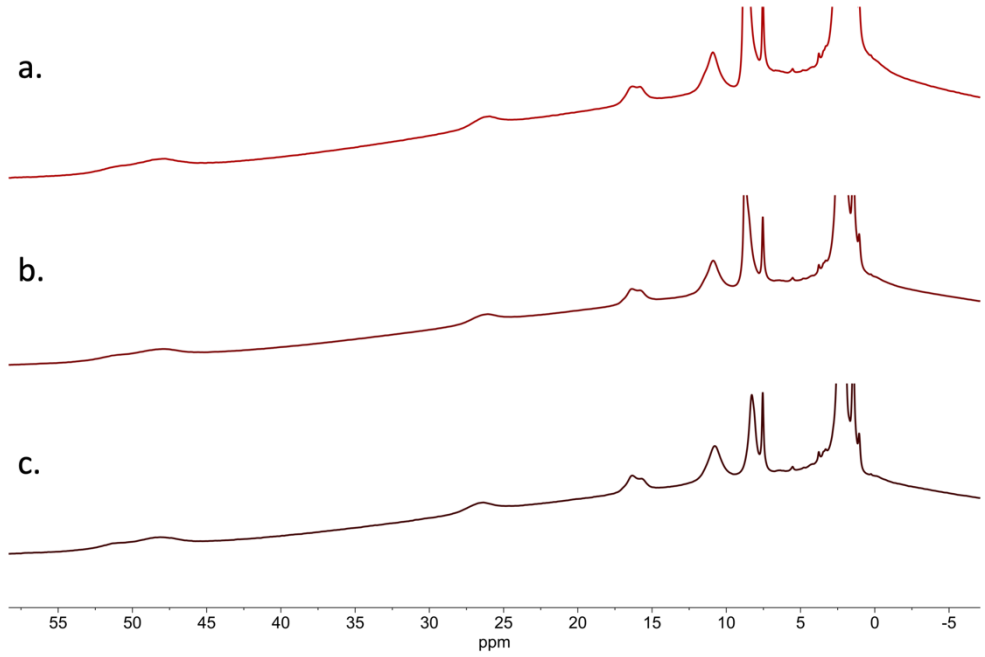

Figure S8: *in situ* oxidation of Nickel phosphine sandwich complex **8** and cage **9** to Nickel phosphine oxide cage **10**. a) Phosphine oxide cage **10** formed from phosphine oxide ligand **S1**. b) Phosphine oxide cage **10** formed *in situ* from the oxidation of phosphine sandwich complex **8** and cage **9** after 16 hours at r.t. c) Phosphine sandwich complex **8** and cage **9** prior to oxidation.

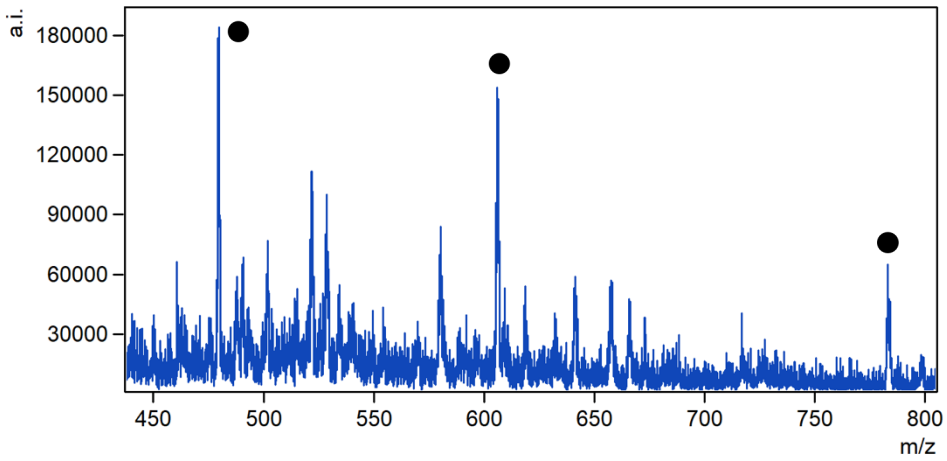

Figure S9: *in situ* oxidation of Nickel phosphine sandwich complex **8** and cage **9** to Nickel phosphine oxide cage **10**. LRMS of sample after oxidation, showing Nickel phosphine oxide cage **10**. Oxidation was less clean when using the nickel system, with by-products observed.

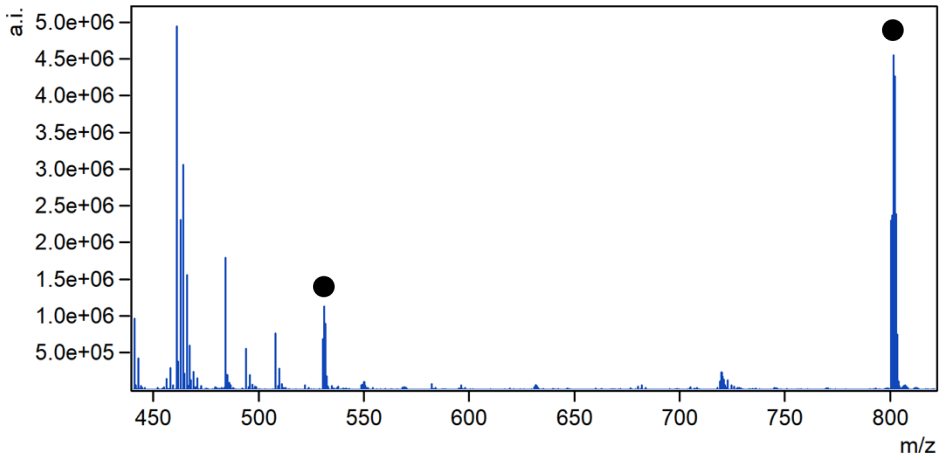

Figure S10: LRMS of sample of nickel phosphine sandwich complex **8** and cage **9**, prior to oxidation, for comparison.

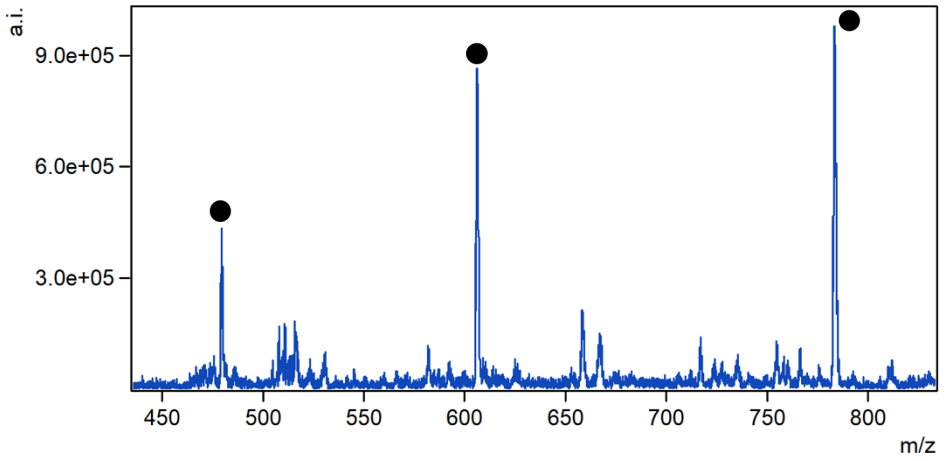

Figure S11: LRMS of Nickel phosphine oxide cage **10**, for comparison.

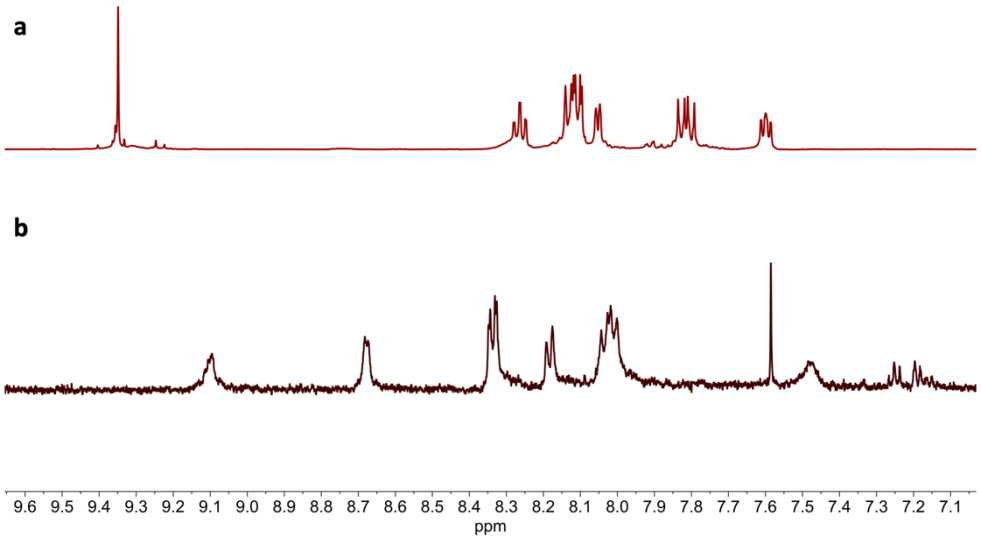

Figure S12: Addition of TBAI to phosphonium salt cage **4**, causing cage disassembly. a. Cage **4** prior to addition of TBAI. b. Product of addition of TBAI after 15 minutes at r.t..

S4. Host Guest Studies

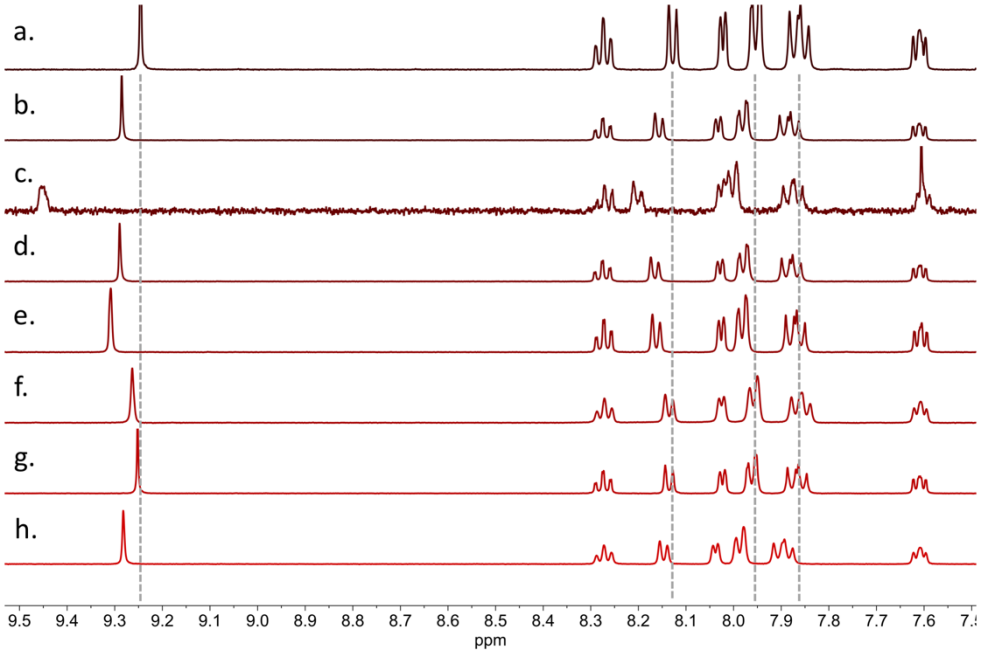

Figure S13: a) Phosphine oxide cage **3**. b) Phosphine oxide cage **3** after addition of $TBAClO_4$. c) Phosphine oxide cage **3** after addition of $TBANO_3$. d) Phosphine oxide cage **3** after addition of $TBABF_4$. e) Phosphine oxide cage **3** after addition of TBAOTf. f) Phosphine oxide cage **3** after addition of TBAOTs. g) Phosphine oxide cage **3** after addition of $TBAPF_6$. h) Phosphine oxide cage **3** after addition of $TBAReO_4$.

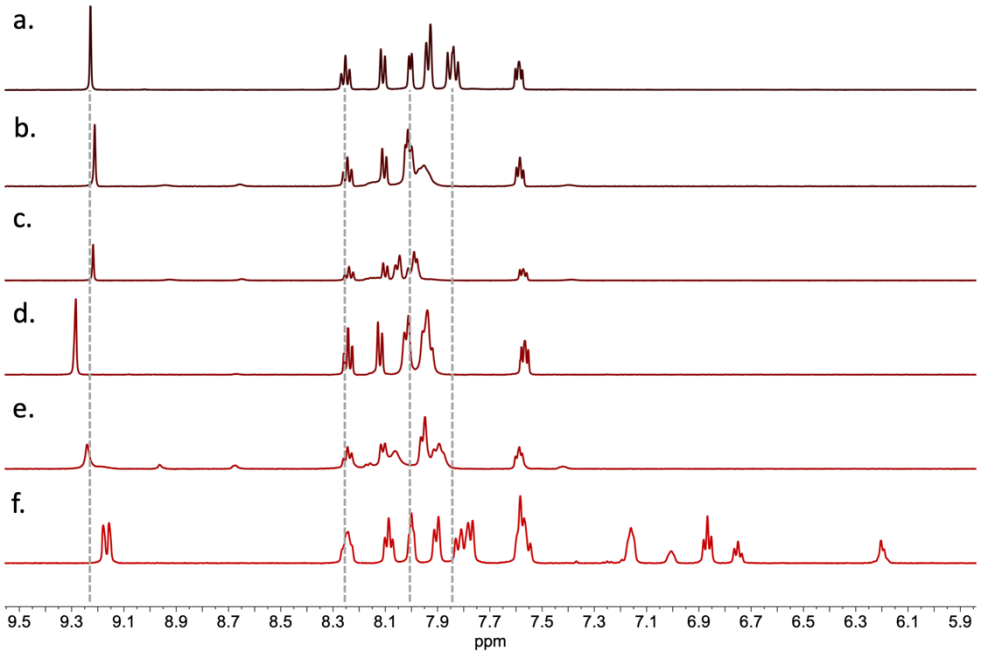

Figure S14: a) Phosphine oxide cage **3**. b) Phosphine oxide cage **3** after addition of TBACl. c) Phosphine oxide cage **3** after addition of TBABr. d) Phosphine oxide cage **3** after addition of TBAI. e) Phosphine oxide cage **3** after addition of NaTFA. f) Phosphine oxide cage **3** after addition of $TBABPh_4$ (note, a significant increase in spectra complexity was observed with this anion due to slow exchange binding).

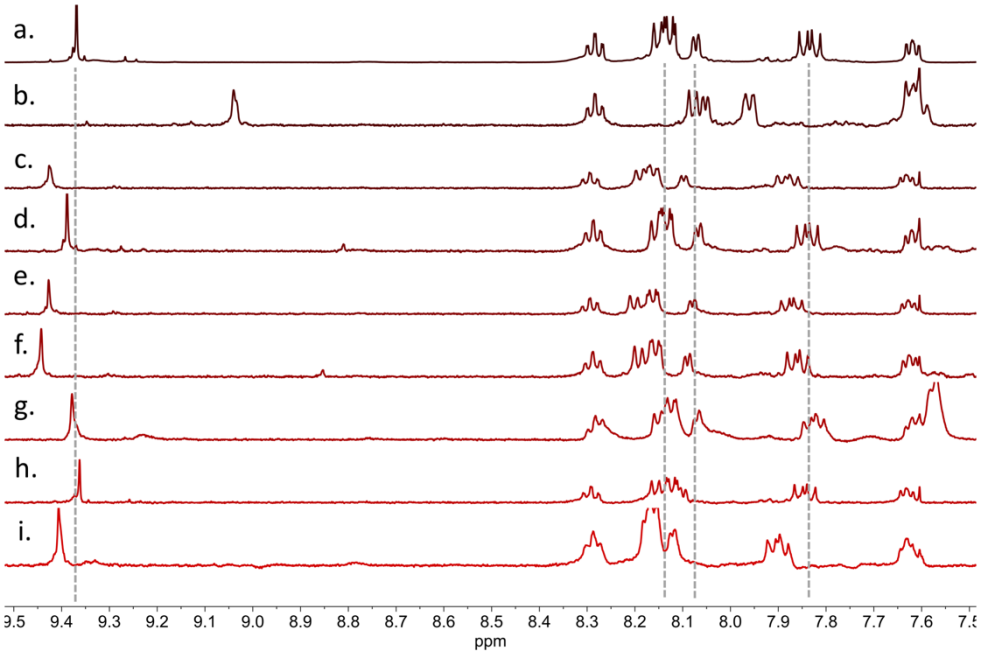

Figure S15: a) Phosphonium salt cage **4**. b) Phosphonium salt cage **4** after addition of $NaBPh_4$. c) Phosphonium salt cage **4** after addition of $TBAClO_4$. d) Phosphonium salt cage **4** after addition of $TBANO_3$. e) Phosphonium salt cage **4** after addition of $TBABF_4$. f) Phosphonium salt cage **4** after addition of TBAOTf. g) Phosphonium salt cage **4** after addition of TBAOTs. h) Phosphonium salt cage **4** after addition of $TBAPF_6$. i) Phosphonium salt cage **4** after addition of $TBAReO_4$.

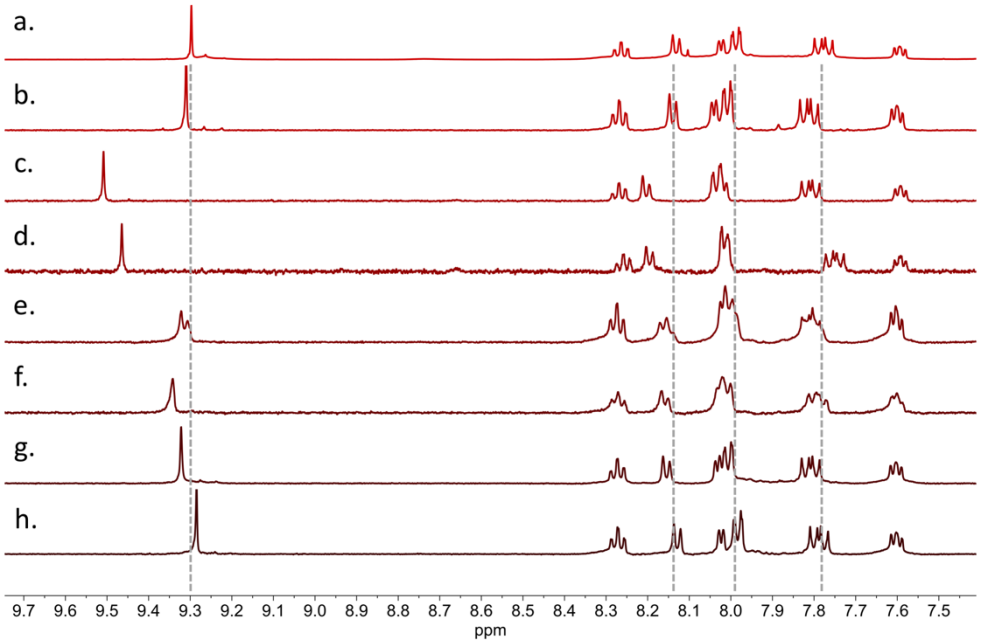

Figure S16: a) Aurated cage **5**. b) Aurated cage **5** after addition of $TBAReO_4$. c) Aurated cage **5** after addition of $TBANO_3$. d) Aurated cage **5** after addition of TBAOTs. e) Aurated cage **5** after addition of $TBABF_4$. f) Aurated cage **5** after addition of TBAOTf. g) Aurated cage **5** after addition of $TBAClO_4$. h) Aurated cage **5** after addition of $TBAPF_6$.

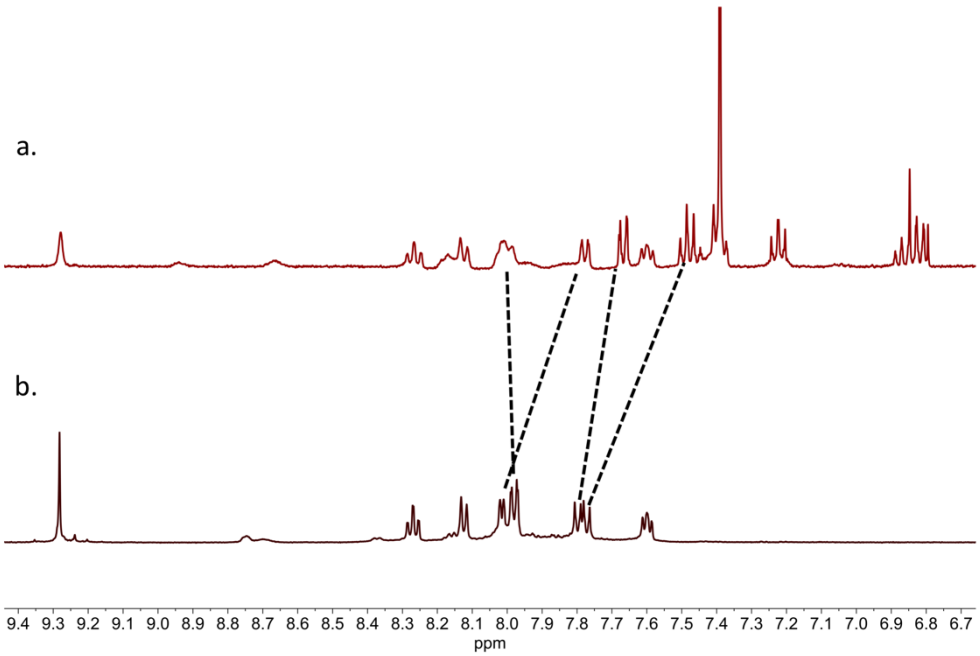

Figure S17: a) 16 hours after addition of $NaBPh_4$ to Aurated cage **5**. The tetraphenylborate anion was bound in slow exchange by cage **5**, leading to the more complex spectra observed. b) Aurated cage **5** prior to addition of $NaBPh_4$.

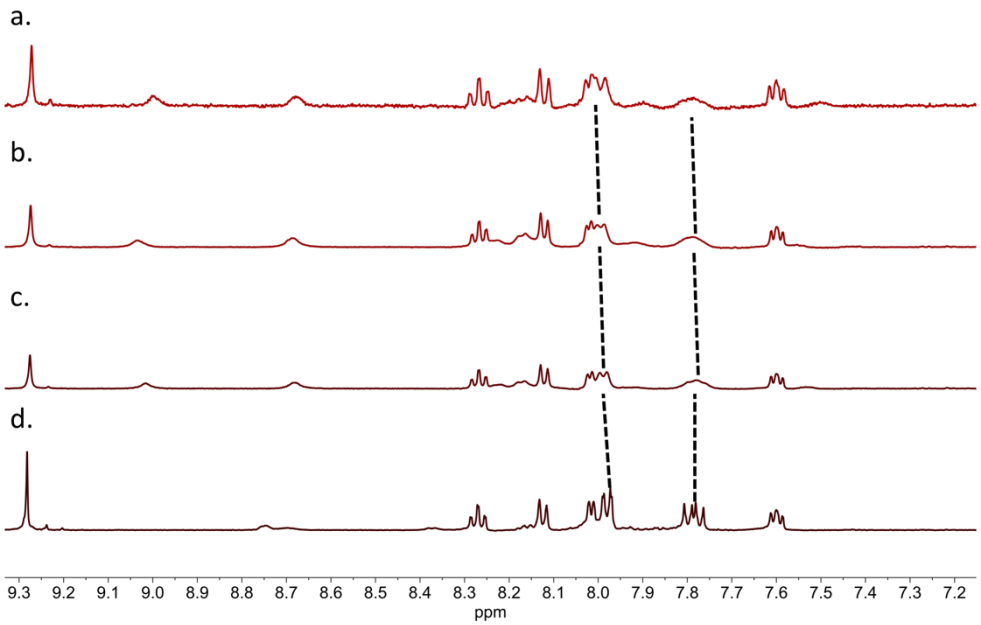

Figure S18: Addition of TBACN to aurated cage **5**. a) Aurated cage **5** after 16 hr at r.t. and an additional 24 hours at 50 °C. b) Aurated cage **5** after 16 hr at r.t.. c) Aurated cage 10 minutes after addition of 16 eq. TBACN. d) Aurated cage **5** prior to addition of TBACN. Signals most affected relate to the P-Aryl ring signals, supporting chloride displacement by cyanide.

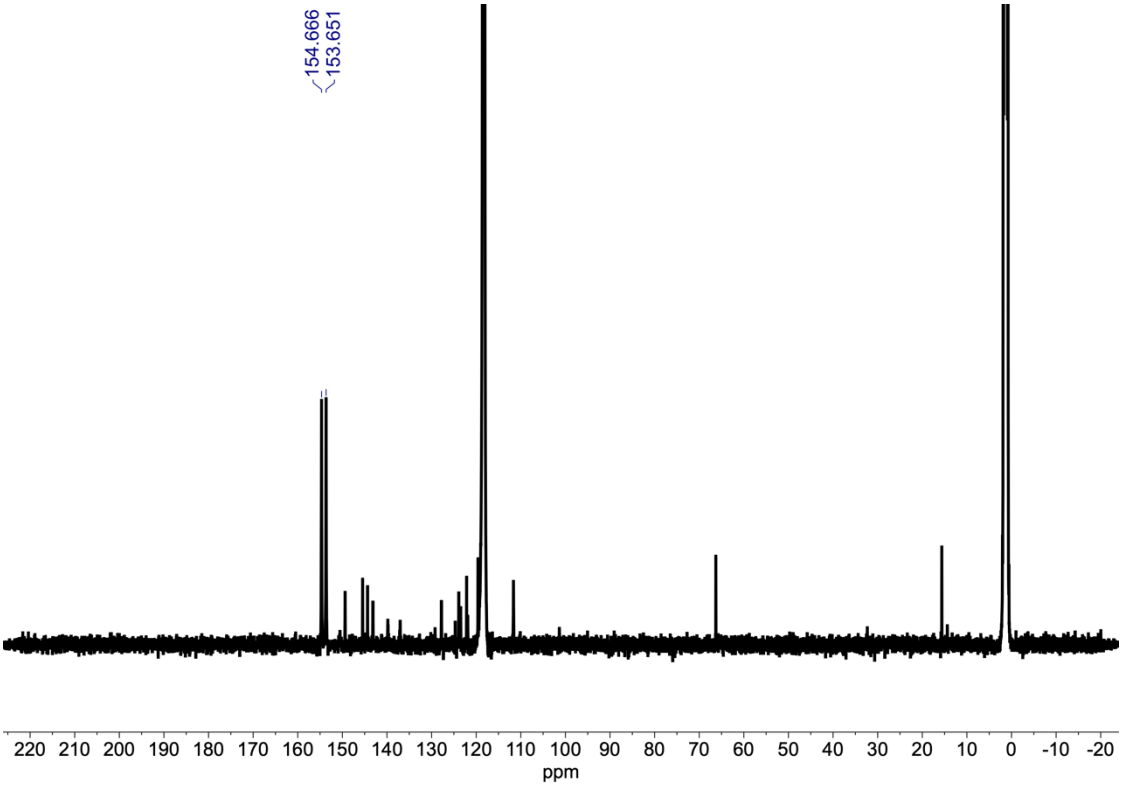

Figure S19: Addition of TBA^{13}CN to aurated cage **5** in MeCN-d_3. Peaks corresponding to P-Au-CN bound cyanide (^{13}C labelled) were observed, and a ^{31}P-Au-^{13}C coupling constant of 128.9 Hz was seen, confirming external binding of the cyanide anion, and explaining the changing in cage behavior regarding cyanide binding/cage destruction with respect to cages **3** and **4**.

S5. Determination of Guest Binding Affinity

Procedure for NMR titrations: A 0.55 mL solution of host in MeCN-d_3 was titrated with a concentrated solution of guest. The total change in concentration of the host was >15 % over the course of the titration, and the error involved was assumed to be negligible. Upon each addition, the solution was manually stirred for 1 min before acquiring the spectrum, which allowed equilibrium to be reached between the host and guest. Binding isotherms for all titrations were calculated using BINDFIT.[3] Data from the titration experiments showed 1:1 binding for all anions which could be fitted. Cages **3**, **4** and **5** showed no binding to triflimide up to the addition of 400 equiv. of $TBANTf_2$. This allowed us to disregard competitive binding by NTf_2 in these systems when calculating binding affinities. Sufficient points were taken in the titration to ensure a binding isotherm could be calculated. Below we show the full data for binding of ReO_4^- (from titration of $TBAReO_4$), and summarise binding affinity calculations for other anions in Table S1.

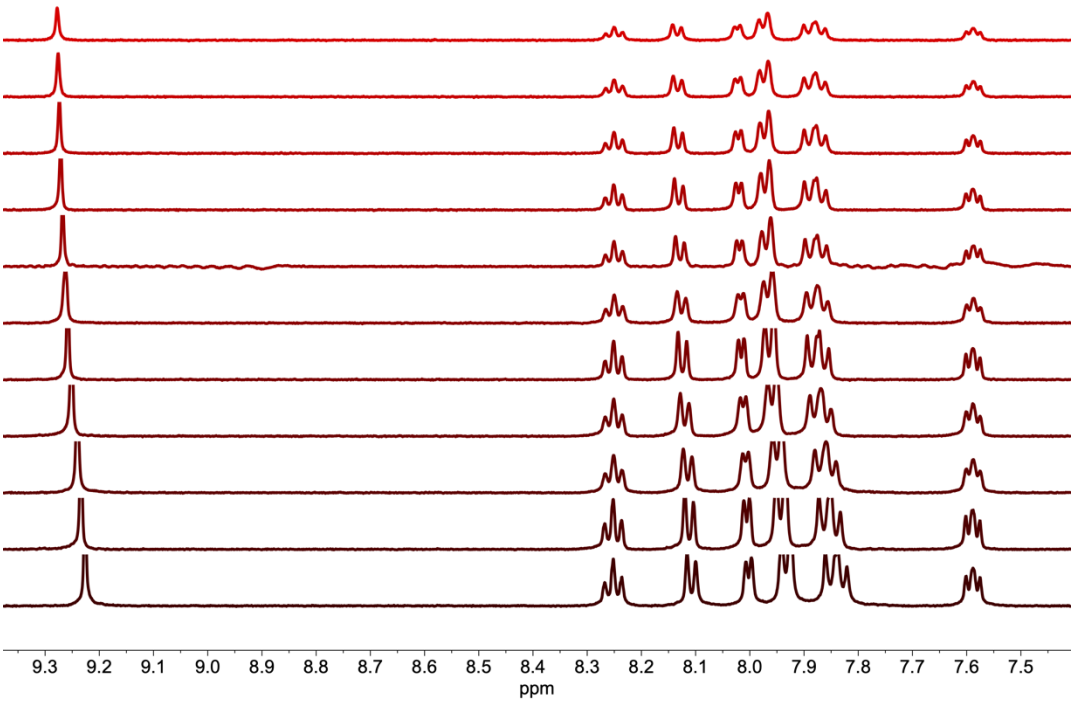

Figure S20: Addition of $TBAReO_4$ to phosphine oxide cage **3**. Titration starts at bottom spectra (0 equiv.).

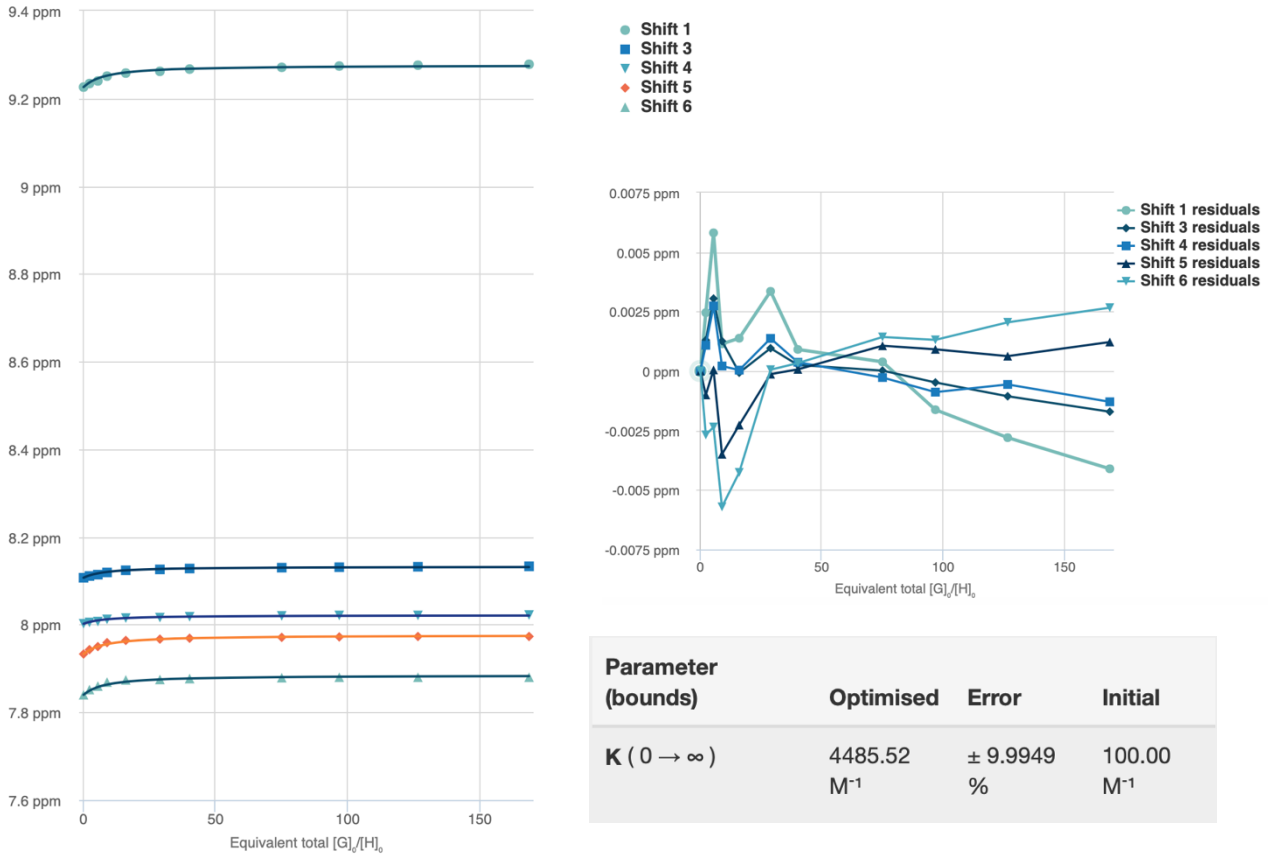

Parameter (bounds)	Optimised	Error	Initial
K (0 → ∞)	4485.52 M^{-1}	± 9.9949 %	100.00 M^{-1}

Figure S21: Binding data for addition of $TBAReO_4$ to phosphine oxide cage **3**.

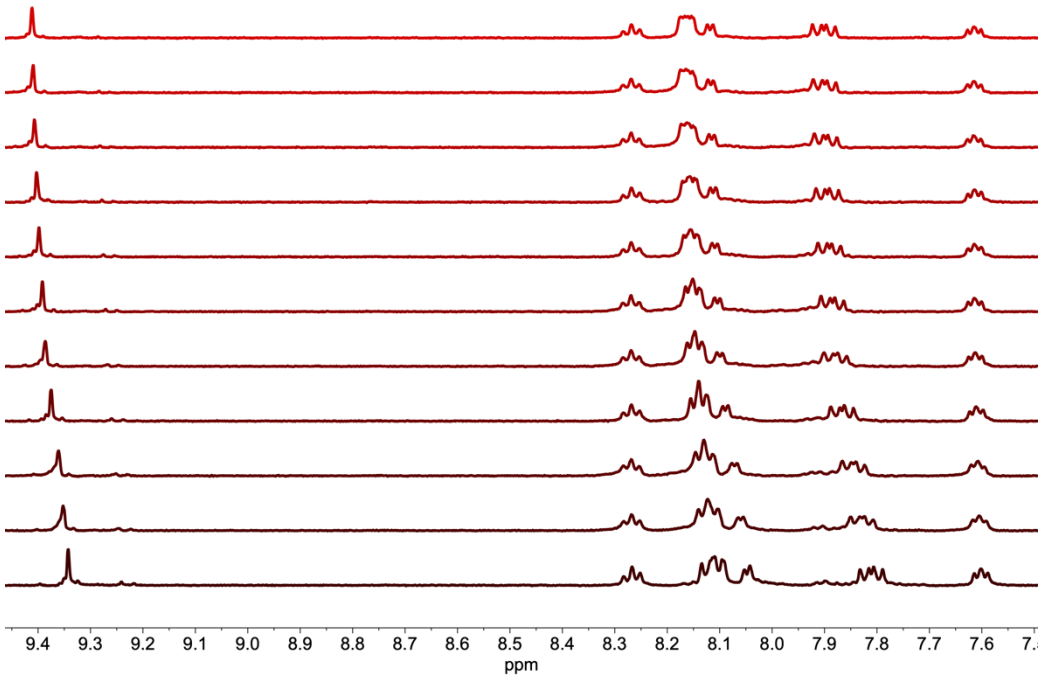

Figure S22: Addition of $TBAReO_4$ to methylated cage **4**. Titration starts at bottom spectra (0 equiv.).

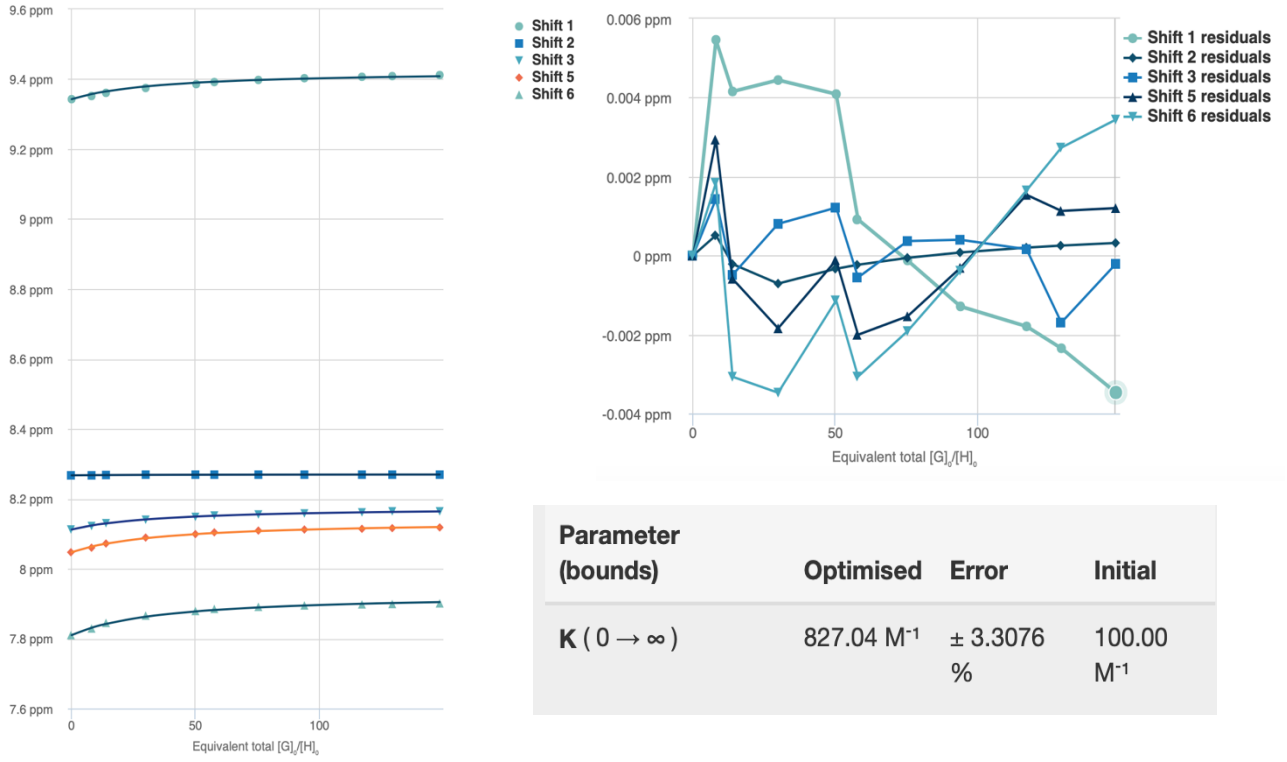

Parameter (bounds)	Optimised	Error	Initial
K (0 → ∞)	827.04 M^{-1}	± 3.3076 %	100.00 M^{-1}

Figure S23: Binding data for addition of $TBAReO_4$ to methylated cage **4**.

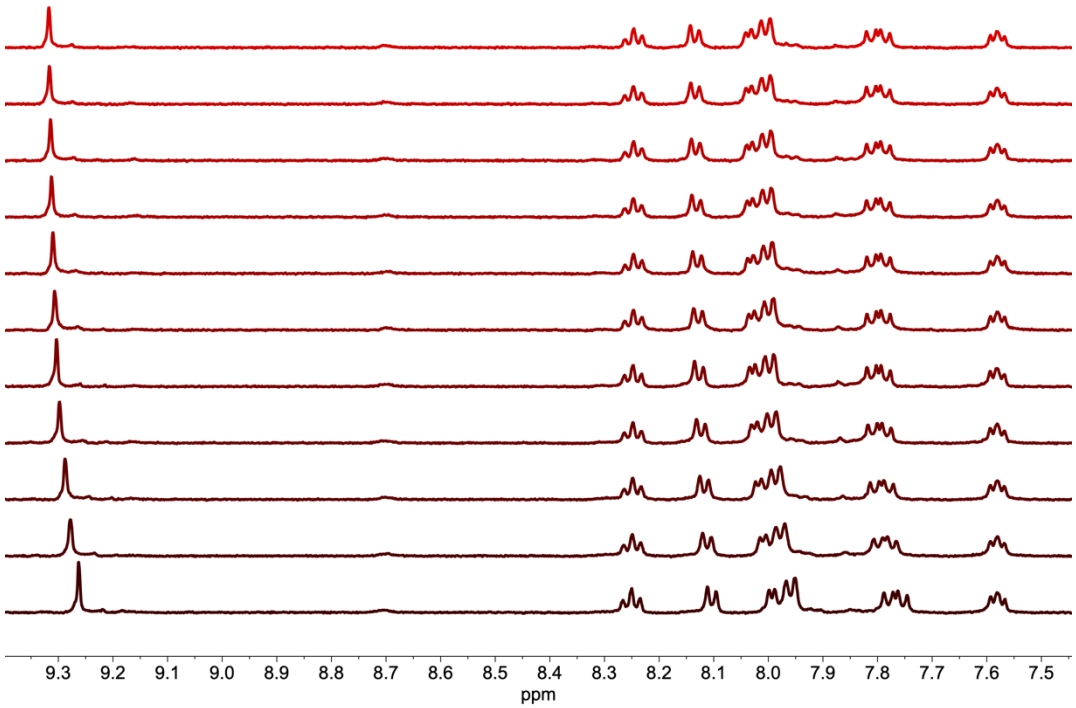

Figure S24: Addition of $TBAReO_4$ to aurated cage **5**. Titration starts at bottom spectra (0 equiv.).

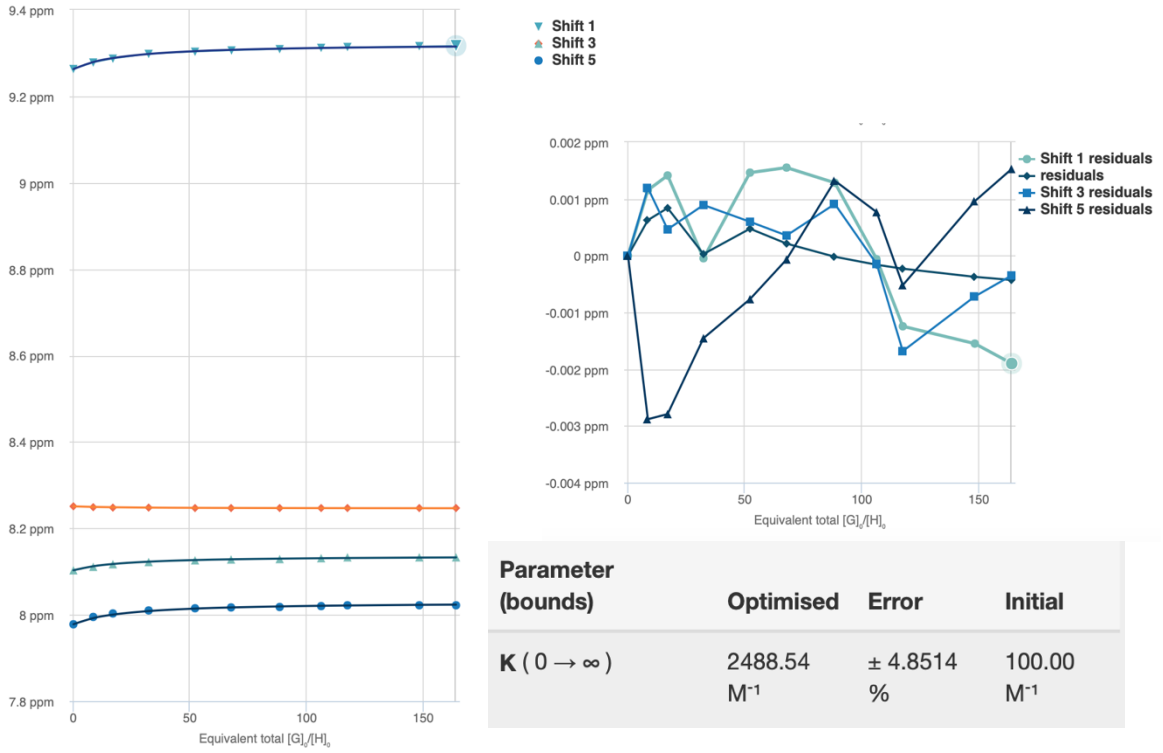

Figure S25: Binding data for addition of $TBAReO_4$ to aurated cage **5**.

	Phosphine Oxide Cage 3		Phosphonium Cage 4		Aurated Cage 5	
	Binding Constant	**Error**	**Binding Constant**	**Error**	**Binding Constant**	**Error**
TBAReO4	4485.52M^{-1}	± 9.9949%	827.04 M^{-1}	± 3.3076%	2488.54M^{-1}	± 4.8514%
TBAClO4	296.52 M^{-1}	± 2.4451%	42.33 M^{-1}	± 2.0337%	100.78 M^{-1}	± 4.6369%
TBAOTf	233.39 M^{-1}	± 2.1935%	52.90 M^{-1}	± 1.8695%	59.21 M^{-1}	± 2.4163%
TBABF4	235.00 M^{-1}	± 3.2962%	32.93 M^{-1}	± 2.4644%	103.62 M^{-1}	± 2.7851%
TBANO3	$	$	$	$	$	$
TBAOTs	$	$	$	$	$	$
TBAPF6	11.56 M^{-1}	± 16.0167%	~	~	37.25 M^{-1}	± 9.0590%
NaBPh4	*	*	26.96 M^{-1}	± 10.6283%	*	*
NaTFA	§	§	No Binding	No Binding	No Binding	No Binding
TBACl	58.03 M^{-1}	± 15.6298%	No Binding	No Binding	No Binding	No Binding
TBABr	§	§	No Binding	No Binding	No Binding	No Binding
TBAI	§	§	No Binding	No Binding	No Binding	No Binding

Table S1: Results of anion binding titrations. Errors calculated from residuals after fitting data to a 1:1 binding isotherm. $ = The cage was observed to precipitate upon addition of larger quantities of anion, preventing determination of a binding isotherm. * = The cage bound BPh_4 in fast and slow exchange simultaneously preventing determination of a binding isotherm. § = The cage was observed to disassemble upon addition of larger quantities of anion, preventing determination of a binding isotherm.

S6. Synthesis and characterization

Tris(4-(4-(pyridin-2-yl)-1*H*-1,2,3-triazol-1-yl)phenyl)phosphine oxide **S1**

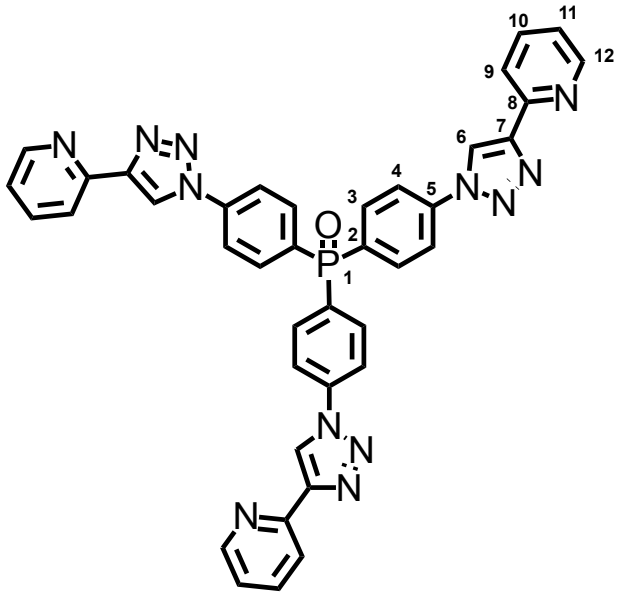

Phosphine oxide triamine **S2** (0.580 g, 1.80 mmol) was dissolved in aqueous HCl (4M, 16 mL), and the resulting solution cooled to 0 °C. Sodium nitrite (0.60 g, 8.70 mmol) was dissolved in H_2O (5 mL) and cautiously added dropwise over 10 minutes. The reaction was stirred vigorously for 15 minutes, before sodium azide (0.70 g, 10.8 mmol) in H_2O (5 mL) was added dropwise over 5 minutes (CARE – ACIDIFIED NaN_3 PRODUCES TOXIC HN_3). The reaction was stirred for 15 minutes, then extracted with EtOAc (200 mL), dried over $MgSO_4$, and concentrated *in vacuo* (n.b. the water bath of the rotary evaporator was maintained below 10 °C during this process). The crude triazide **S3** was immediately used to prevent decomposition. The crude was taken up in DMF (10 mL) and sparged with nitrogen for 15 minutes. Pyridyl acetylene (0.80 mL, 7.92 mmol) was added, and the reaction sparged for a further 5 minutes. Copper sulfate (180 mg, 1.13 mmol) and sodium ascorbate (400 mg, 2.02 mmol) were added, and the reaction stirred at r.t. for 16 hours. $EDTA_{(aq)}$ (0.1 M, 50 mL) followed by CH_2Cl_2 (200 mL) were added, and the reaction stirred at r.t. for 2 hours. The phases were separated, the aqueous layer washed with CH_2Cl_2 (50 mL), and the organic phases combined. The organic phases were washed with $NaOH_{(aq)}$ (1 M, 100 mL), brine (100 mL) followed by H_2O (2 × 100 mL). The organic phase was dried over Na_2SO_4, then concentrated *in vacuo* after the addition of toluene (10 mL). The crude was purified by flash column chromatography (CH_2Cl_2:MeOH 20:1) to furnish phosphine oxide ligand **S1** (0.901 g, 1.27 mmol, 71%) as an off-white powder.

^{1}H NMR (500 MHz, CD_3CN) δ: 8.91 (s, 3H, H_6), 8.66 (d, *J* = 4.6 Hz, 3H, H_{12}), 8.20 (d, *J* = 7.9 Hz, 3H, H_9), 8.16 (dd, *J* = 8.6, 2.0 Hz, 6H, H_4), 7.99 (dd, *J* = 11.3, 8.7 Hz, 6H, H_3), 7.91 (td, *J* = 7.6, 1.7 Hz, 3H, H_{10}), 7.37 (ddd, *J* = 7.6, 4.9, 0.9 Hz, 3H, H_{11}). **^{13}C NMR** (126 MHz, CD_2Cl_2) δ: 150.2, 150.0, 140.5 (d, *J* = 2.4 Hz), 137.5, 134.4 (d, *J* = 10.6 Hz), 132.9 (d, *J* = 105.3 Hz), 123.9, 120.9 (d, *J* = 12.4 Hz), 120.8, 120.5. **^{31}P NMR** (162 MHz, CD_3CN) *δ*: 24.0. **HRMS** (ESI^+): m/z = 711.2237 $[M+H]^+$, calculated for $C_{39}H_{28}N_{12}OP$ = 711.2241.

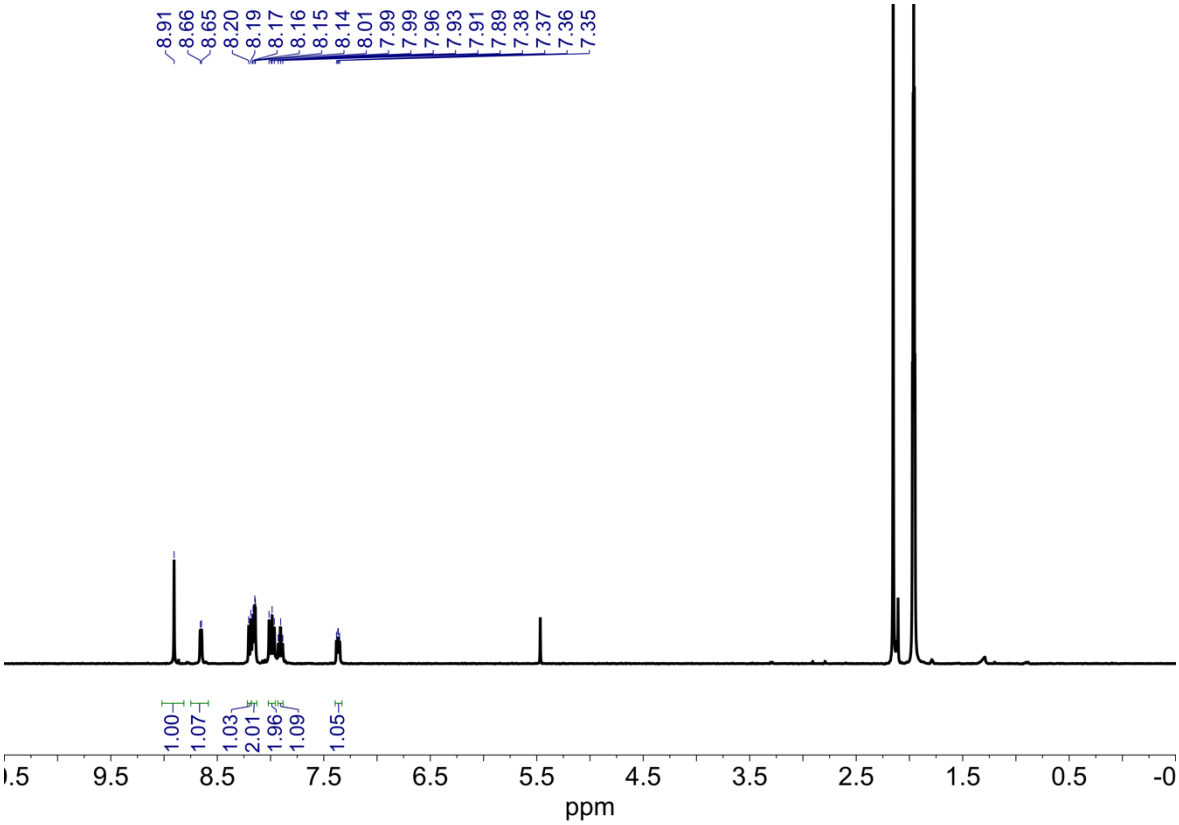

Figure S26: ^{1}H NMR (CD_3CN, 500 MHz, 298 K) spectrum of **S1**.

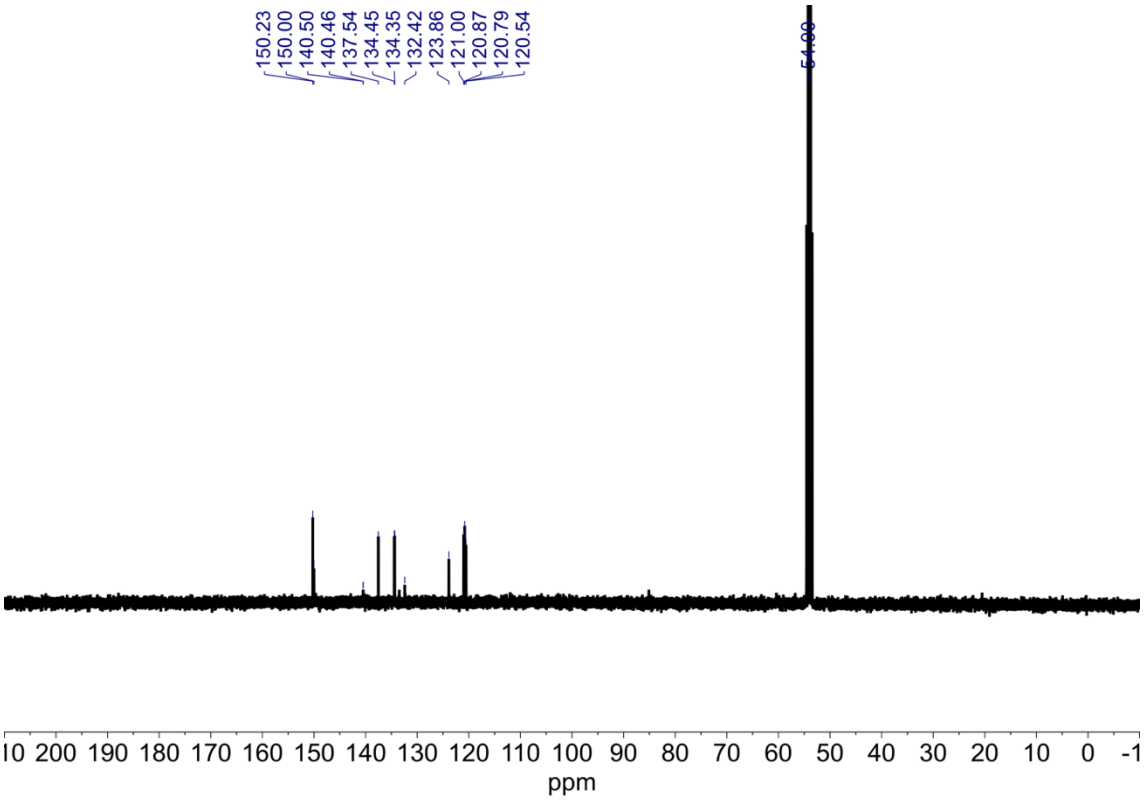

Figure S27: ^{13}C NMR (CD_3CN, 126 MHz, 298 K) Spectrum of **S1**.

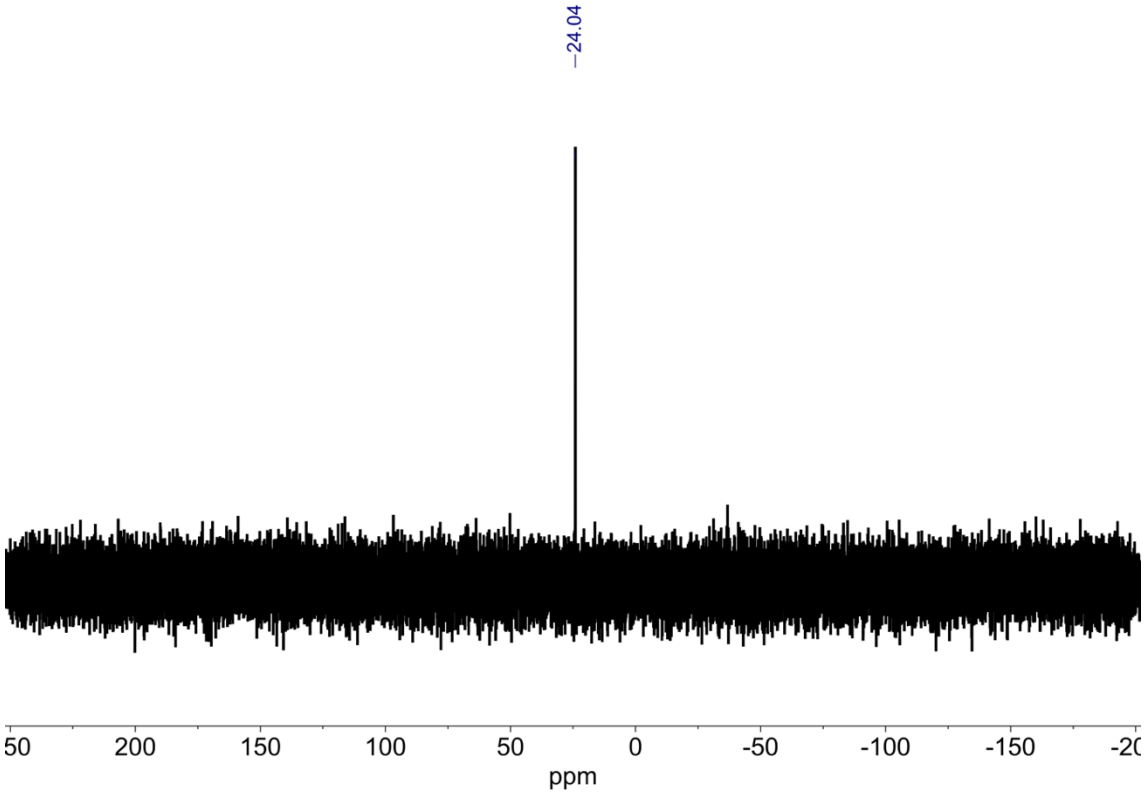

Figure S28: ^{31}P NMR (CD_3CN, 162 MHz, 298 K) spectrum of **S1**

Tris(4-(4-(pyridin-2-yl)-1*H*-1,2,3-triazol-1-yl)phenyl)phosphane **1**

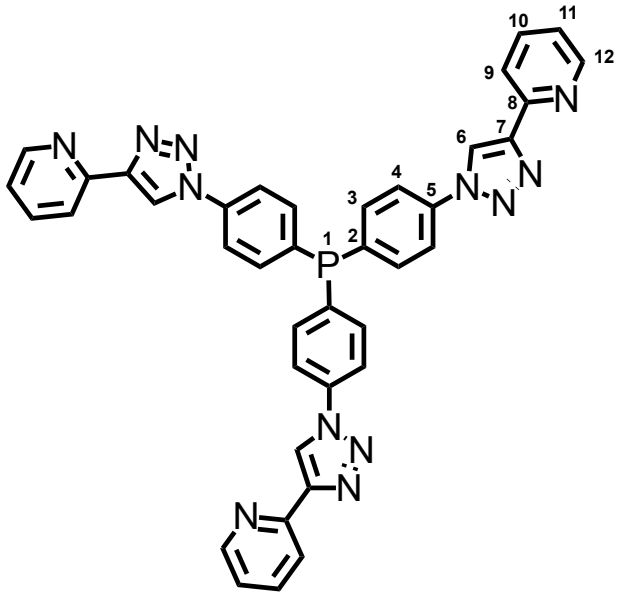

Phosphine oxide **S1** (86 mg, 0.121 mmol) was suspended in toluene (10 mL) and thoroughly sparged with nitrogen. Trichlorosilane (1.5 mL, 14.8 mmol) and sparged, dry, Et_3N (1 mL, 7.2 mmol) were added simultaneously with vigorous stirring. The reaction was immediately heated to reflux for 2.5 h. The reaction was cooled to r.t. and sparged MeOH (5 mL) was added with caution until all solids had dissolved. Silica was then added and the solvent removed *in vacuo*. The crude residue was purified by flash column chromatography under an atmosphere of N_2, with all solvents and glassware thoroughly sparged with N_2 prior to use (EtOAc:MeOH 50:1) to furnish **1** (77 mg, 0.111 mmol, 92%) as a colourless oil. **1** was stored in matrix of sparged benzene until required.

^{1}H NMR (500 MHz, CD_3CN) δ: 8.86 (s, 3H, H_6), 8.65 (d, *J* = 4.6 Hz, 3H, H_{12}), 8.19 (d, *J* = 7.9 Hz, 3H, H_9), 8.01 (d, *J* = 8.2 Hz, 6H, H_4), 7.91 (td, *J* = 7.8, 1.8 Hz, 3H, H_{10}), 7.64 (dd, *J* = 8.3, 7.2 Hz, 6H, H_3), 7.36 (ddd, *J* = 7.4, 4.8, 1.2 Hz, 3H, H_{11}). **^{13}C NMR** (126 MHz, CD_3CN) δ: 150.9, 150.8, 149.8, 138.7, 138.1 (*J* = 12.8 Hz), 138.0, 135.9 (*J* = 20.7 Hz), 124.2, 121.8 (*J* = 7.0 Hz), 121.6, 120.9. **^{31}P NMR** (162 MHz, CD_3CN) *δ*: − 7.6. **HRMS** (ESI^+): m/z = 695.2288 $[M+H]^+$, calculated for $C_{39}H_{28}N_{12}P$ = 695.2292.

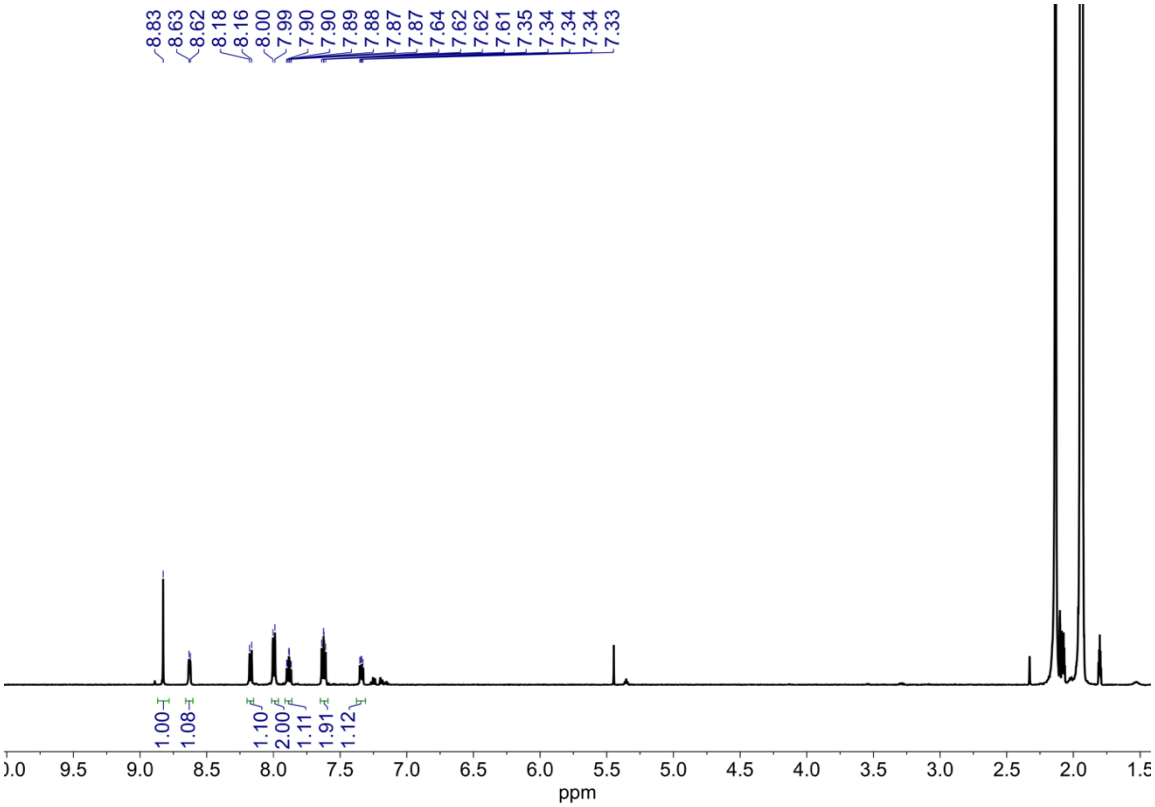

Figure S29: ^{1}H NMR (CD_3CN, 500 MHz, 298 K) spectrum of **1**.

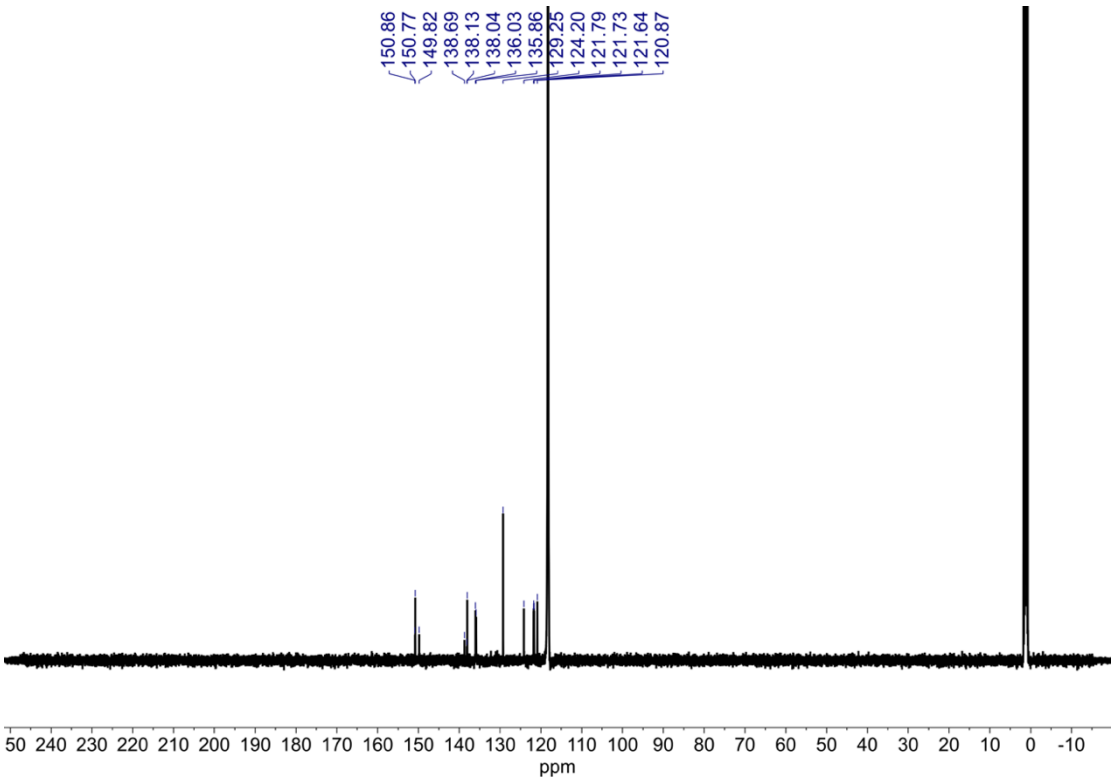

Figure S30: ^{13}C NMR (CD_3CN, 126 MHz, 298 K) spectrum of **1**.

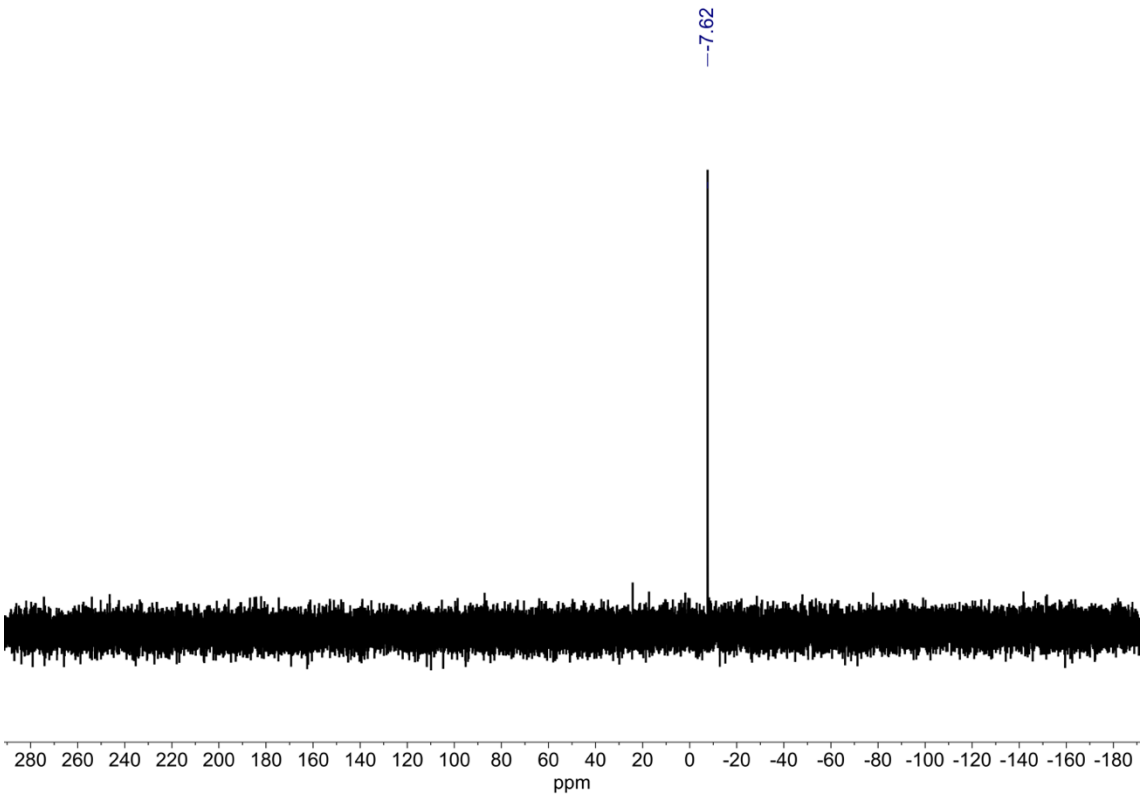

Figure S31: ^{31}P NMR (CD_3CN, 162 MHz, 298 K) spectrum of **1**.

Methyltris(4-(4-(pyridin-2-yl)-1*H*-1,2,3-triazol-1-yl)phenyl)phosphonium bis((trifluoromethyl)sulfonyl)amide **S4**

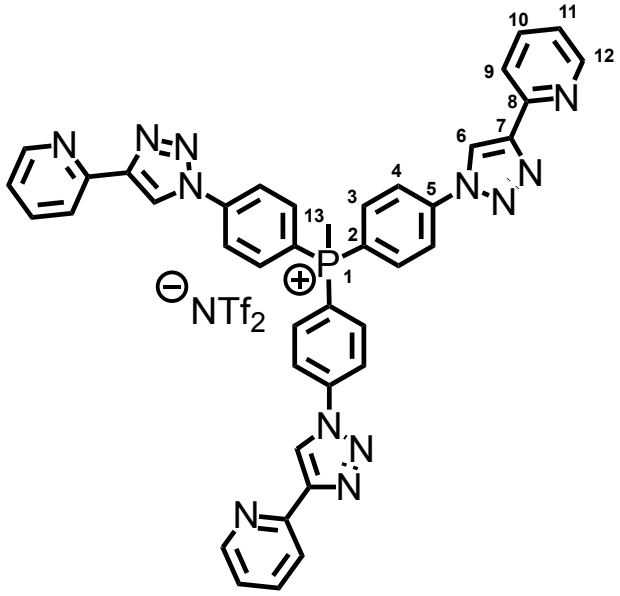

Phosphine ligand **1** (12 mg, 0.0173 mmol) was dissolved in MeCN (3 mL). Methyl iodide (40 µL, 0.643 mmol) was added after being filtered through basic alumina. The reaction was heated at 70 °C for 1 hour before being cooled to r.t.. Benzene (15 mL) was added and the precipitate formed collected by centrifugation. The precipitate was washed with benzene (10 mL) and Et_2O (10 mL) before being taken up in MeCN (5 mL). $LiNTf_2$ (50 mg, 0.173 mmol) was added as a solution in MeCN (5 mL). The reaction was stirred for 15 minutes, and concentrated *in vacuo*. The residue was taken up in CH_2Cl_2 (3 mL) and centrifuged to remove insoluble material. The filtrate was azeotroped with toluene (3 x 5 mL) and concentrated *in vacuo* to furnish phosphonium salt ligand **S4** (14.2 mg, 0.0144 mmol, 83%).

^{1}H NMR (500 MHz, CD_3CN) δ: 9.02 (s, 3H, H_6), 8.67 (br, 3H, H_{12}), 8.35 (dd, *J* = 8.6, 2.4 Hz, 6H, H_4), 8.21 (d, *J* = 8.0 Hz, 3H, H_9), 7.96 (dd, *J* = 13.4, 8.8 Hz, 6H, H_3), 7.93 (td, *J* = 7.4, 1.3 Hz, 3H, H_{10}), 7.39 (dd, *J* = 7.2, 5.1 Hz, 3H, H_{11}), 2.93 (d, *J* = 14.0 Hz, 3H, H_{13}). **^{13}C NMR** (126 MHz, CD_3CN) δ: 150.9, 150.3, 142.9, 138.2, 136.5 (d, *J* = 11.7 Hz), 122.5 (d, *J* = 13.7 Hz), 122.1, 120.8 (q, *J* = 320.3 Hz), 120.0, 119.6, 119.3, 9.4*. **^{31}P NMR** (162 MHz, CD_3CN) *δ*: 22.0. **^{19}F NMR** (376 MHz, CD_3CN) *δ*: − 80.2. **HRMS** (ESI^+): m/z = 709.2444 $[M+H]^+$, calculated for $C_{40}H_{30}N_{12}P$ = 709.2449.

* Denotes signal extracted from HSQC data.

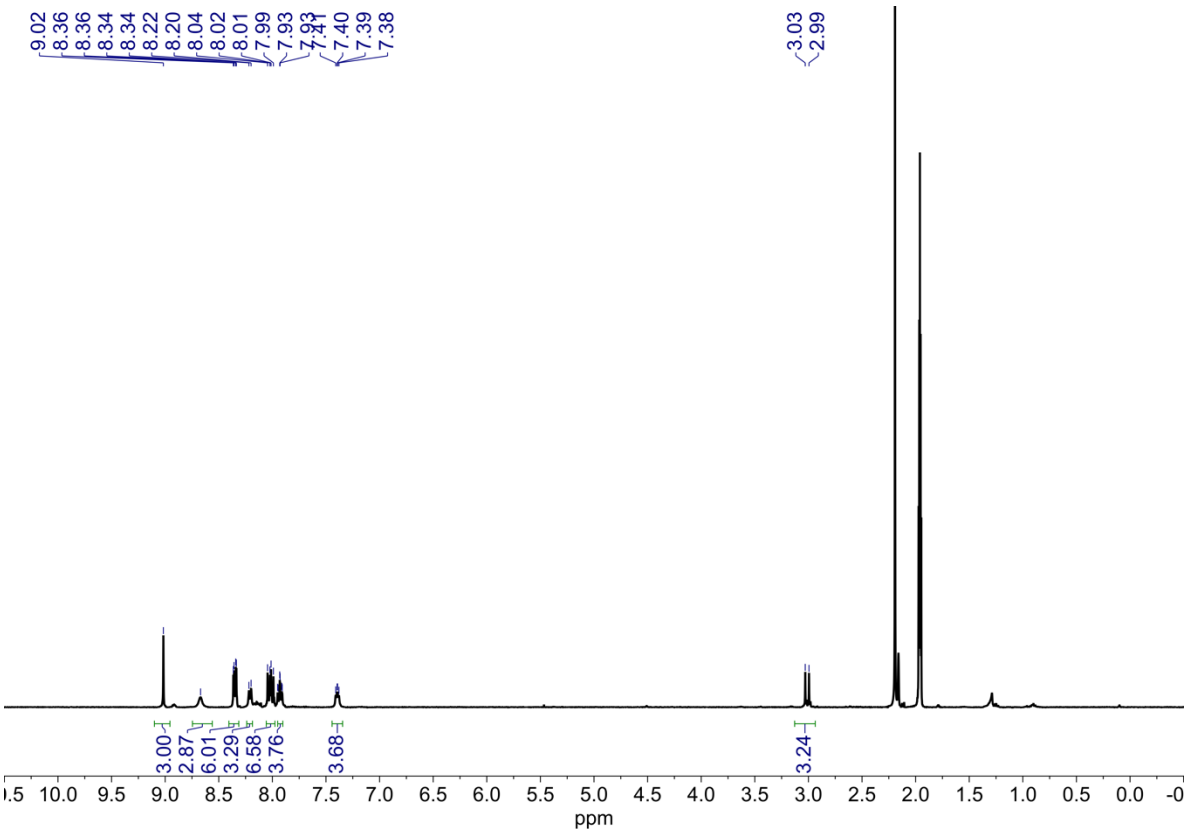

Figure S32: ^{1}H NMR (CD_3CN, 500 MHz, 298 K) spectrum of **S4**.

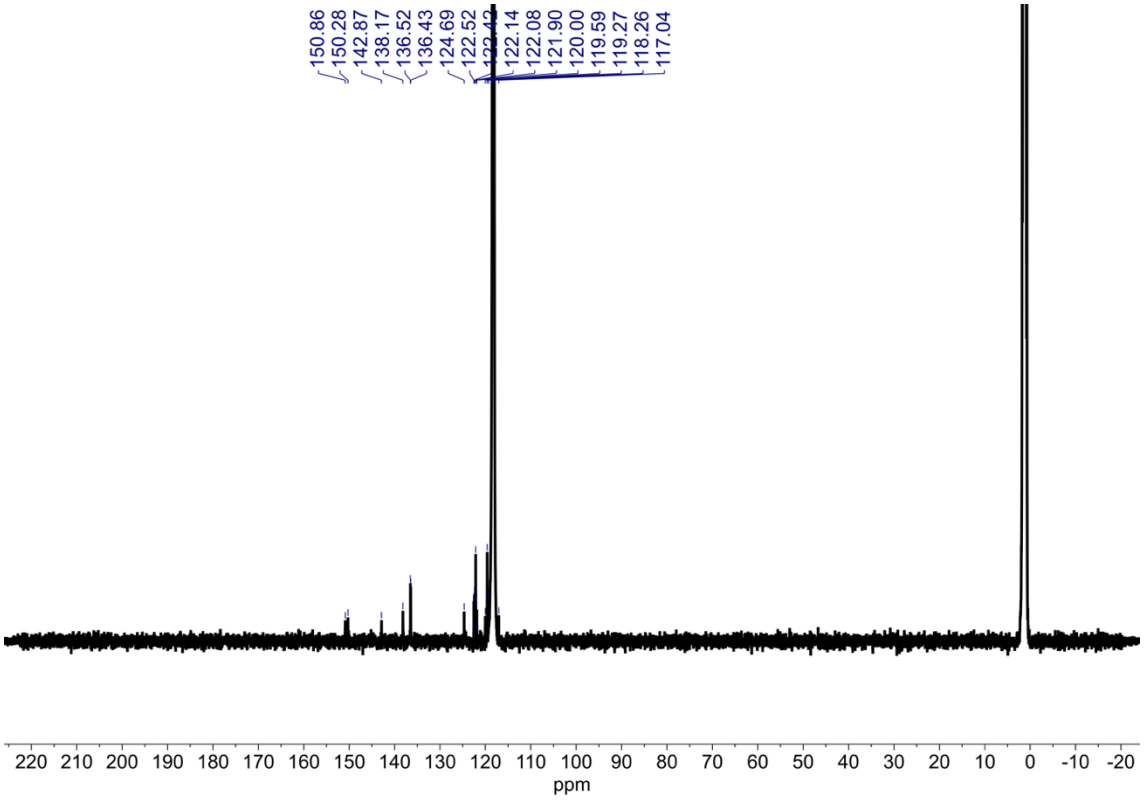

Figure S33: ^{13}C NMR (CD_3CN, 126 MHz, 298 K) spectrum of **S4**.

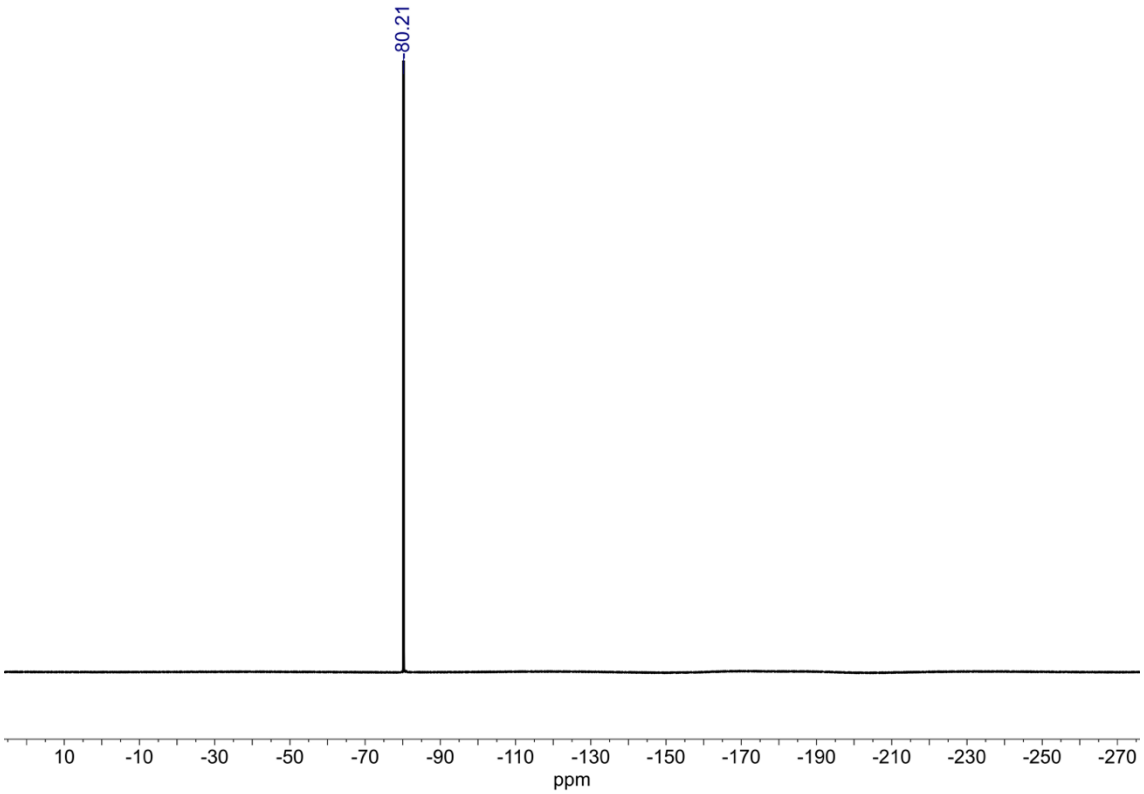

Figure S34: ^{19}F NMR (CD_3CN, 376 MHz, 298 K) spectrum of **S4**.

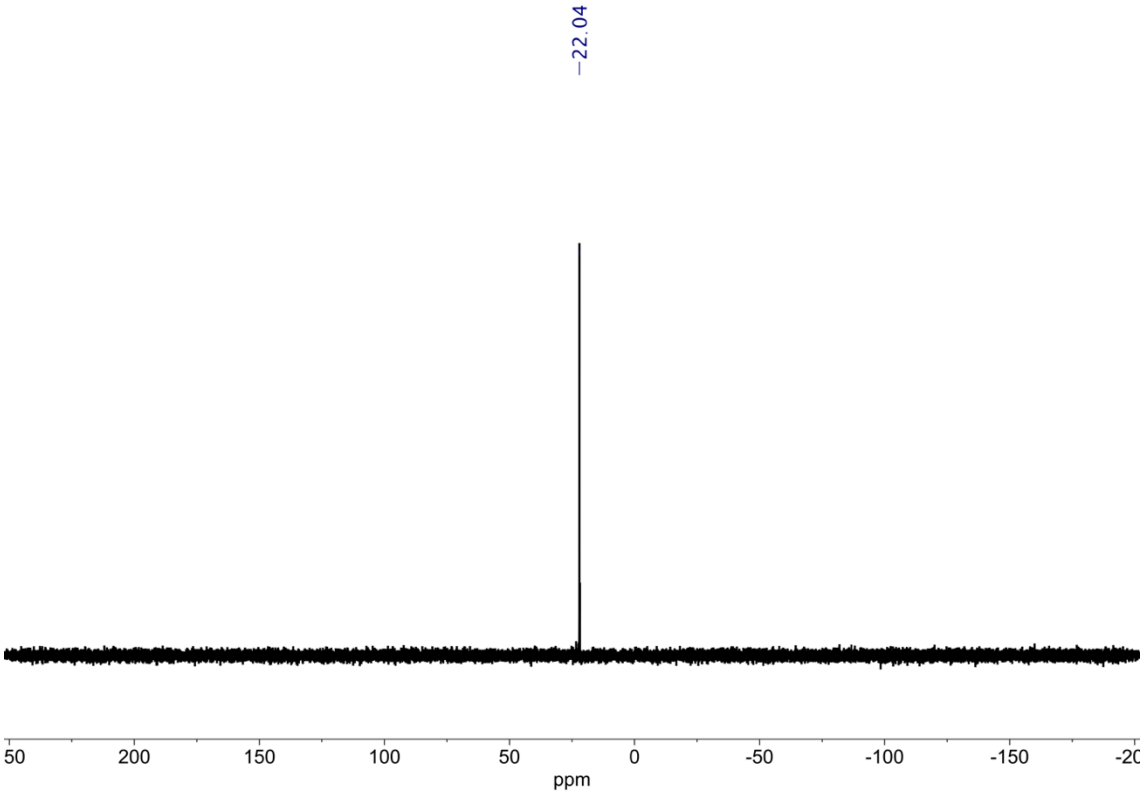

Figure S35: ^{31}P NMR (CD_3CN, 162 MHz, 298 K) spectrum of **S4**.

Phosphine Paneled Cage **2**

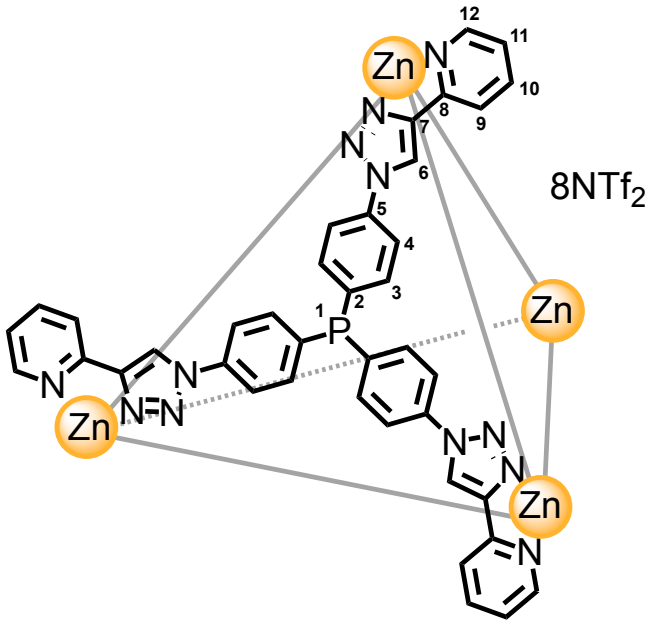

Phosphine ligand **1** (2.0 mg, 2.88 µmol) was dissolved in thoroughly sparged MeCN-d_3 (0.5 mL). $Zn(NTf_2)_2$ (2.16 mg, 3.46 µmol) was added and the reaction heated to 70 °C for 1 hour, under N_2. The formed cage was used as synthesised.

^{1}H NMR (500 MHz, CD_3CN) δ: 9.24 (s, 3H, H_6), 8.26 (t, *J* = 8.0 Hz, 3H, H_{11}), 8.12 (d, *J* = 8.0 Hz, 3H, H_9), 8.00 (d, *J* = 5.1 Hz, 3H, H_{12}), 7.85 (d, *J* = 8.2 Hz, 6H, H_4), 7.58 (t, *J* = 6.4 Hz, 3H, H_{10}), 7.53 (d, *J* = 7.6 Hz, 6H, H_3). **^{13}C NMR** (126 MHz, CD_3CN) δ: 149.2, 145.5, 144.2, 143.0, 139.2 (d, *J* = 12.8 Hz), 137.6, 136.1 (d, *J* = 20.7 Hz), 127.6, 123.8, 123.1, 121.2 (d, *J* = 7.2 Hz), 120.8 (q, *J* = 320.8 Hz). **^{31}P NMR** (162 MHz, CD_3CN) *δ*: − 6.0. **^{19}F NMR** (376 MHz, CD_3CN) *δ*: − 80.2.

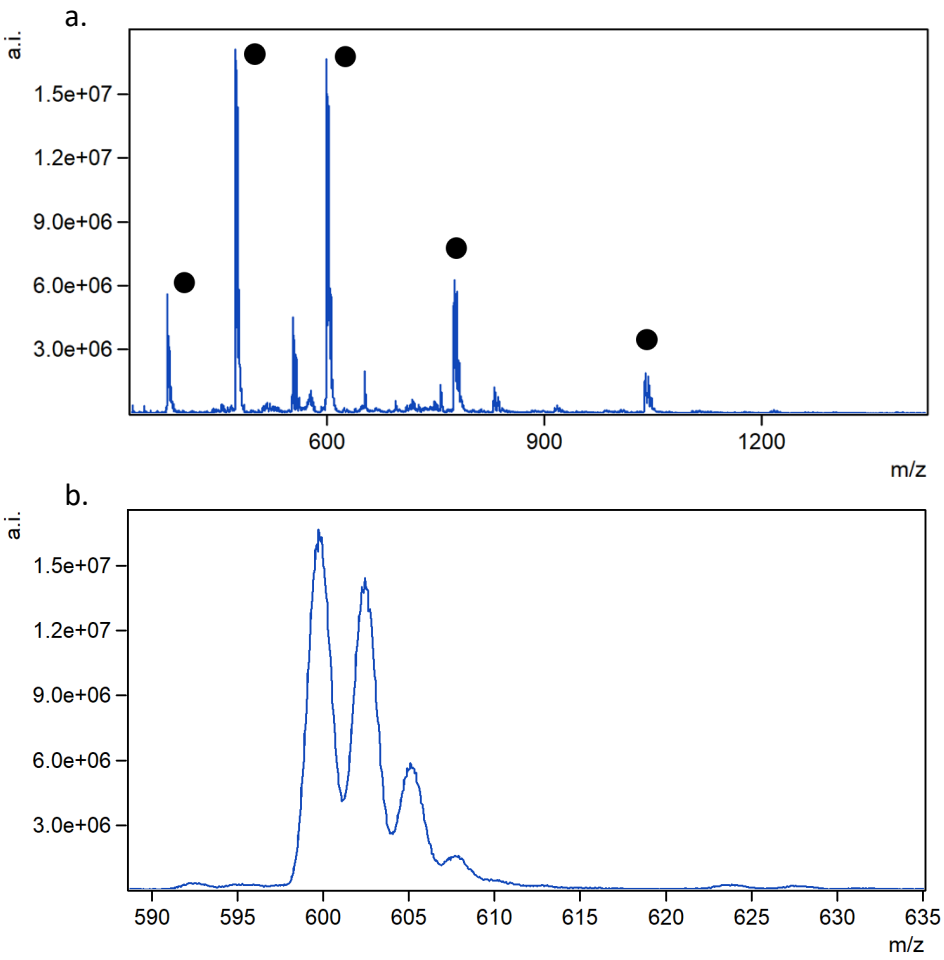

Figure S36: a. LRMS spectrum of **2**, showing partial oxidation during ionisation (peaks observed for 0-4 additional oxygen atoms per cage). b. Single cage charge species showing 0-4 additional oxygen atoms per cage.

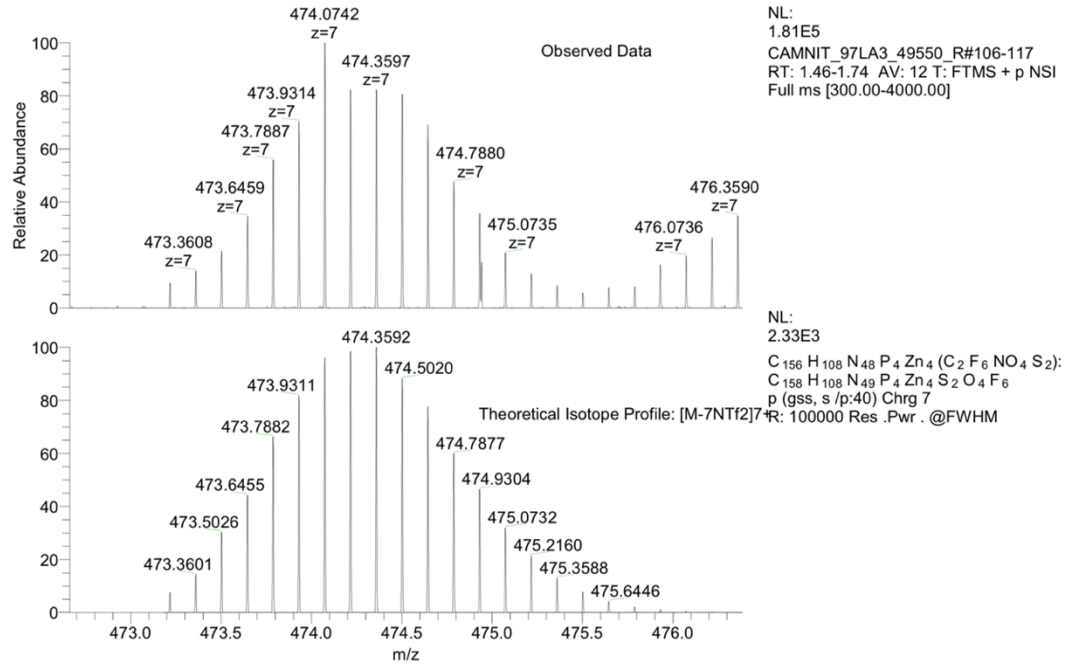

Figure S37: HRMS spectrum of **2**, 7+ cation.

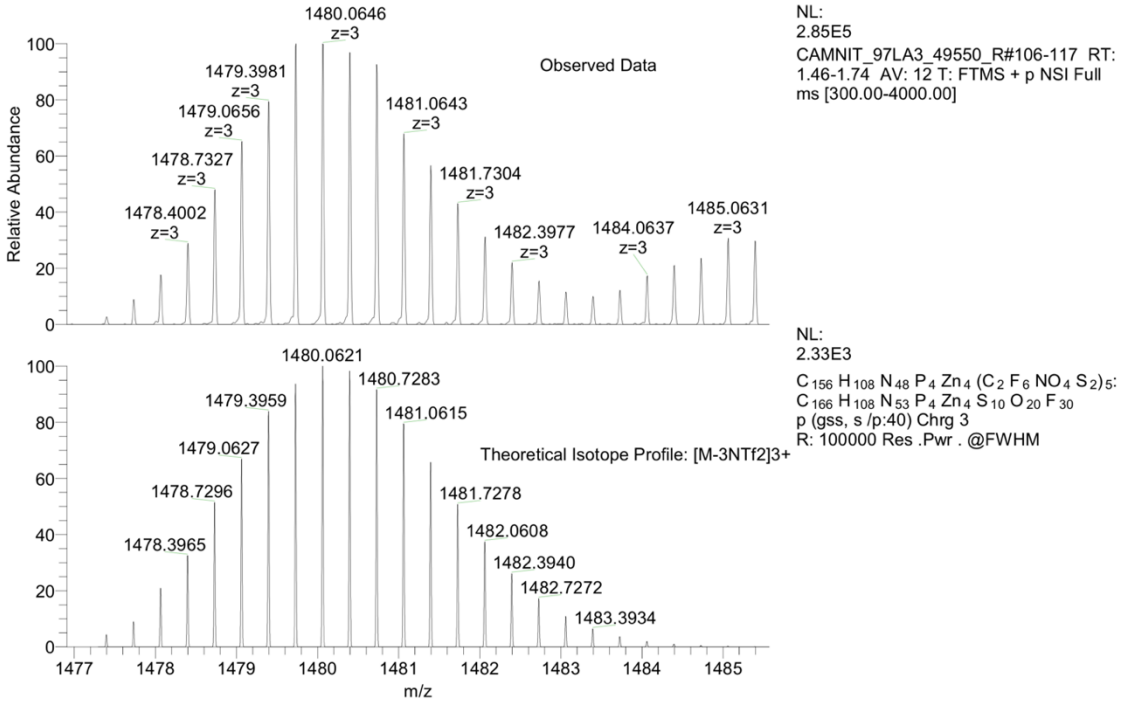

Figure S38: HRMS spectrum of **2**, 3+ cation.

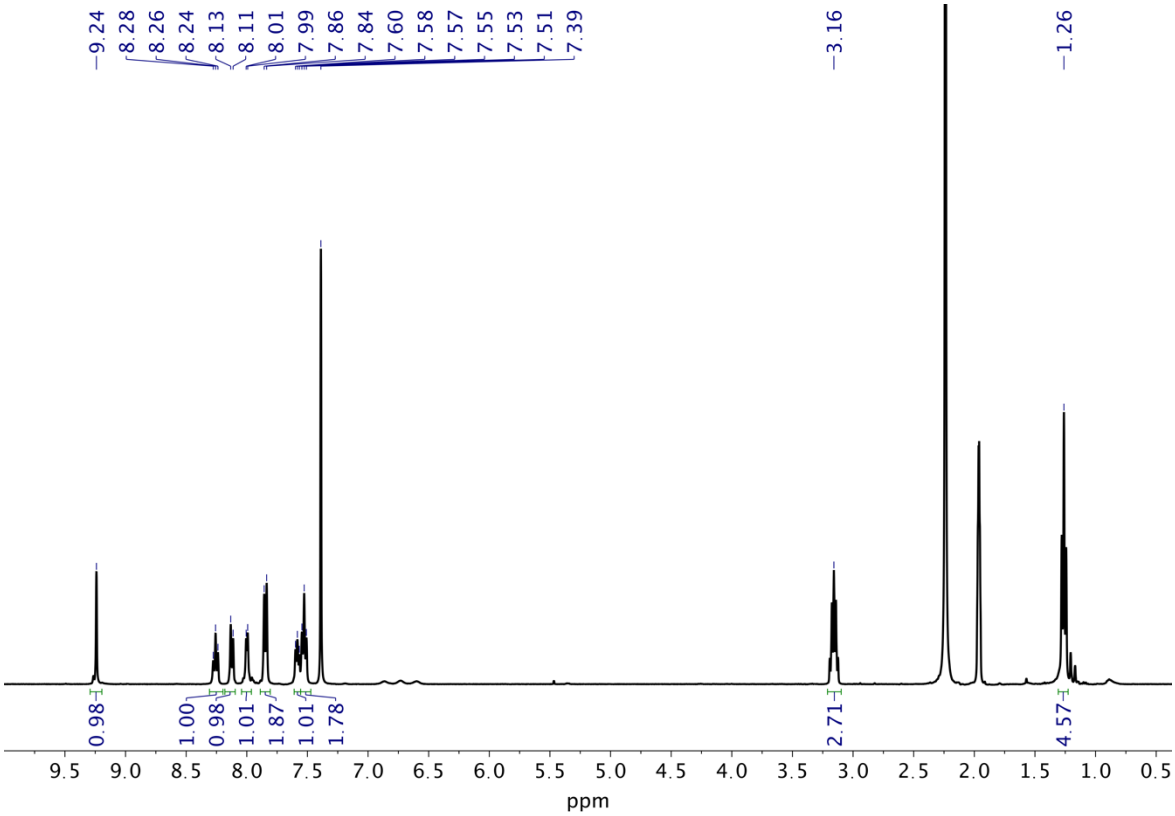

Figure S39: ^{1}H NMR (CD_3CN, 500 MHz, 298 K) spectrum of **2**.

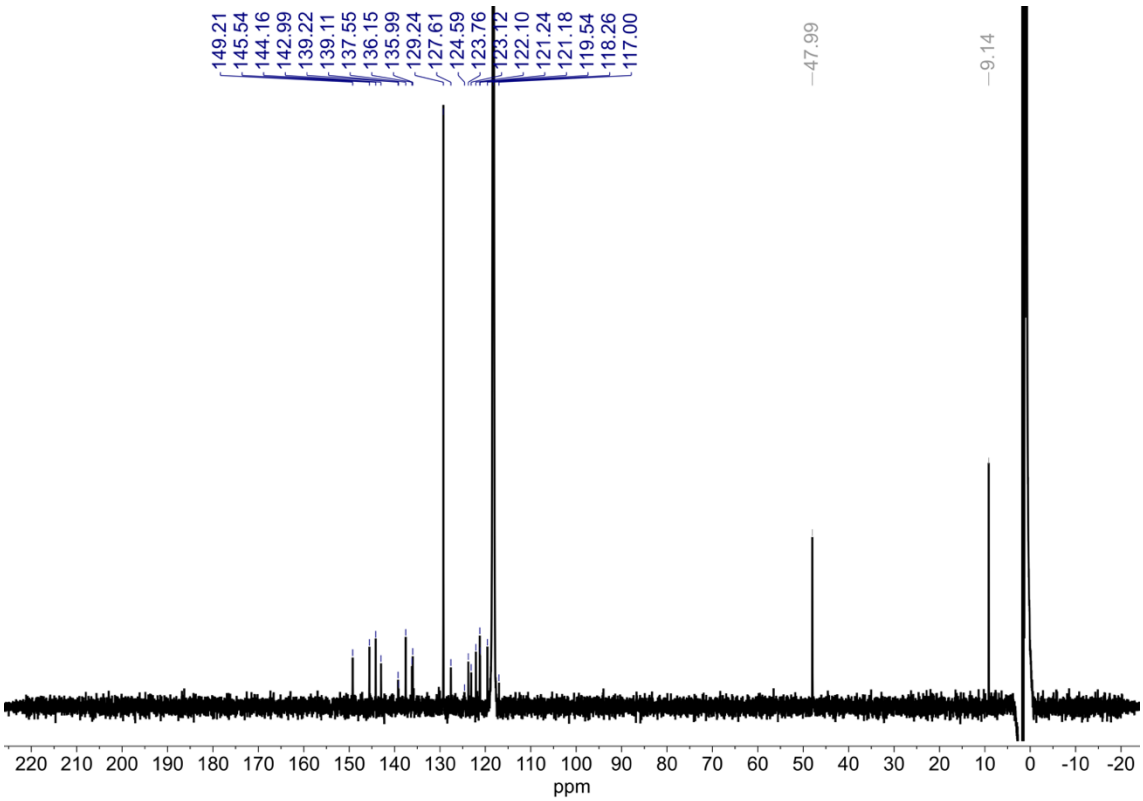

Figure S40: ^{13}C NMR (CD_3CN, 126 MHz, 298 K) spectrum of **2**.

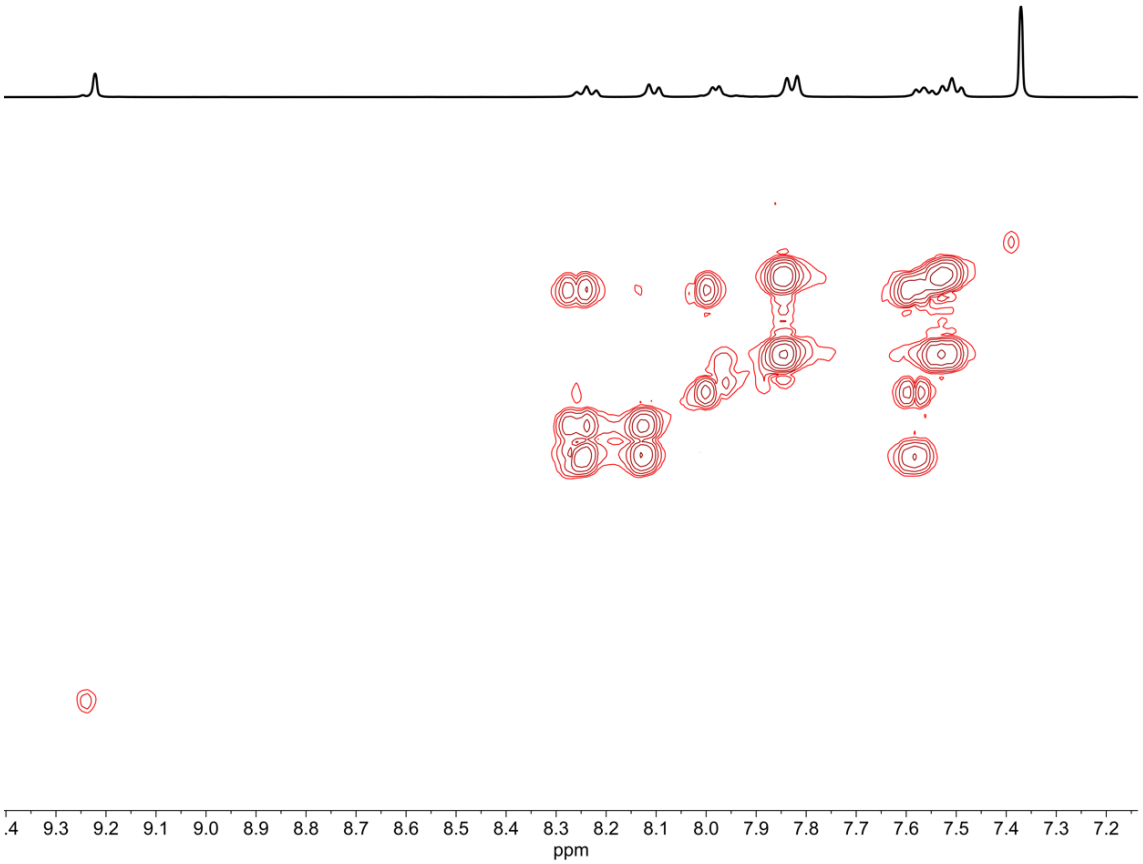

Figure S41: Partial COSY spectrum of **2**.

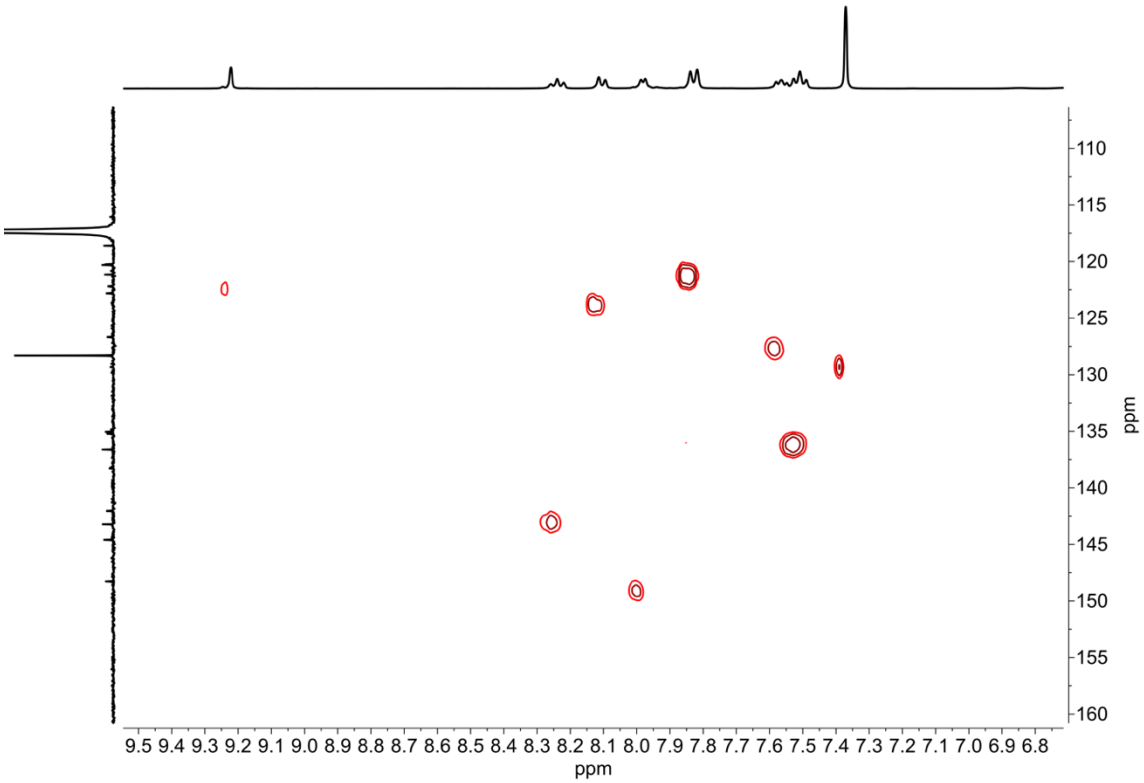

Figure S42: Partial HSQC spectrum of **2**.

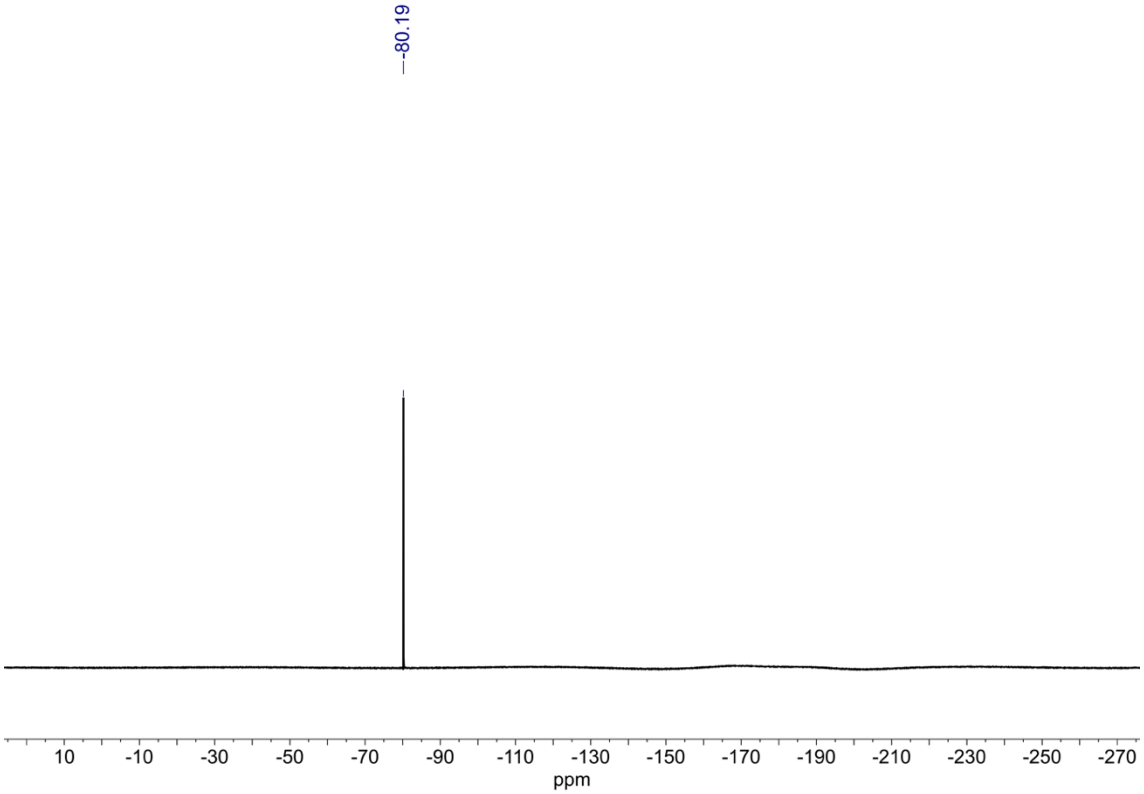

Figure S43: ^{19}F NMR (CD_3CN, 376 MHz, 298 K) spectrum of **2**.

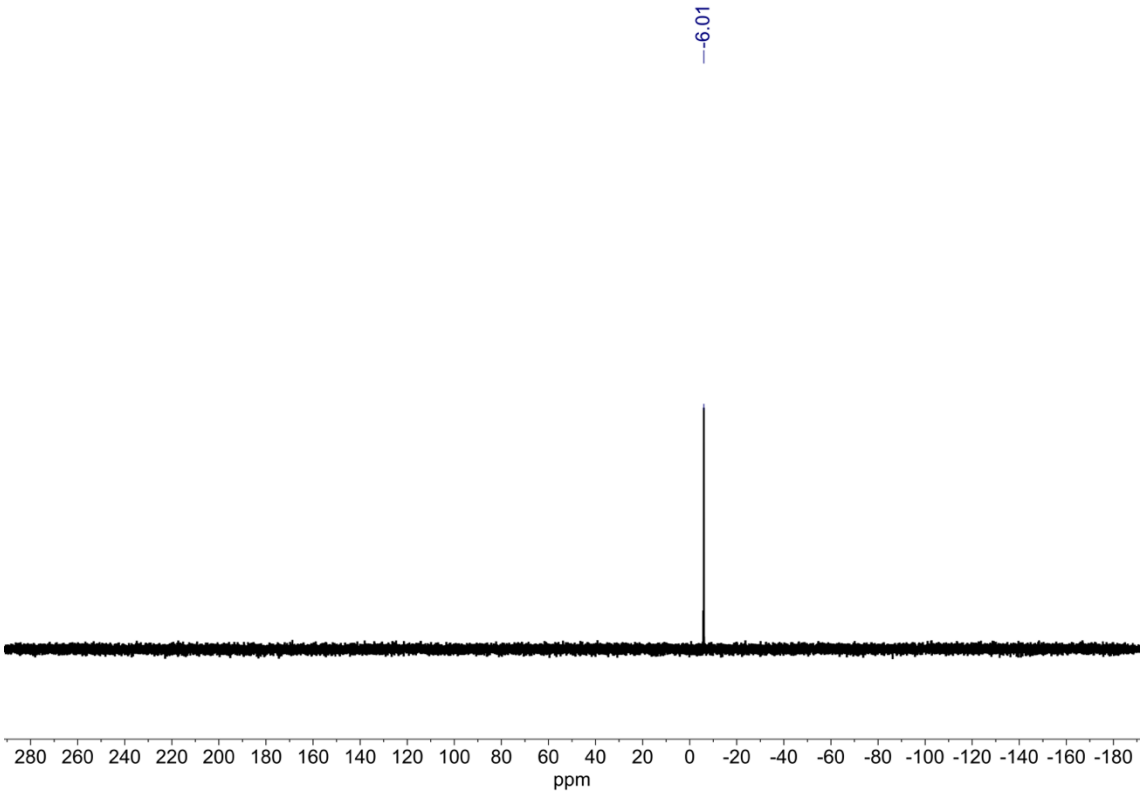

Figure S44: ^{31}P NMR (CD_3CN, 162 MHz, 298 K) spectrum of **2**.

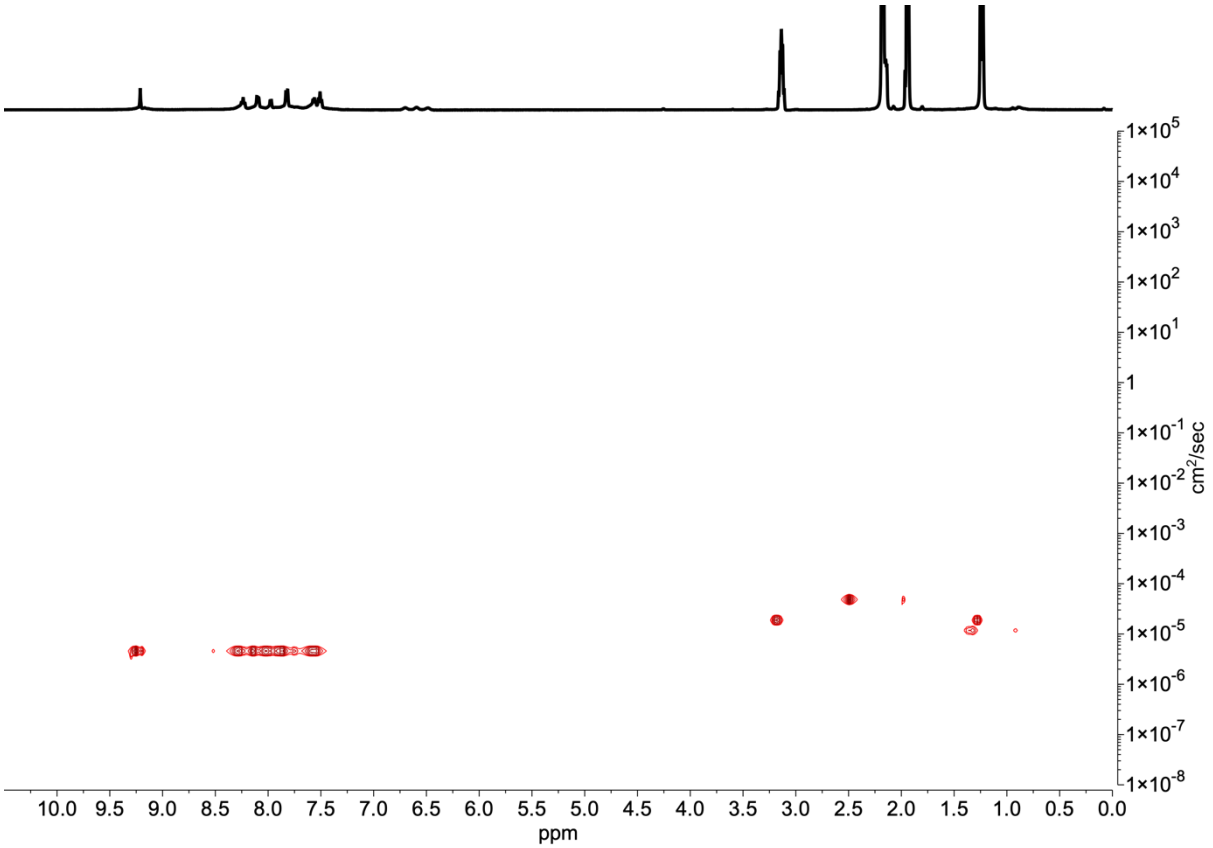

Figure S45: DOSY NMR spectrum of **2**. Diffusion coefficient: 4.62×10^{-10} m^2s^{-1}. R_H from DOSY: 13.8 Å. Calculated R_H: 12.1 Å.

Phosphine Oxide Paneled Cage **3**

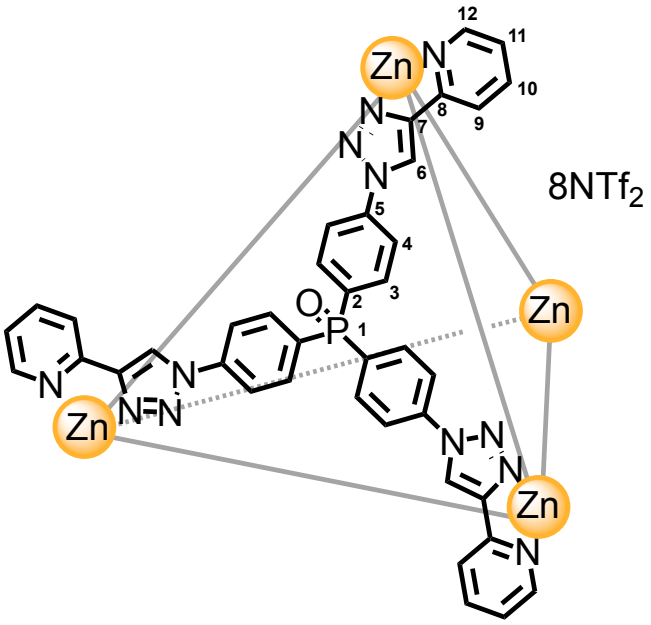

Phosphine oxide ligand **S1** (2.0 mg, 2.82 mmol) was dissolved in MeCN-d_3 (0.5 mL). $Zn(NTf_2)_2$ (2.16 mg, 3.46 mmol) was added and the reaction heated to 70 °C for 1 hour. The formed cage was used as synthesised.

^{1}H NMR (500 MHz, CD_3CN) δ: 9.25 (s, 3H, H_6), 8.27 (td, *J* = 7.8, 1.4 Hz, 3H, H_{11}), 8.13 (d, *J* = 7.9 Hz, 3H, H_9), 8.02 (d, *J* = 5.2 Hz, 3H, H_{12}), 7.95 (dd, *J* = 8.5, 1.6 Hz, 6H, H_4), 7.86 (d, *J* = 11.5, 8.7 Hz, 6H, H_3), 7.61 (dd, *J* = 8.1, 5.0 Hz, 3H, H_{10}). **^{13}C NMR** (126 MHz, CD_3CN) δ: 149.3, 145.5, 144.3, 143.1, 139.8 (d, *J* = 2.5 Hz), 134.8 (d, *J* = 11.1 Hz), 134.6 (d, *J* = 104.7 Hz), 127.7, 123.9, 123.8, 121.8 (d, *J* = 12.5 Hz), 120.8 (q, *J* = 319.8 Hz). **^{31}P NMR** (162 MHz, CD_3CN) *δ*: 24.2. **^{19}F NMR** (376 MHz, CD_3CN) *δ*: − 81.0.

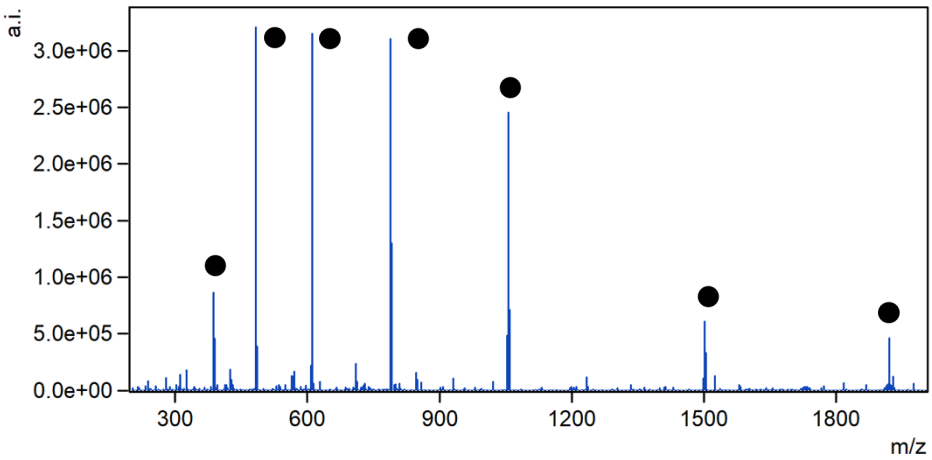

Figure S46: LRMS spectrum of **3**.

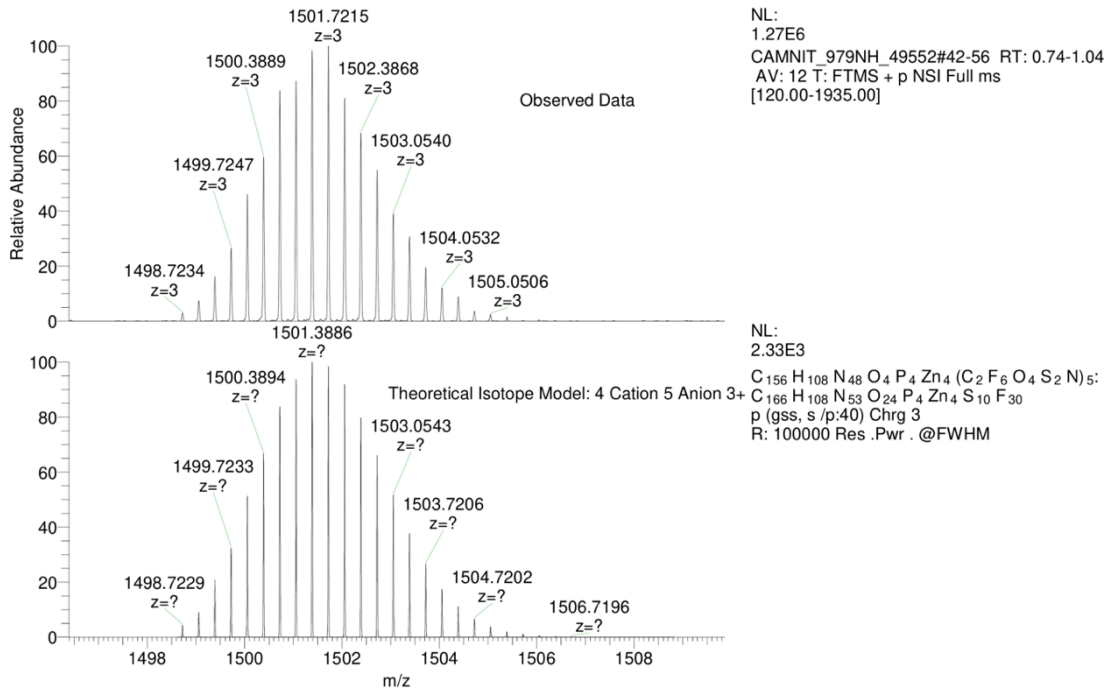

Figure S47: HRMS spectrum of **3**, 5+ cation.

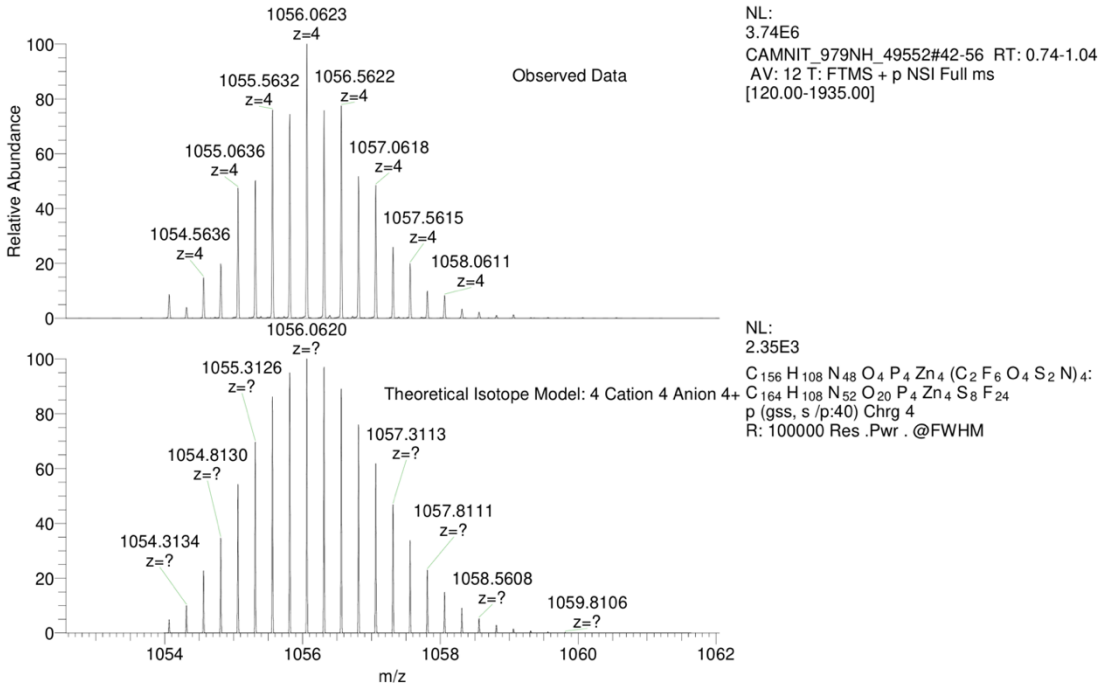

Figure S48: HRMS spectrum of **3**, 4+ cation.

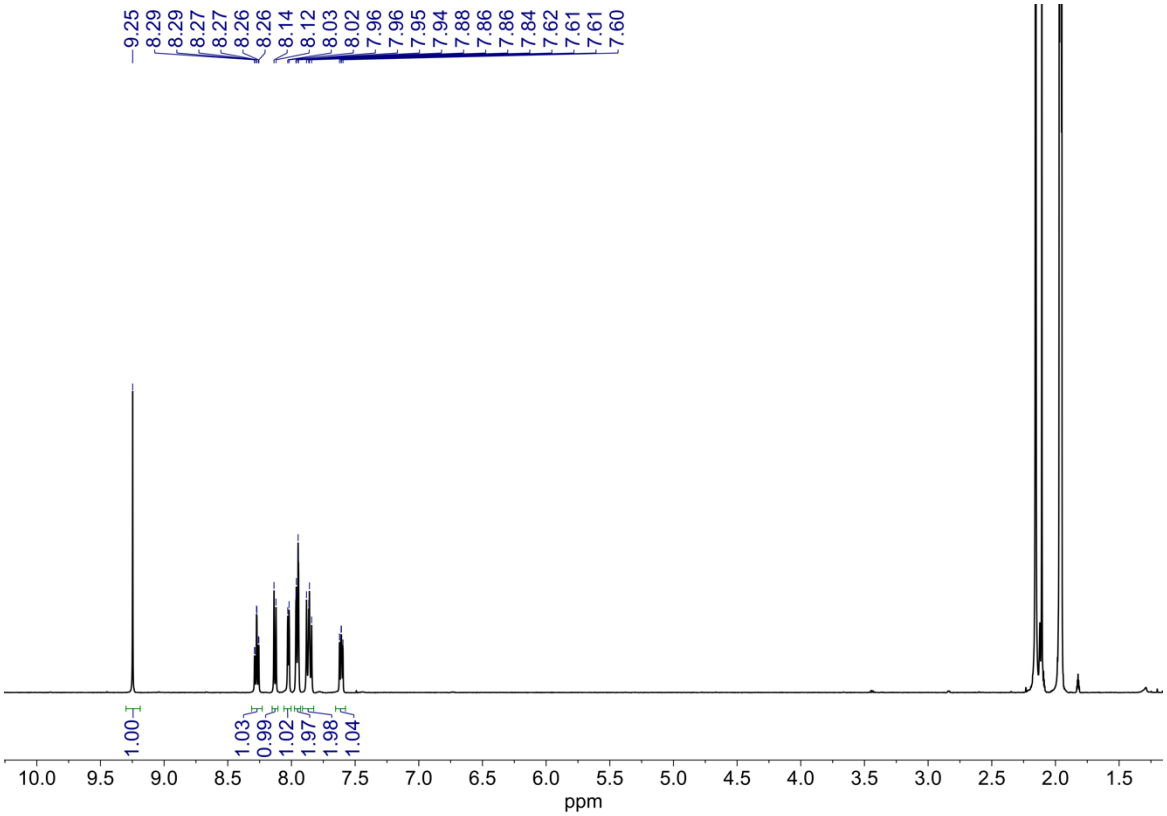

Figure S49: ^{1}H NMR (CD_3CN, 500 MHz, 298 K) spectrum of **3**.

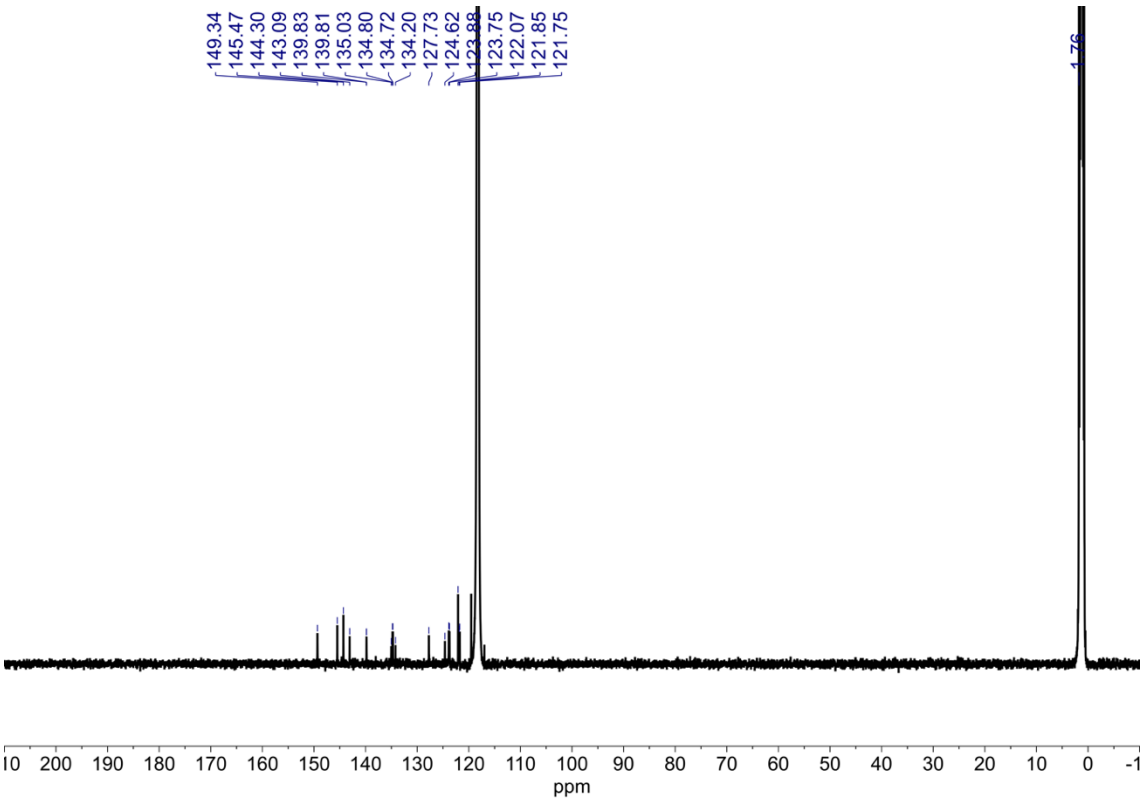

Figure S50: ^{13}C NMR (CD_3CN, 126 MHz, 298 K) spectrum of **3**.

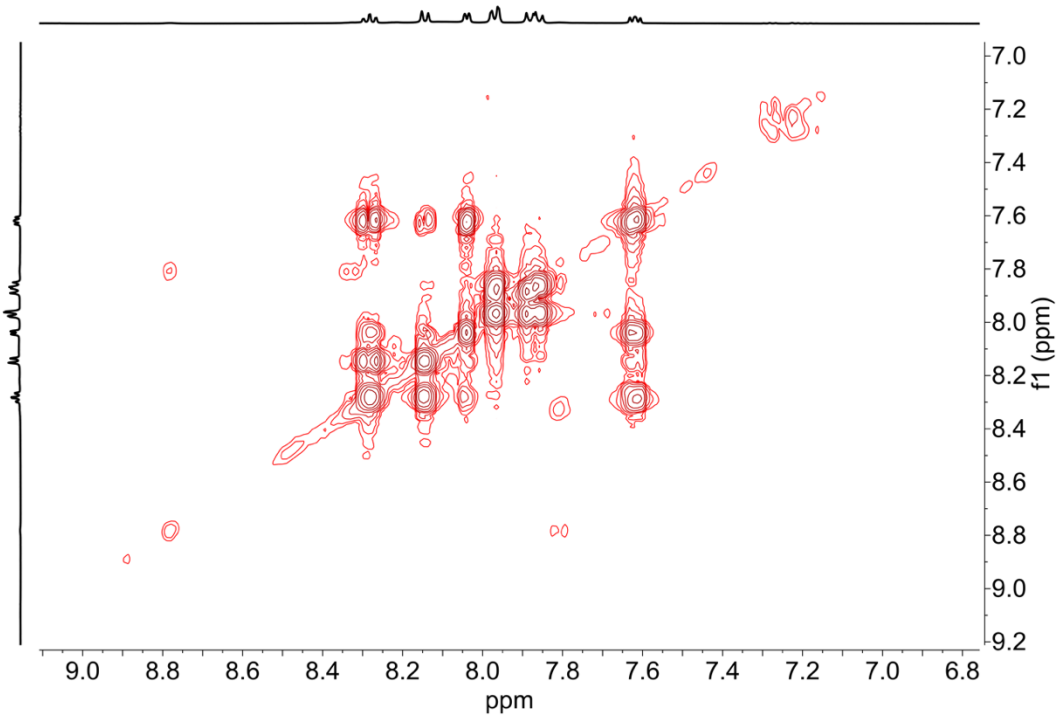

Figure S51: Partial COSY spectrum of **3**.

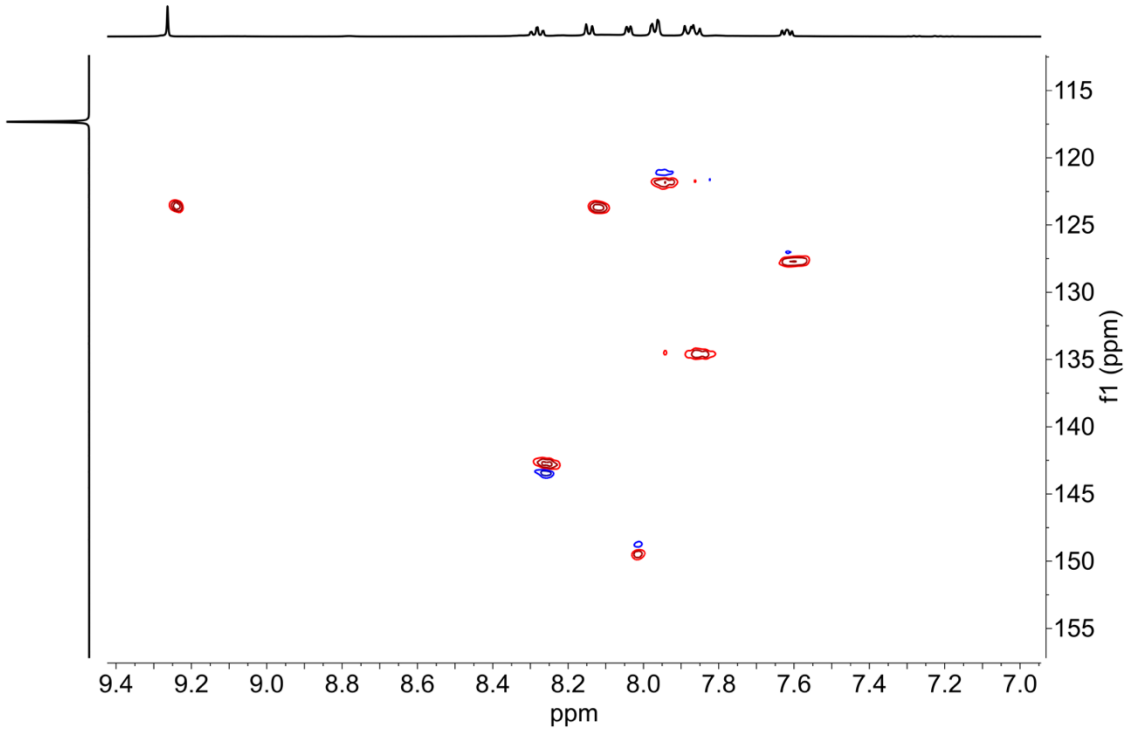

Figure S52: Partial HSQC spectrum of **3**.

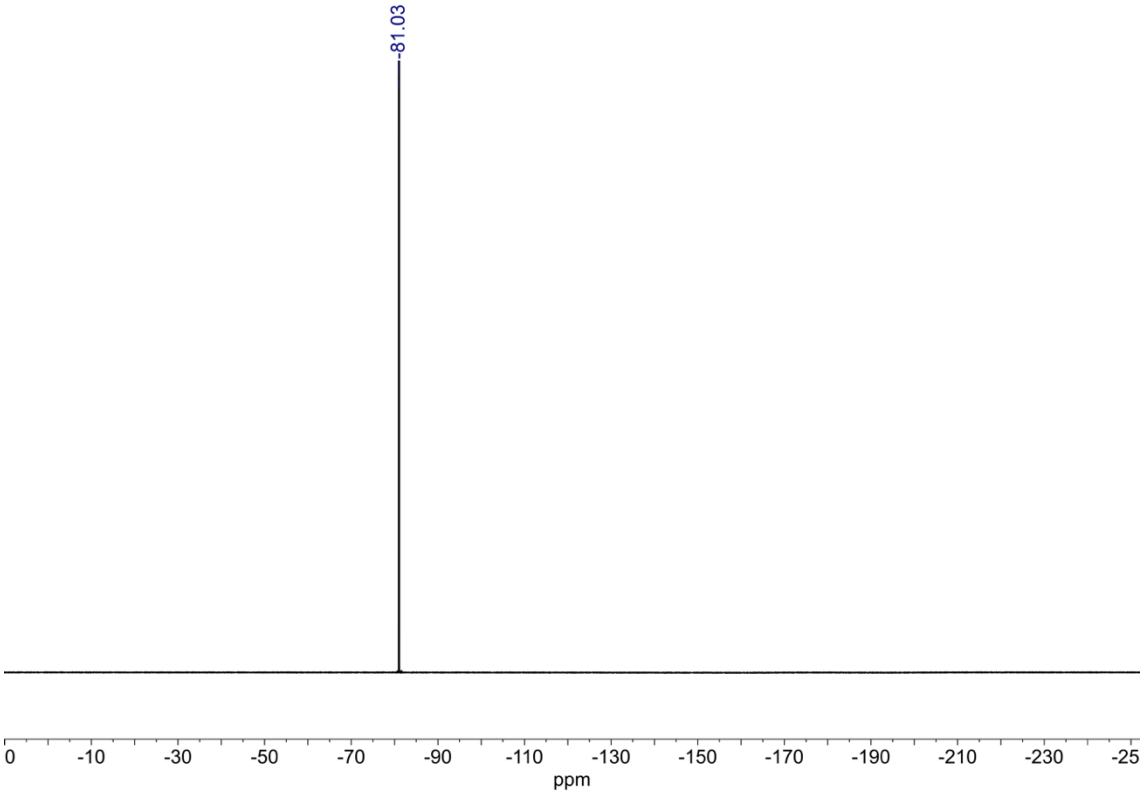

Figure S53: ^{19}F NMR (CD_3CN, 376 MHz, 298 K) spectrum of **3**.

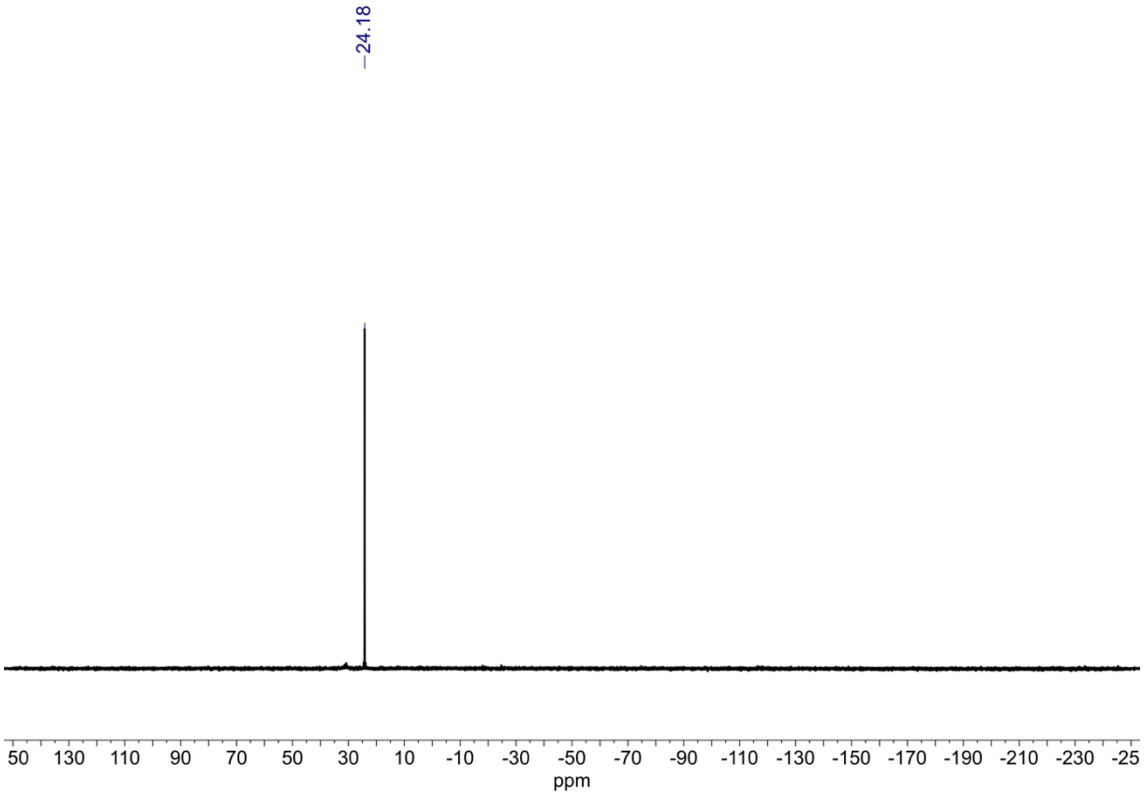

Figure S54: ^{31}P NMR (CD_3CN, 162 MHz, 298 K) spectrum of **3**.

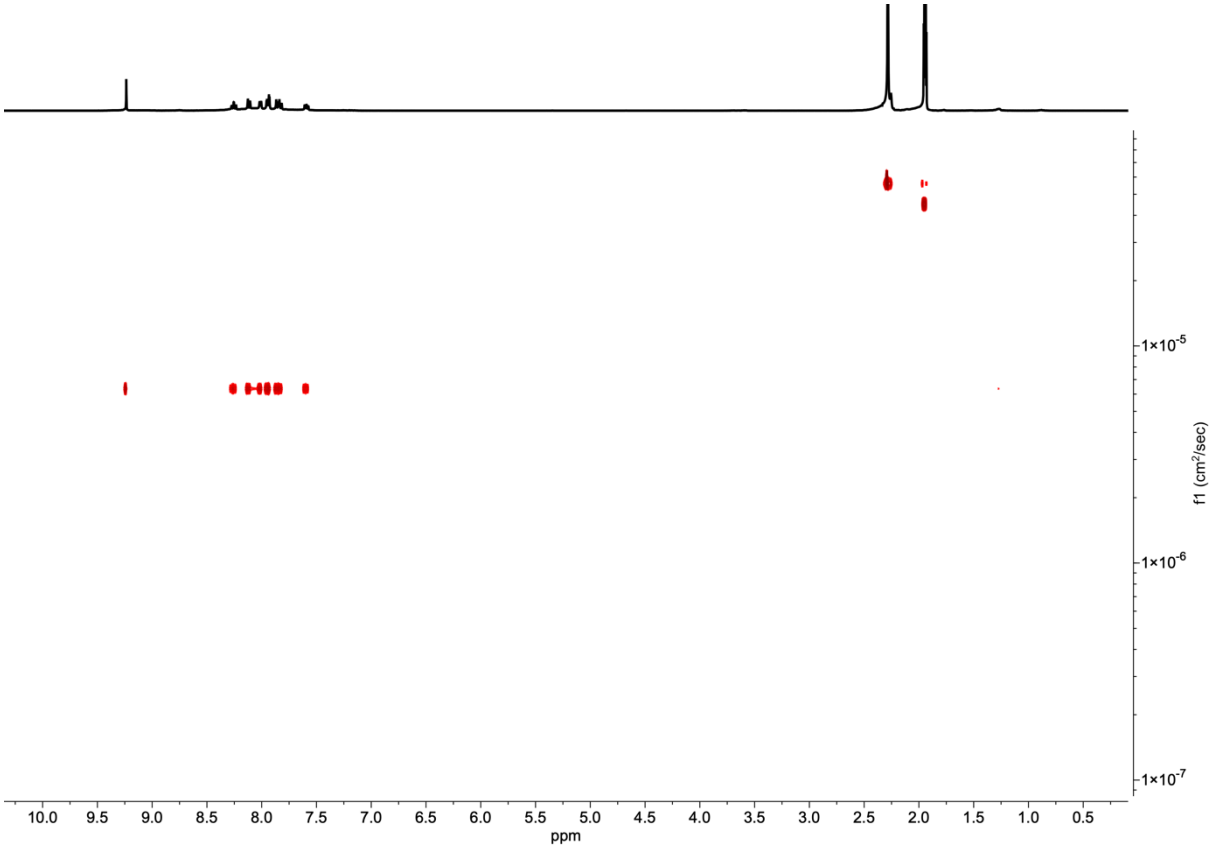

Figure S55: DOSY NMR spectrum of **2**. Diffusion coefficient: 6.34 × 10^{-10} m^2s^{-1}. R_H from DOSY: 10.0 Å. Calculated R_H: 12.1 Å.

Phosphonium Paneled Cage **4**

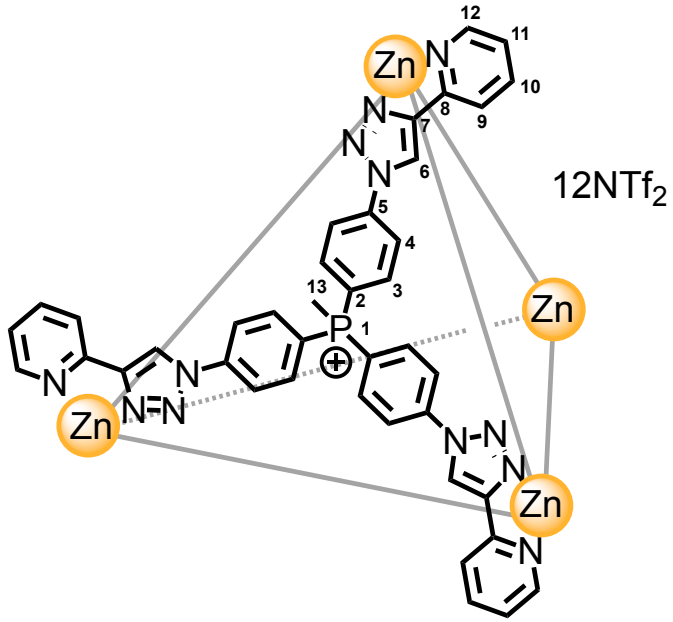

Phosphonium salt ligand **S4** (2 mg, 2.02 µmol) was dissolved in MeCN-d_3 (0.5 mL). $Zn(NTf_2)_2$ (1.52 mg, 2.42 µmol) was added and the reaction heated to 70 °C for 1 hour. The formed cage was used as synthesised.

^{1}H NMR (500 MHz, CD_3CN) δ: 9.37 (s, 3H, H_6), 8.28 (td, *J* = 7.9, 1.5 Hz, 3H, H_{11}), 8.15 (d, *J* = 8.1 Hz, 3H, H_9), 8.13 (dd, *J* = 9.0, 2.5 Hz, 6H, H_4), 8.07 (d, *J* = 8.1 Hz, 3H, H_{12}), 7.83 (d, *J* = 13.3, 8.9 Hz, 6H, H_3), 7.62 (dd, *J* = 7.9, 0.8 Hz, 3H, H_{10}), 2.89 (d, *J* = 14.2 Hz, 3H, H_{13}). **^{13}C NMR** (126 MHz, CD_3CN) δ: 149.4 , 145.3, 144.4, 143.2, 141.7 (d, *J* = 3.5 Hz), 136.7 (d, *J* = 11.9 Hz), 127.8, 123.9, 123.5, 122.2 (d, *J* = 14.5 Hz), 120.8 (q, *J* = 320.9 Hz), 120.5 (d, *J* = 91.7 Hz), 8.19*. **^{31}P NMR** (162 MHz, CD_3CN) *δ*: 23.2. **^{19}F NMR** (376 MHz, CD_3CN) *δ*: − 80.1.

* Denotes signal extracted from HSQC data.

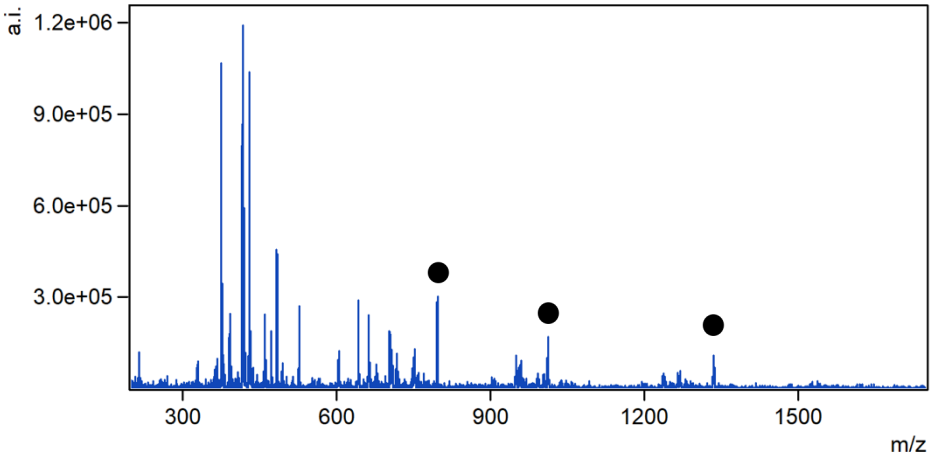

Figure S56: LRMS spectrum of **4**. Phosphonium derived cages required gentle ionisation conditions, and extensive fragmentation was still observed under the best conditions.

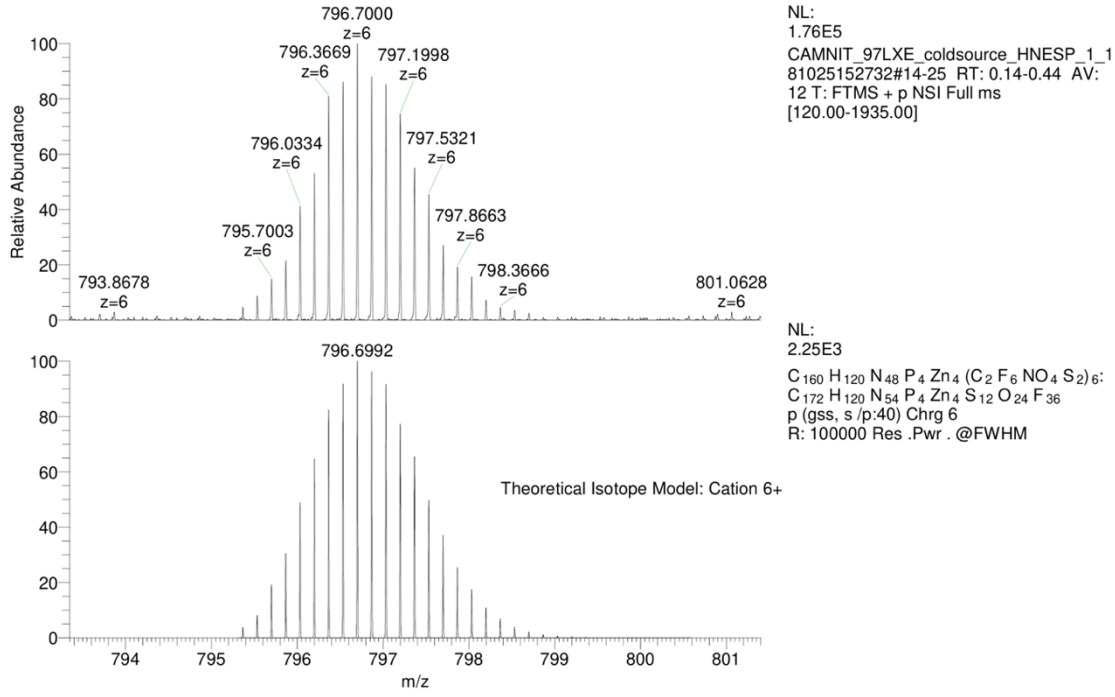

Figure S57: HRMS spectrum of **4**, 6+ cation.

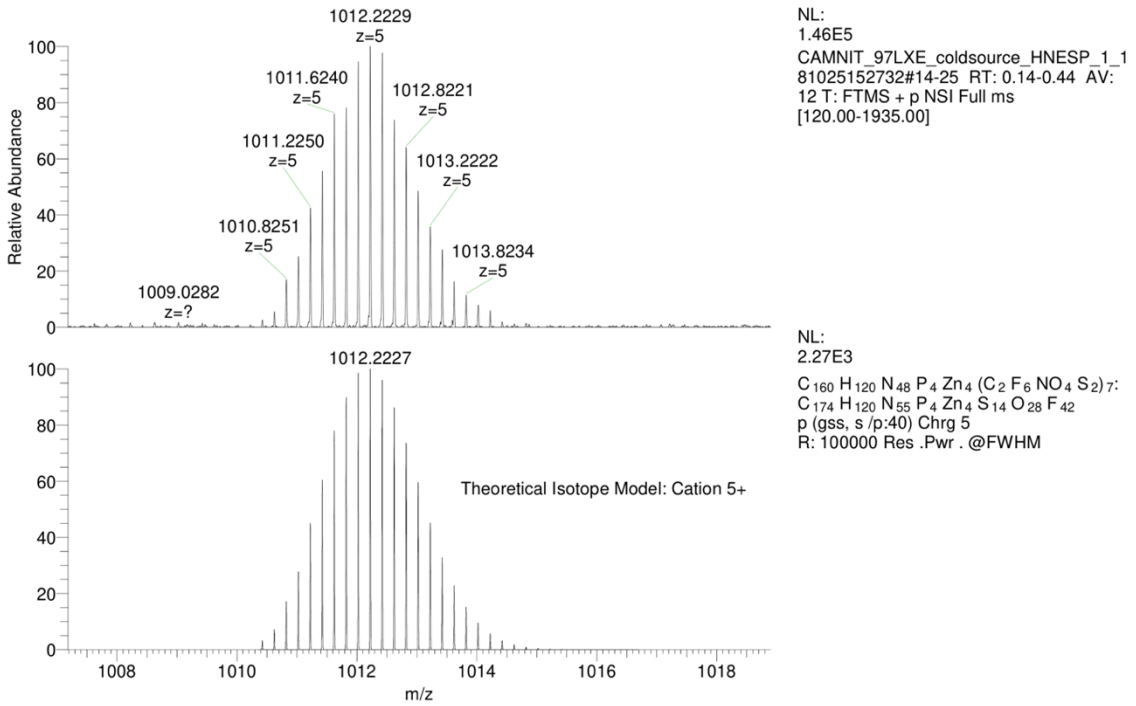

Figure S58: HRMS spectrum of **4**, 5+ cation.

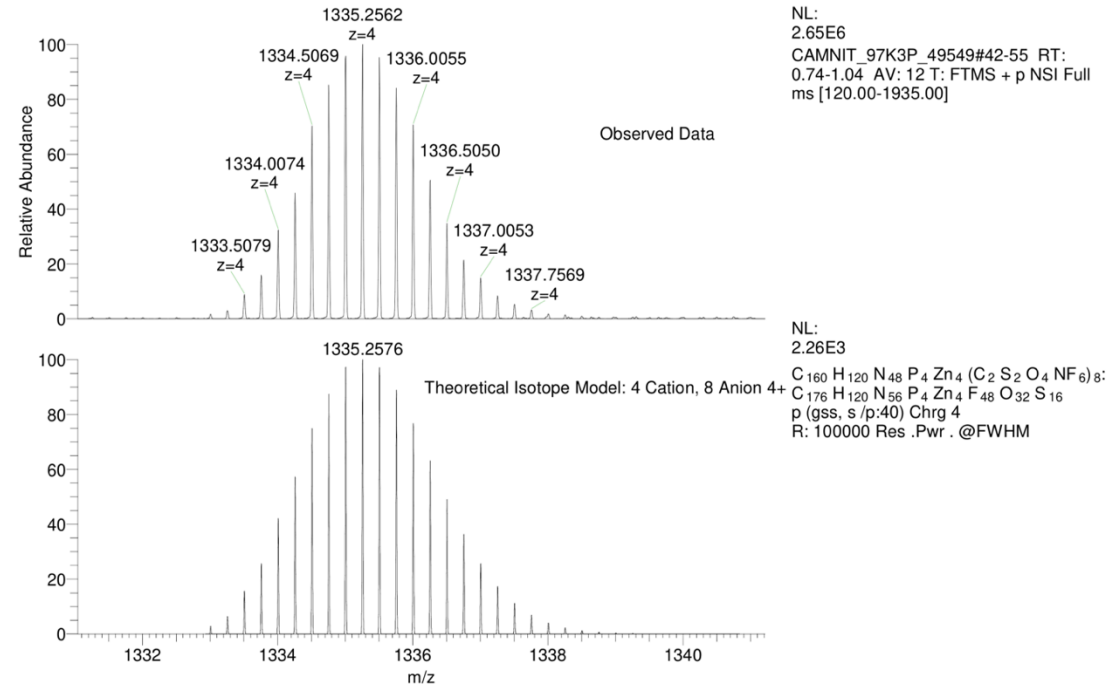

Figure S59: HRMS spectrum of **4**, 4+ cation.

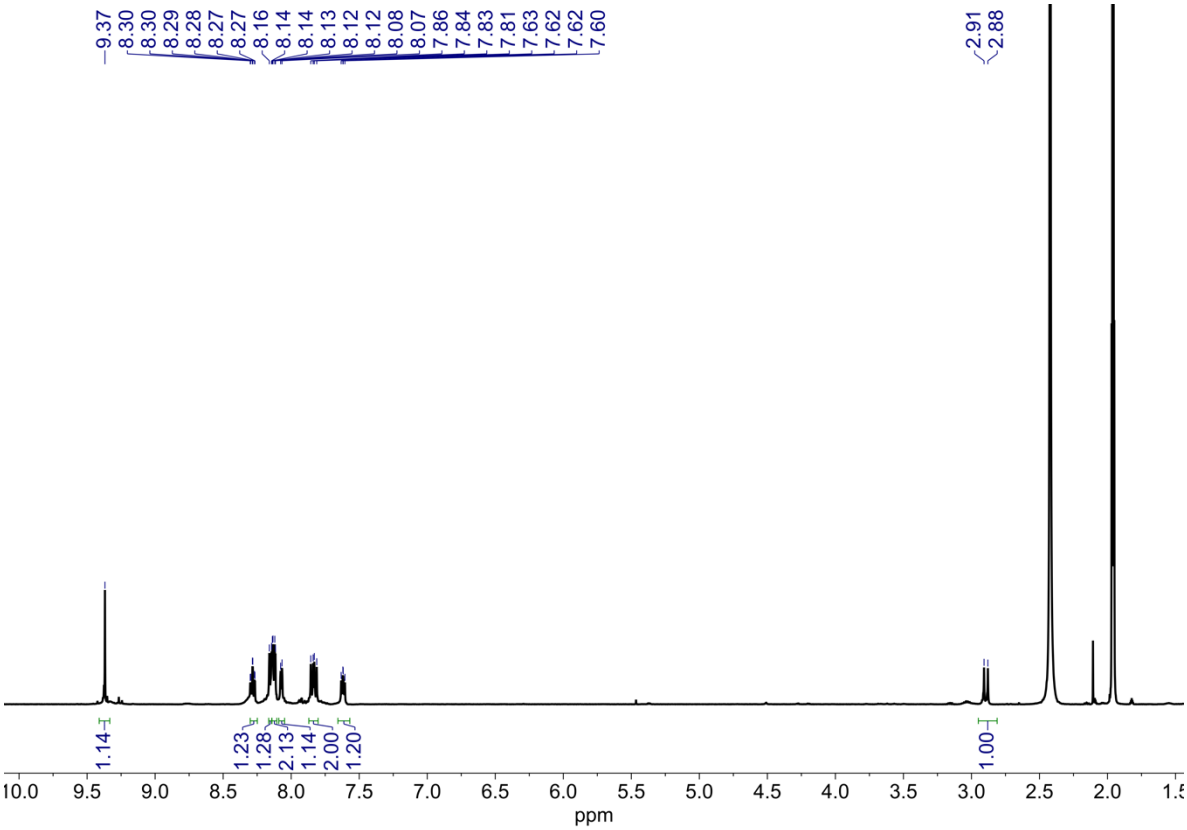

Figure S60: ^{1}H NMR (CD_3CN, 500 MHz, 298 K) spectrum of **4**.

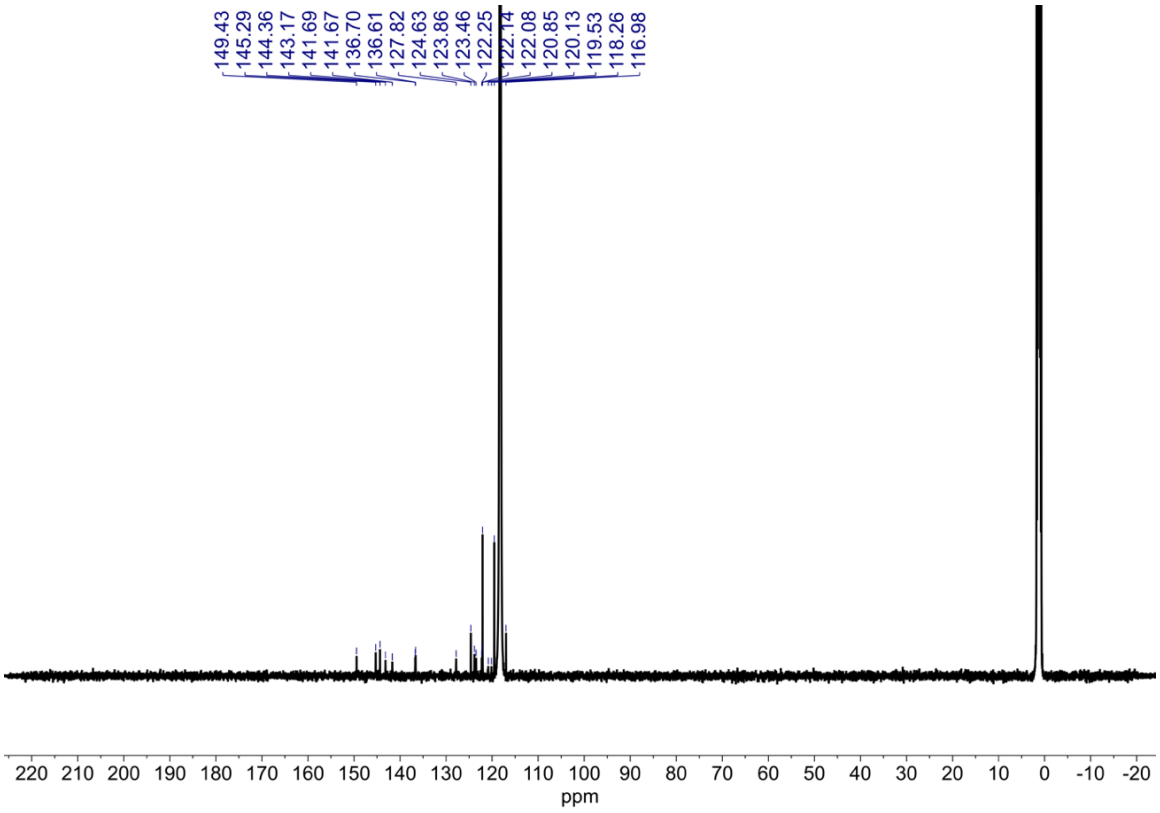

Figure S61: ^{13}C NMR (CD_3CN, 126 MHz, 298 K) spectrum of **4**.

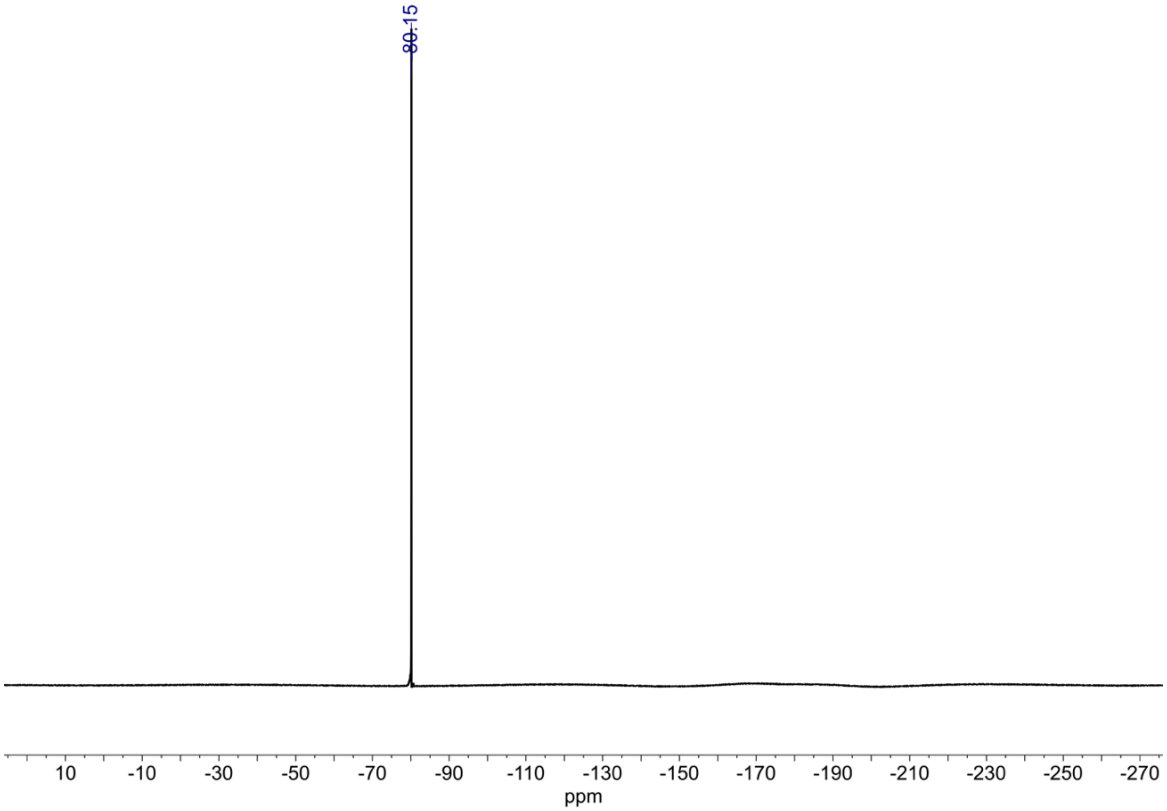

Figure S62: ^{19}F NMR (CD_3CN, 376 MHz, 298 K) spectrum of **4**.

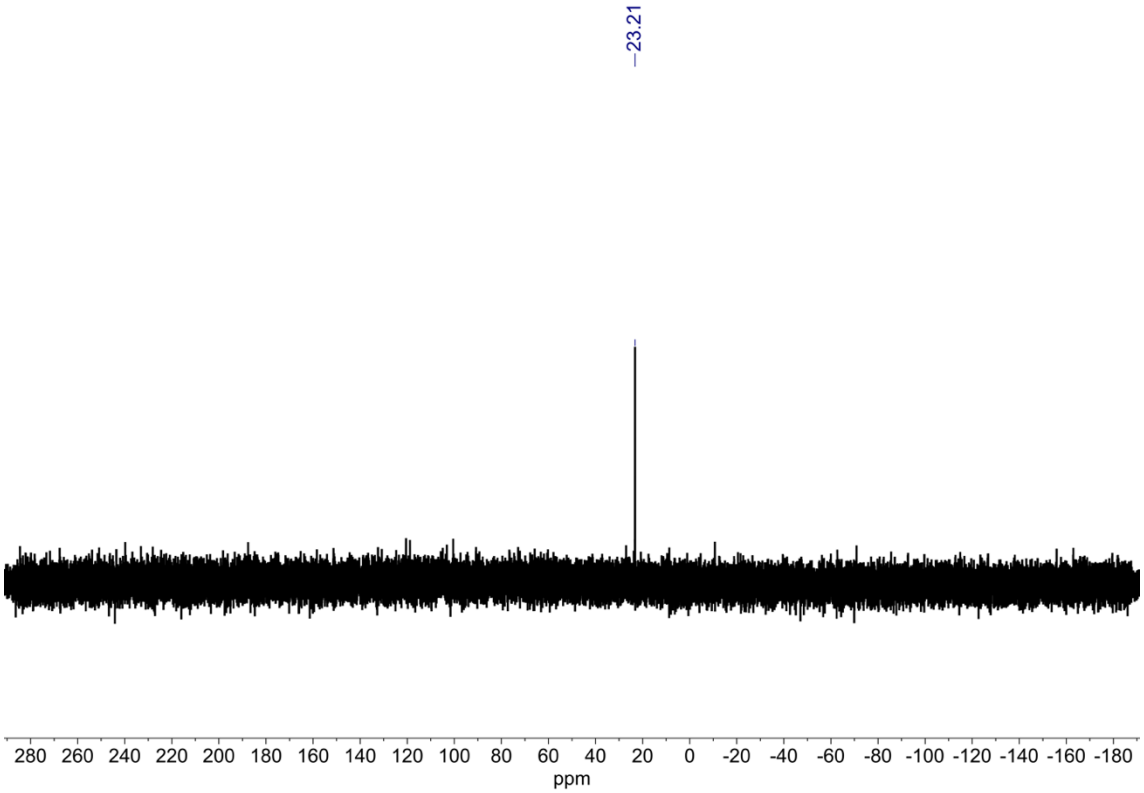

Figure S63: ^{31}P NMR (CD_3CN, 162 MHz, 298 K) spectrum of **4**.

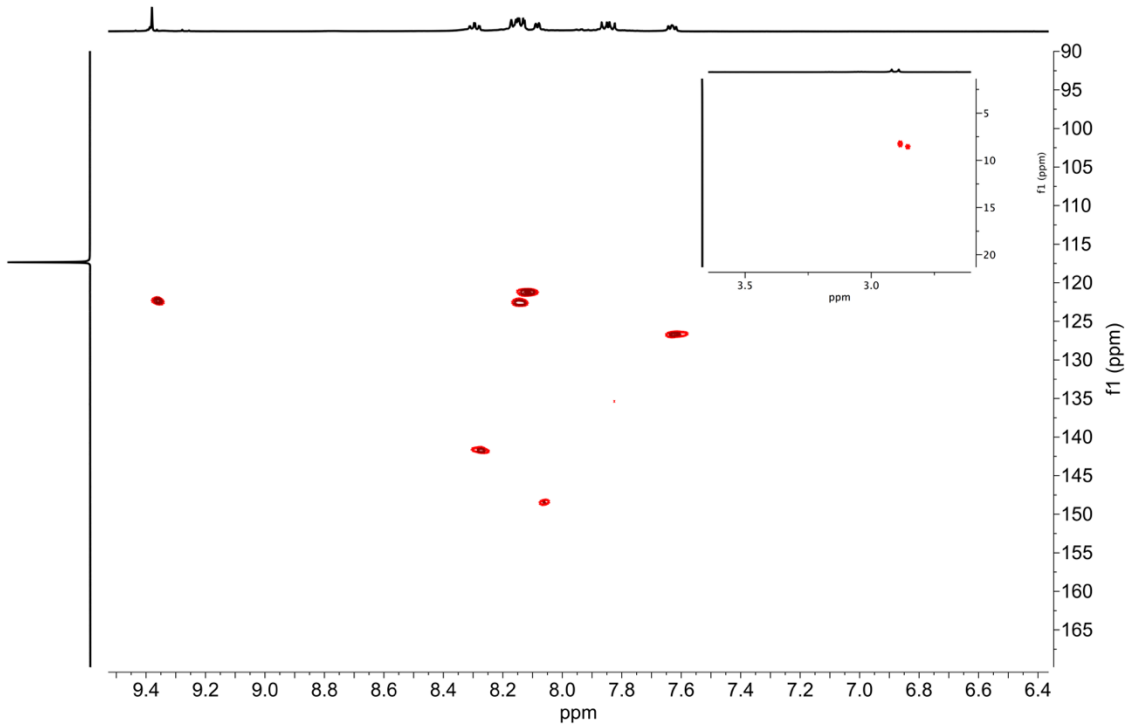

Figure S64: Partial HSQC spectrum of **4**.

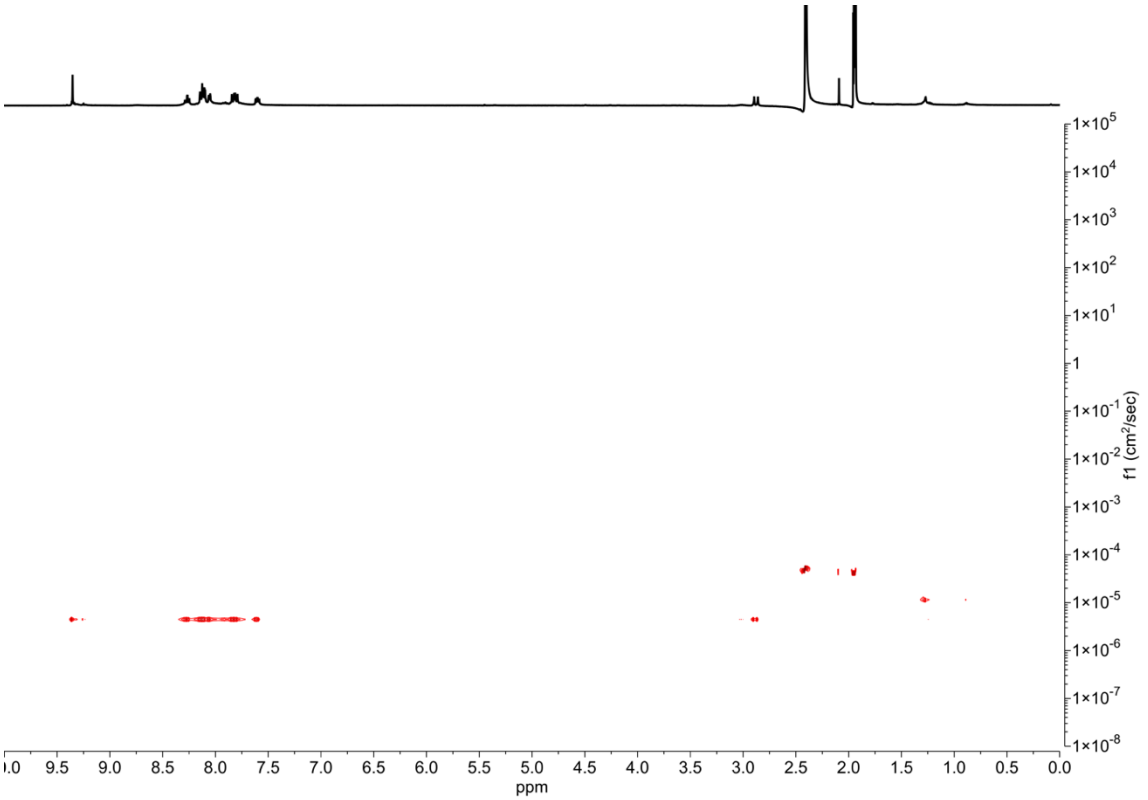

Figure S65: DOSY NMR spectrum of **4**. Diffusion coefficient: 4.42×10^{-10} m^2s^{-1}. R_H from DOSY: 14.4 Å. Calculated R_H: 12.3 Å.

Aurated Phosphine Paneled Cage **5**

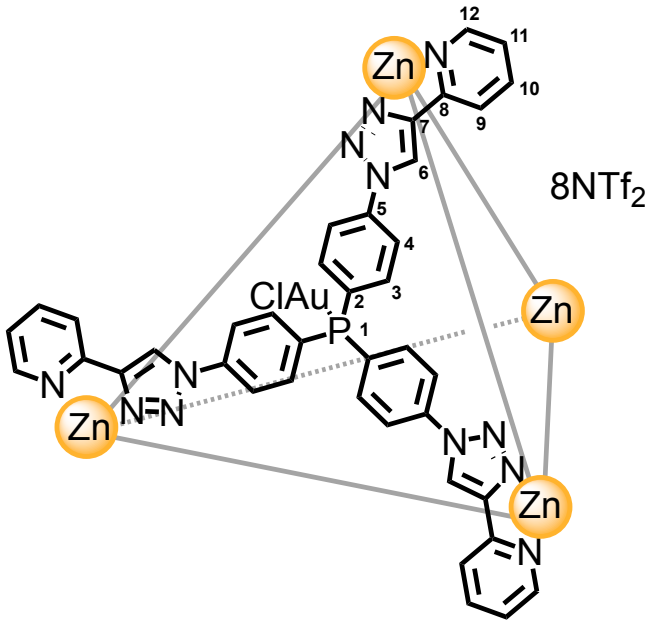

(DMS)AuCl (6.8 mg, 23.0 µmol) was added to phosphine cage **2** (3.80 mg, 2.88 µmol) in MeCN-d_3 (0.5 mL). The reaction was heated to 70 °C for 16 hours, and the precipitate formed removed by centrifugation. The filtrate was washed with benzene (5 mL) then dried under a flow of N_2. Aurated cage **5** was then used directly from the filtrate.

^{1}H NMR (500 MHz, CD_3CN) δ: 9.30 (s, 3H, H_6), 8.26 (td, *J* = 7.8, 1.3 Hz, 3H, H_{11}), 8.13 (d, *J* = 7.9 Hz, 3H, H_9), 8.02 (d, *J* = 5.2 Hz, 3H, H_{12}), 7.99 (dd, *J* = 8.9, 1.7 Hz, 6H, H_4), 7.78 (d, *J* = 13.1, 8.7 Hz, 6H, H_3), 7.59 (dd, *J* = 7.5, 5.6 Hz, 3H, H_{10}). **^{13}C NMR** (126 MHz, CD_3CN) δ: 149.3, 145.3, 144.3, 143.1, 139.7 (d, *J* = 2.4 Hz), 136.9 (d, *J* = 15.0 Hz), 130.3 (d, *J* = 62.8 Hz), 127.7, 123.8, 123.4, 121.8 (d, *J* = 12.5 Hz), 120.8 (d, *J* = 320.1 Hz). **^{31}P NMR** (162 MHz, CD_3CN) *δ*: 32.0. **^{19}F NMR** (376 MHz, CD_3CN) *δ*: − 81.1.

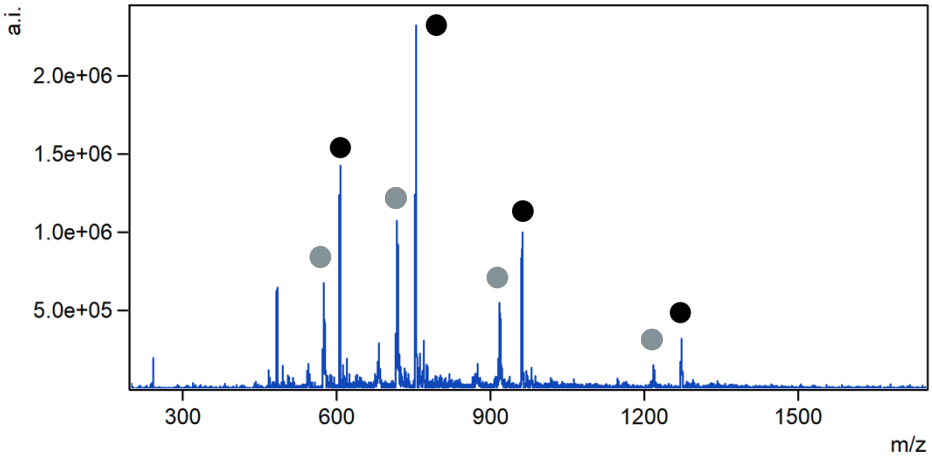

Figure S66: LRMS spectrum of **5**. Light grey represents Cages having lost a single AuCl unit.

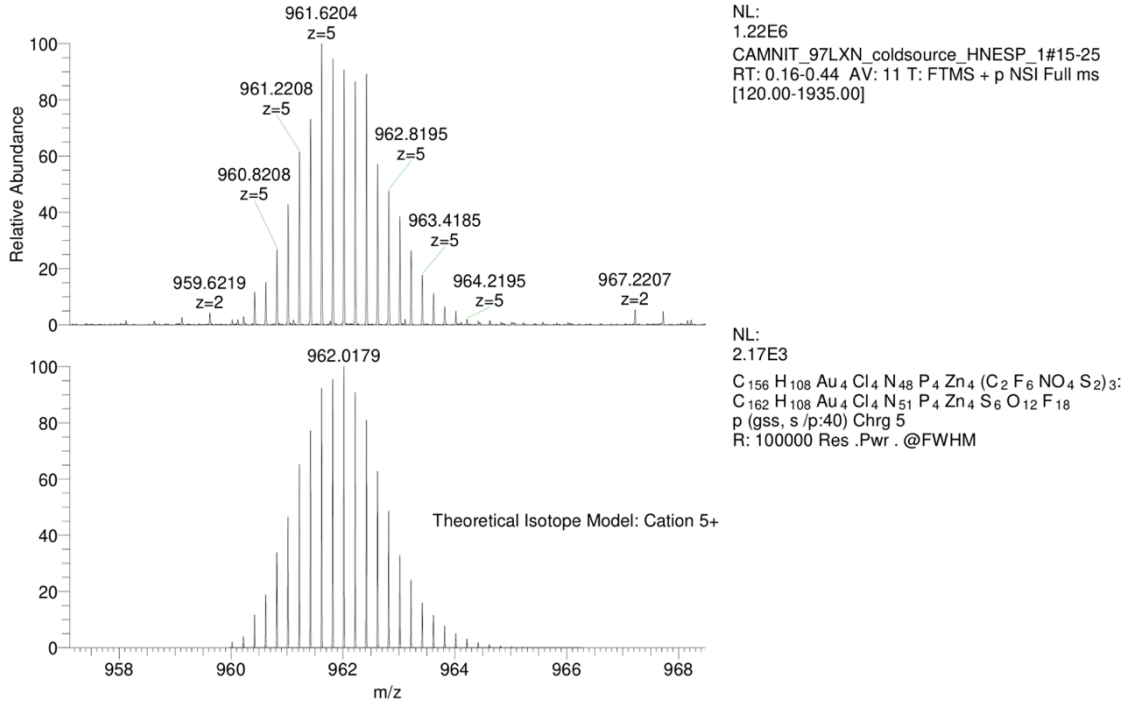

Figure S67: HRMS spectrum of **5**, 5+ cation.

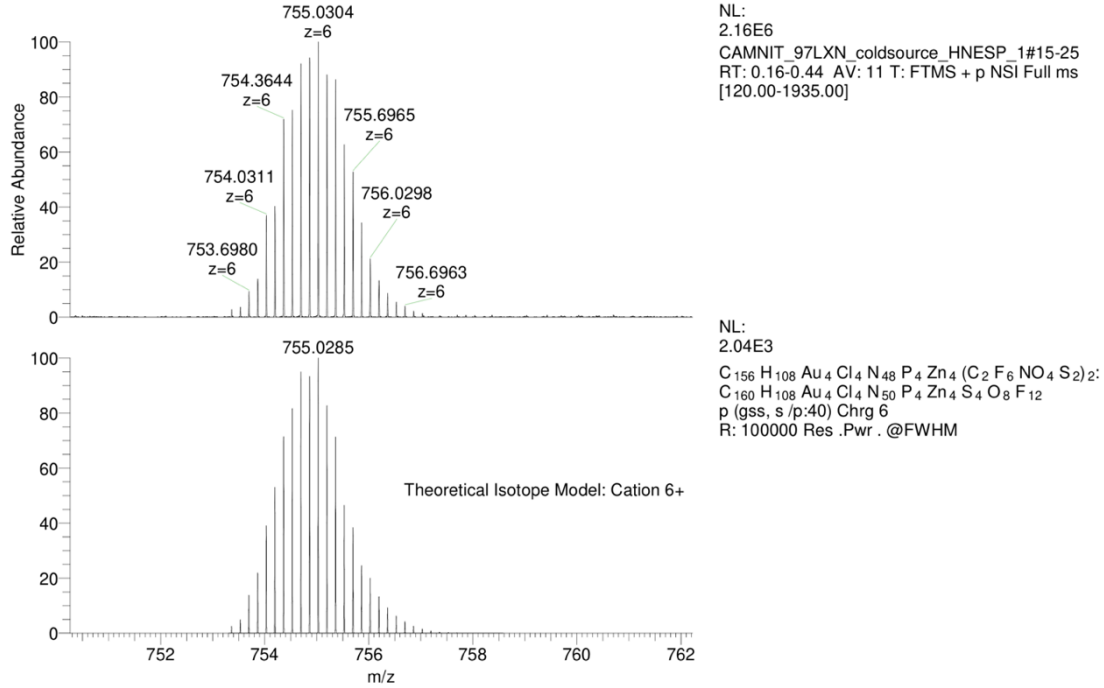

Figure S68: HRMS spectrum of **5**, 6+ cation.

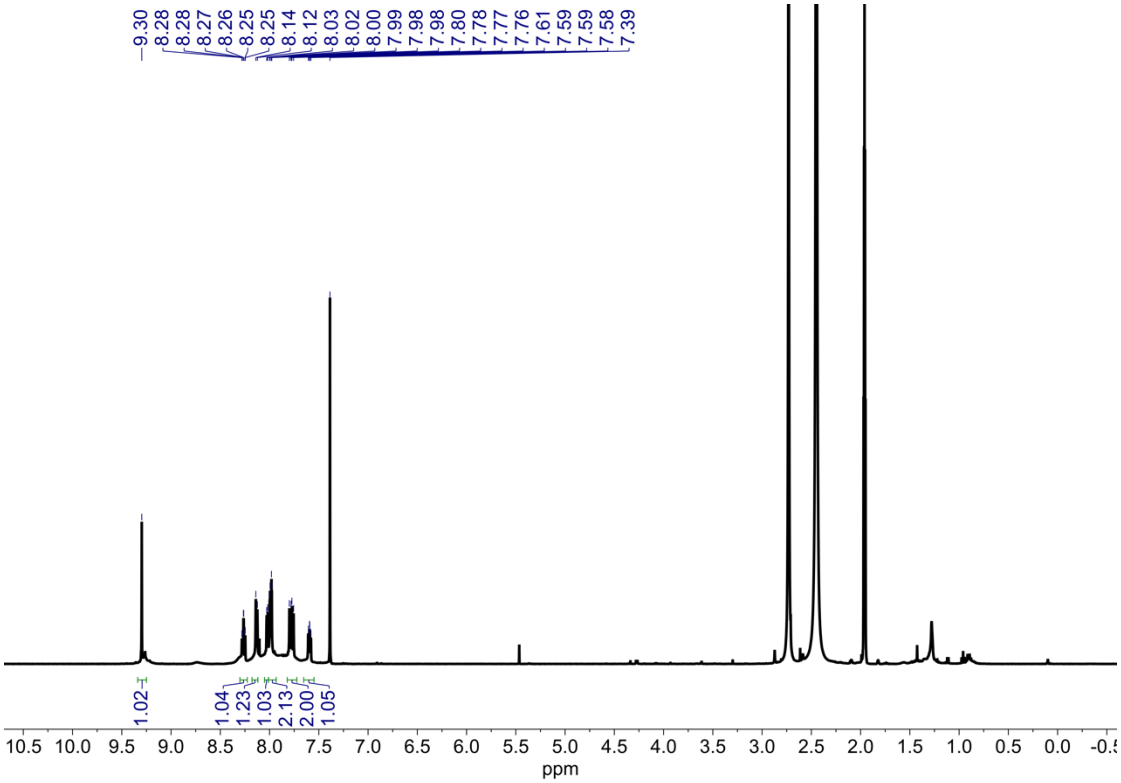

Figure S69: ^{1}H NMR (CD_3CN, 500 MHz, 298 K) spectrum of **5**.

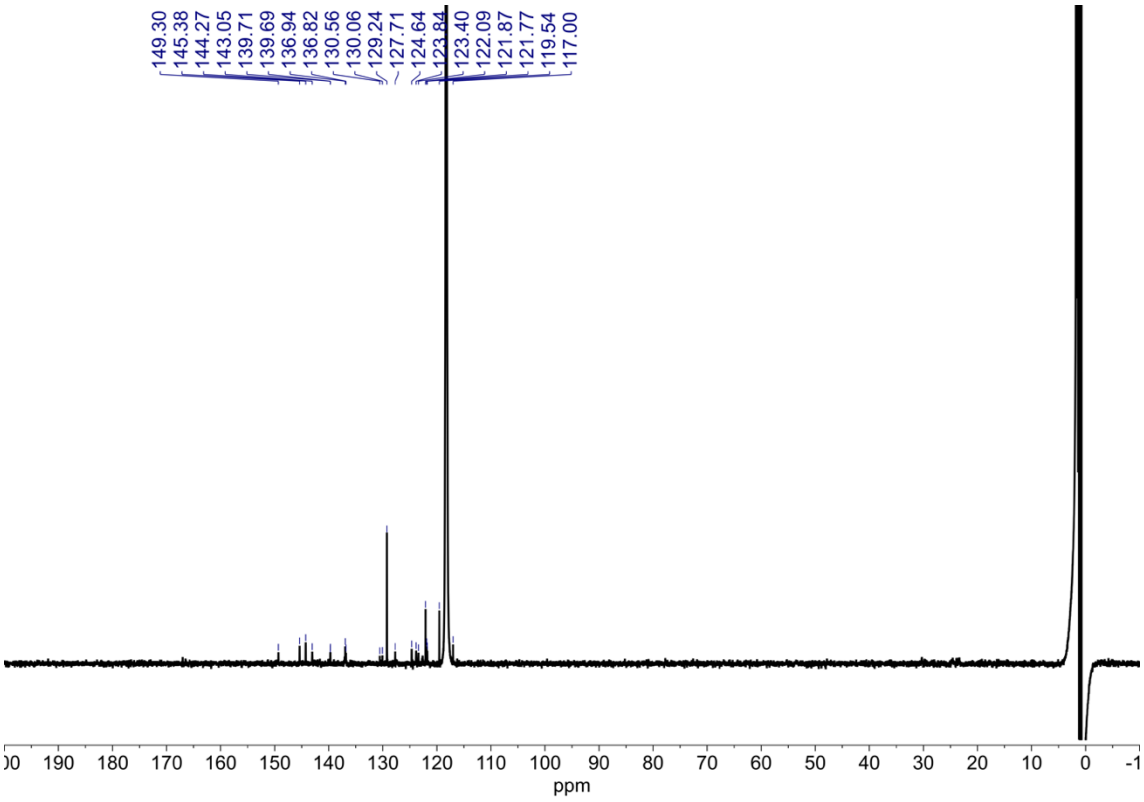

Figure S70: ^{13}C NMR (CD_3CN, 126 MHz, 298 K) spectrum of **5**.

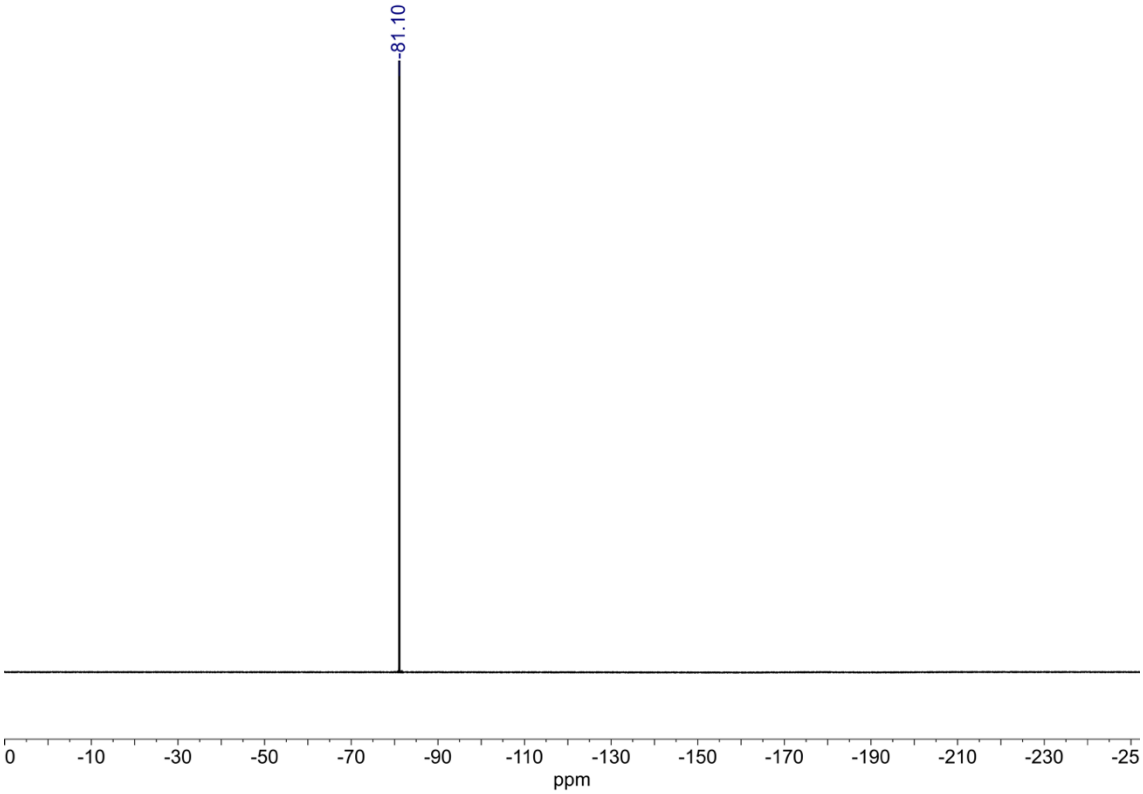

Figure S71: ^{19}F NMR (CD_3CN, 376 MHz, 298 K) spectrum of **5**.

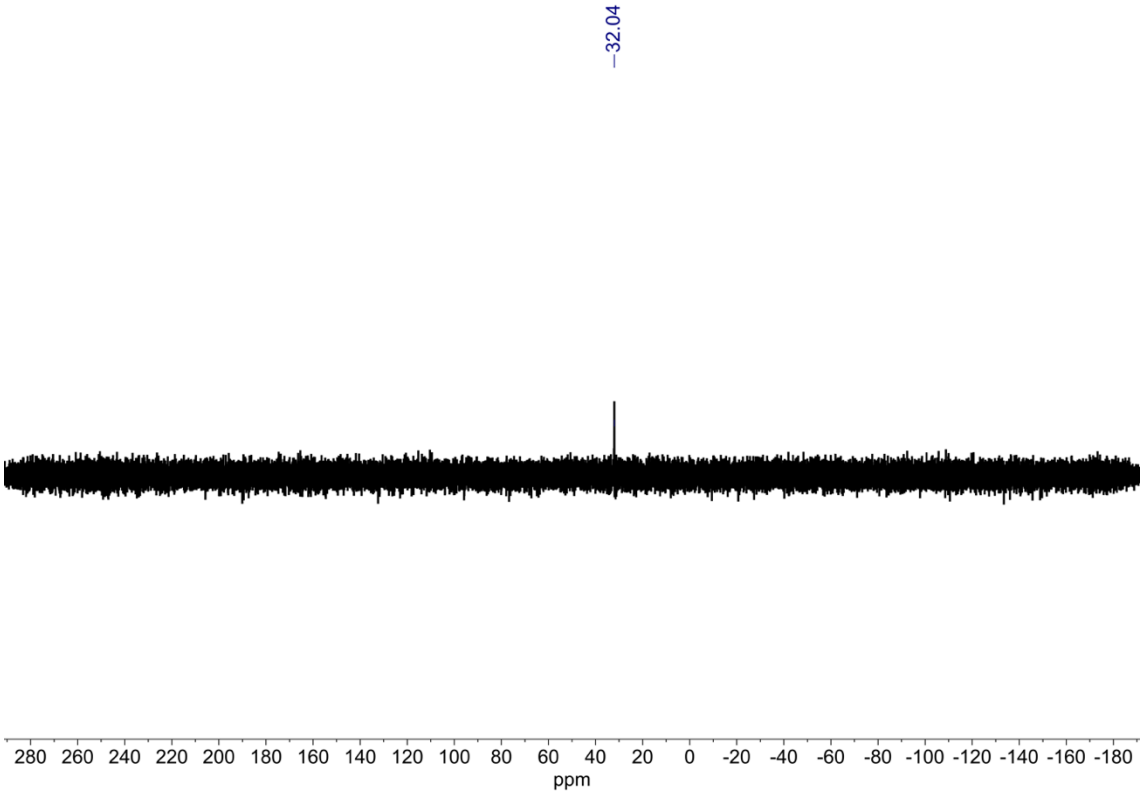

Figure S72: ^{31}P NMR (CD_3CN, 162 MHz, 298 K) spectrum of **5**.

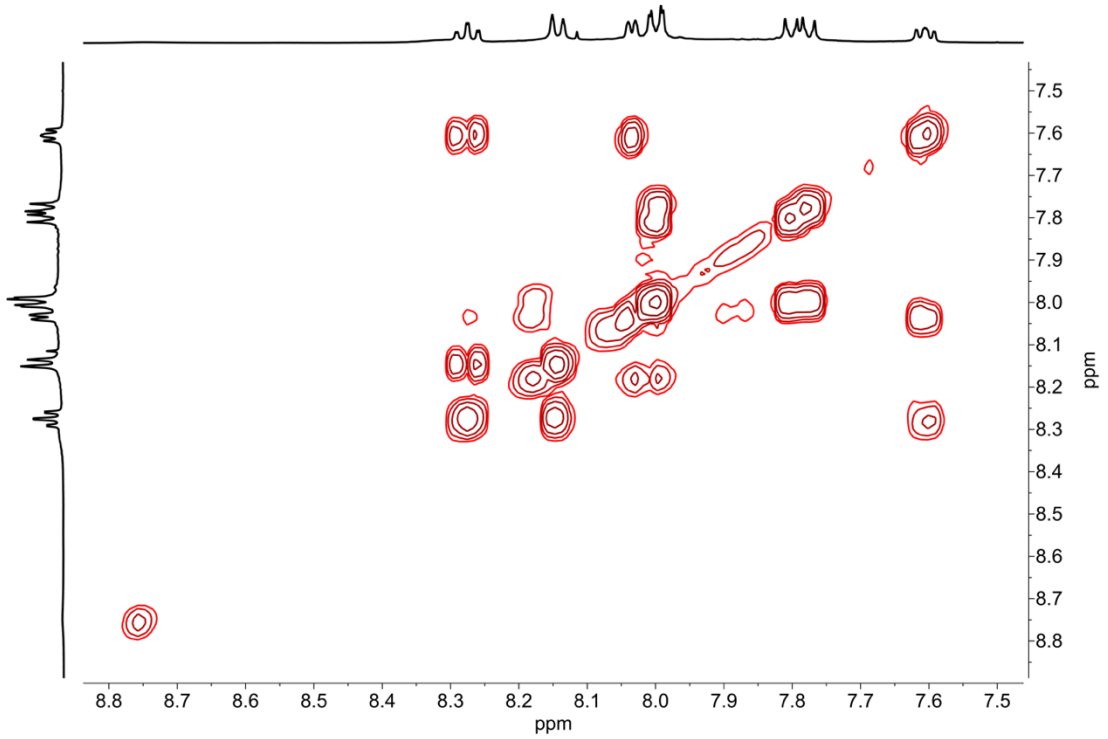

Figure S73: Partial COSY NMR spectrum of **5**.

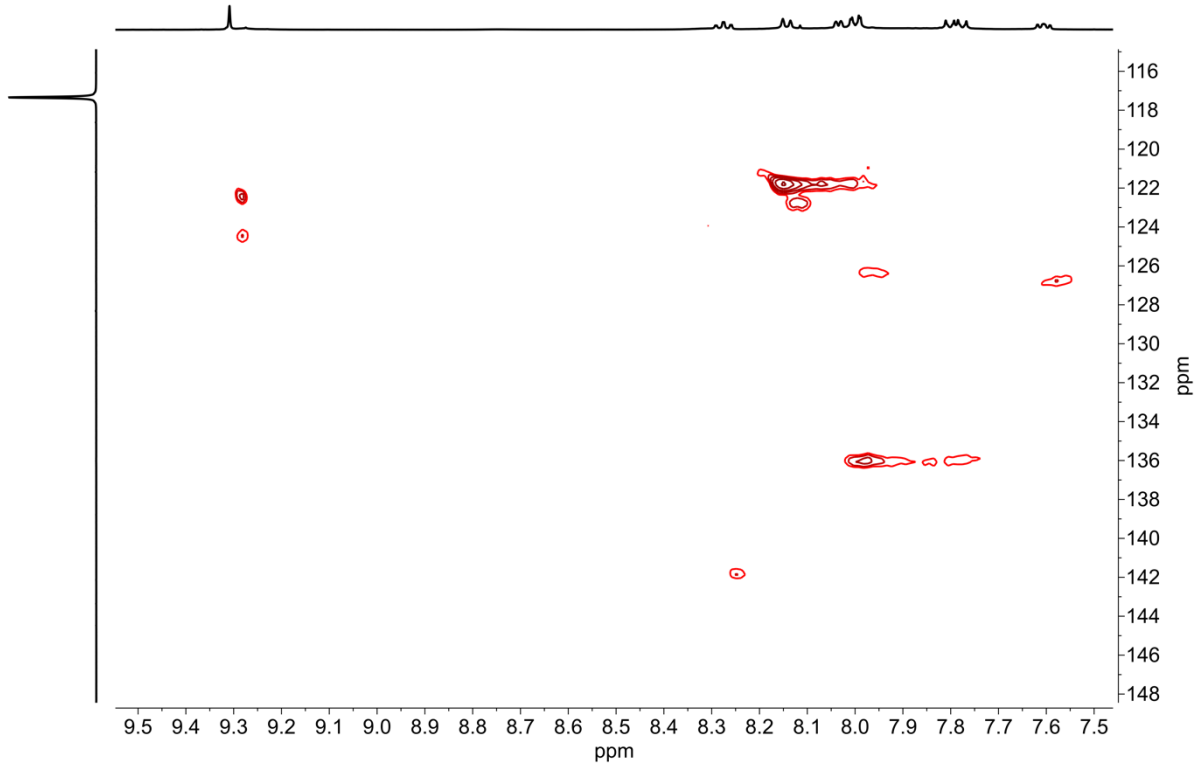

Figure S74: Partial HSQC NMR spectrum of **5**.

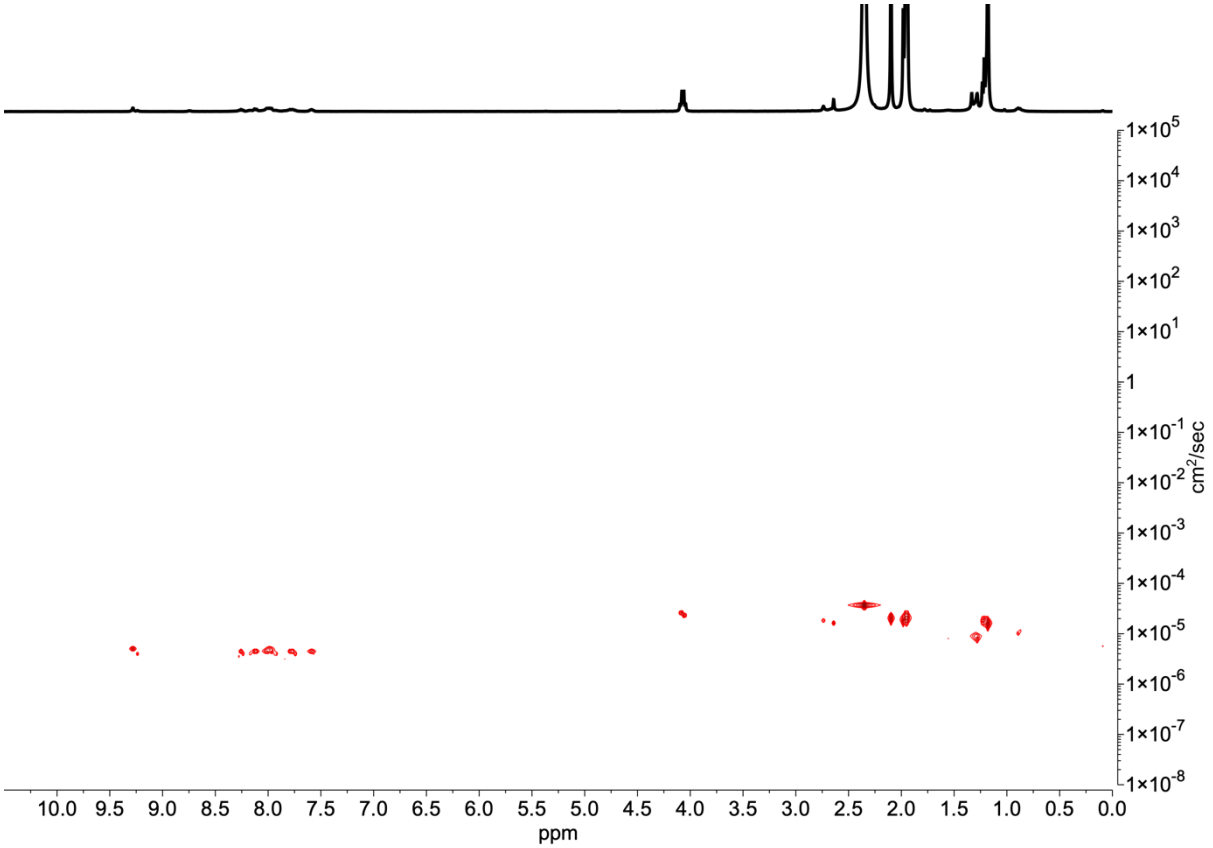

Figure S75: DOSY NMR spectrum of **5**. Diffusion coefficient: 4.58×10^{-10} m^2s^{-1}. R_H from DOSY: 13.9 Å. Calculated R_H: 13.6 Å.

Sandwich Complex **8** and Phosphine Cage **9** formed from $Ni(NTf_2)_2$ with **1**

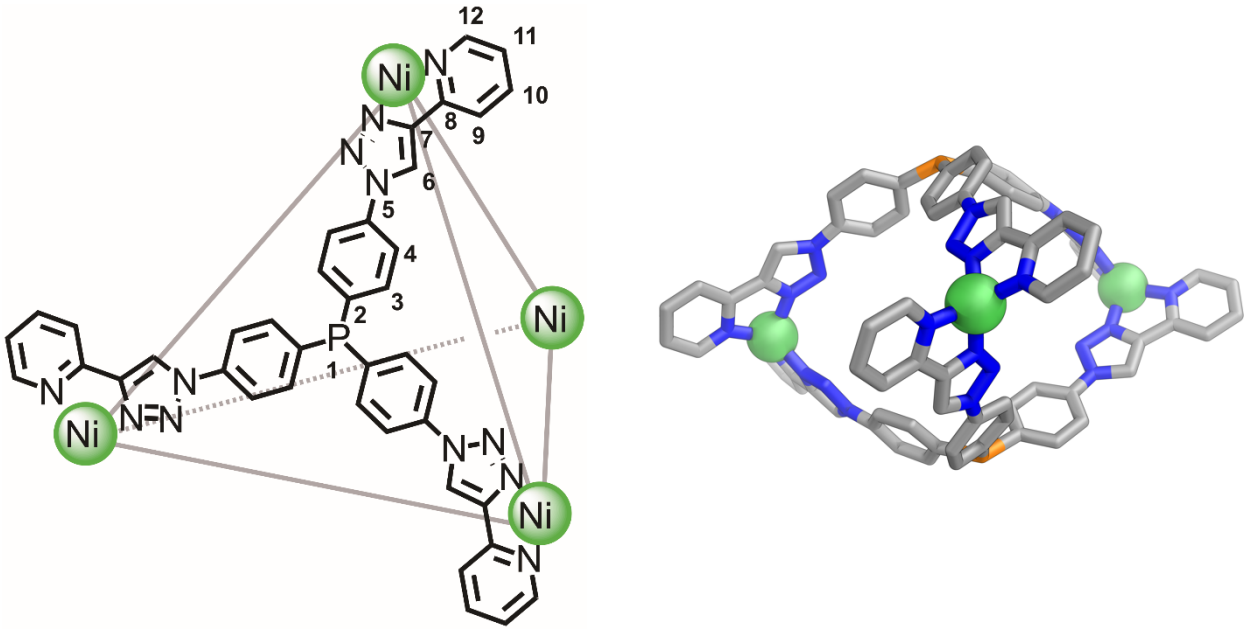

Phosphine ligand **1** (2.0 mg, 2.88 µmol) was dissolved in MeCN-d_3 (0.5 mL). $Ni(NTf_2)_2$ (1.78 mg, 2.88 µmol) was added and the reaction heated to 70 °C for 1 hour. The formed cage system was used as synthesised. Sandwich complex shown above is a MM3 optimised molecular model, please see the main text for a discussion the proposed tetrahedral geometry of the nickel centre.

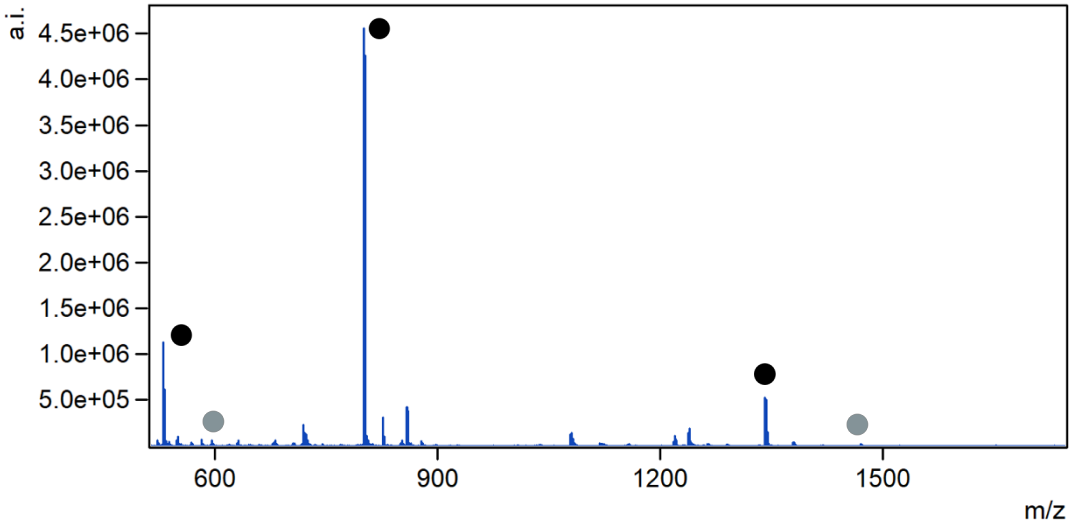

Figure S76: LRMS of complexes formed from $Ni(NTf_2)_2$ and phosphine ligand **1**. Peaks correlating with sandwich complex **8** marked in black, trace peaks for cage **9** marked in grey.

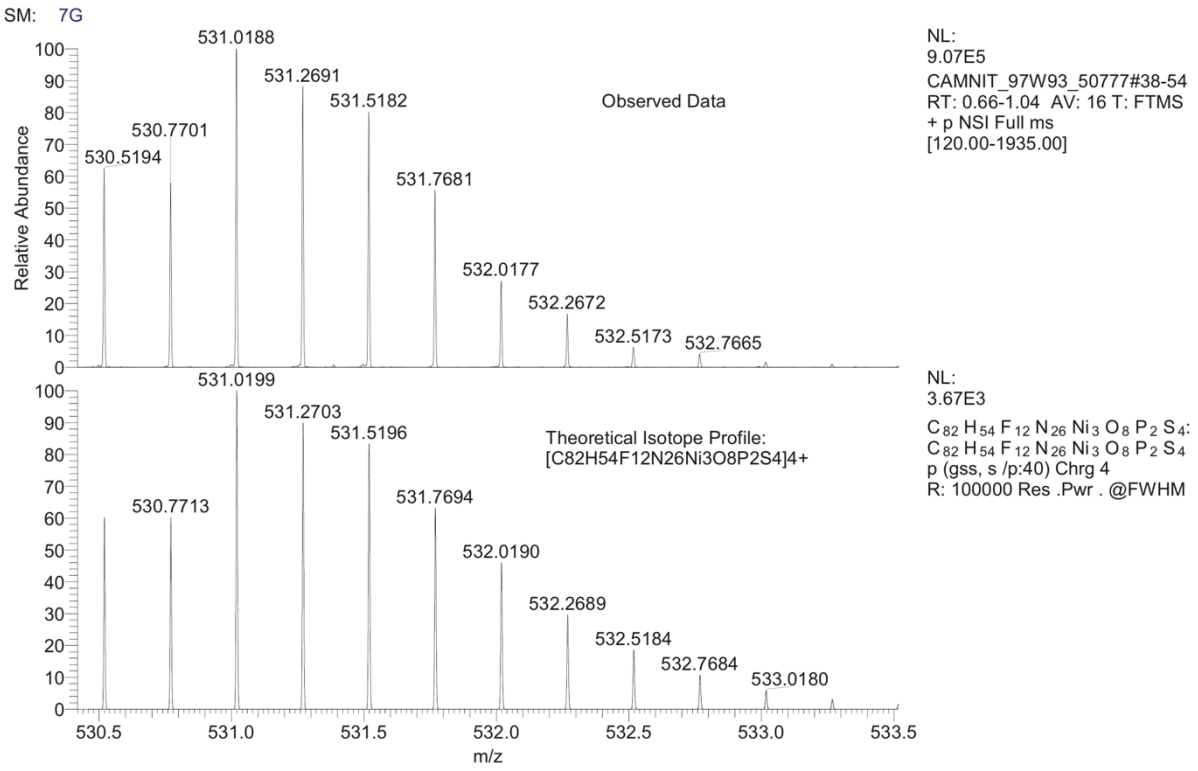

Figure S77: HRMS of sandwich complex **8**.

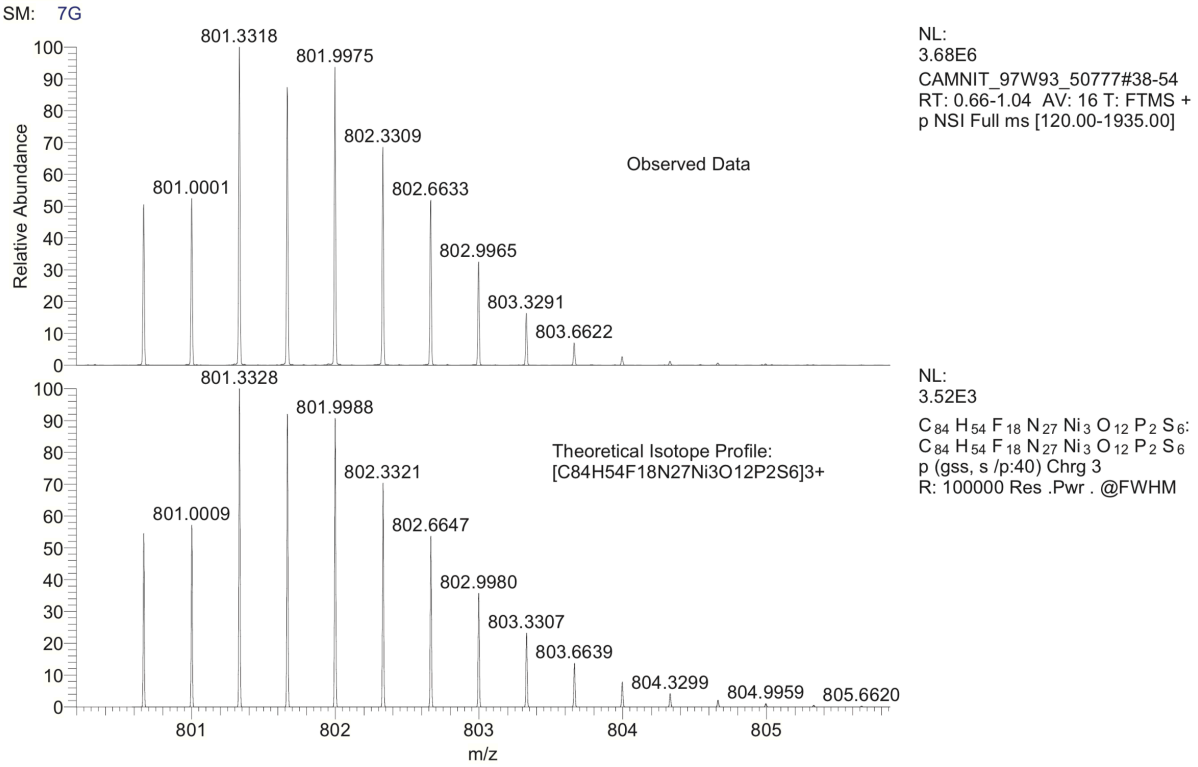

Figure S78: HRMS of sandwich complex **8**.

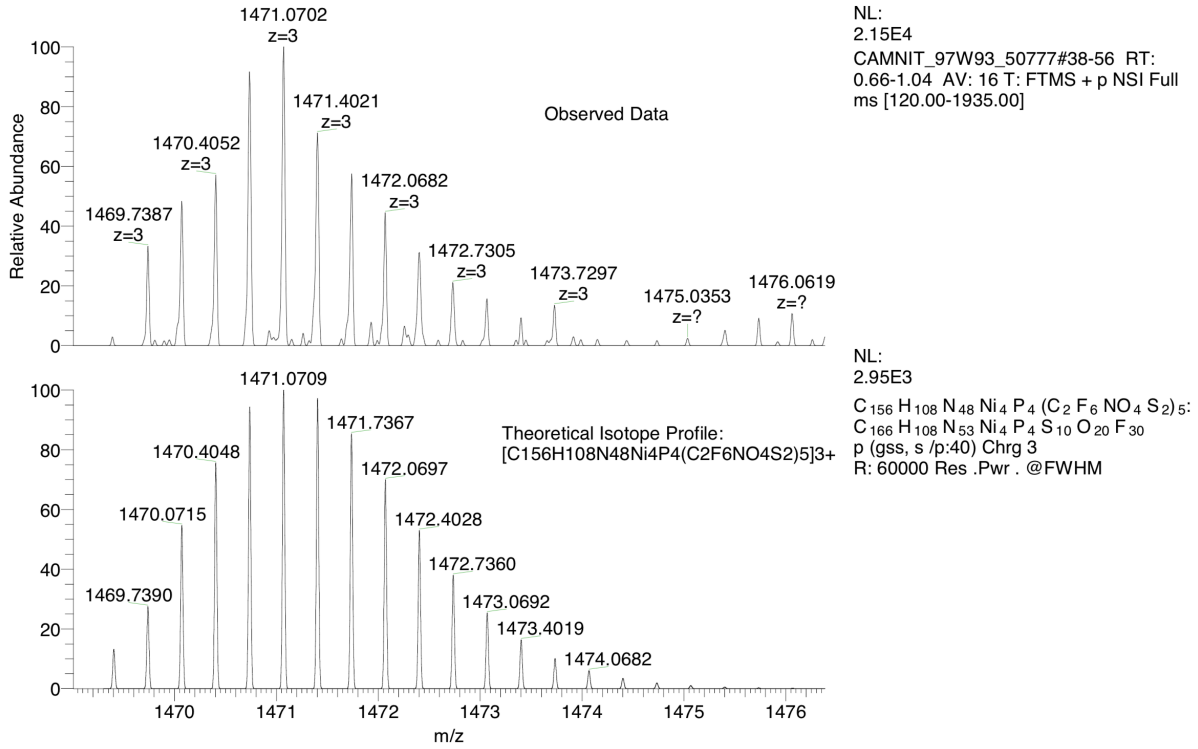

Figure S79: HRMS of cage **9**.

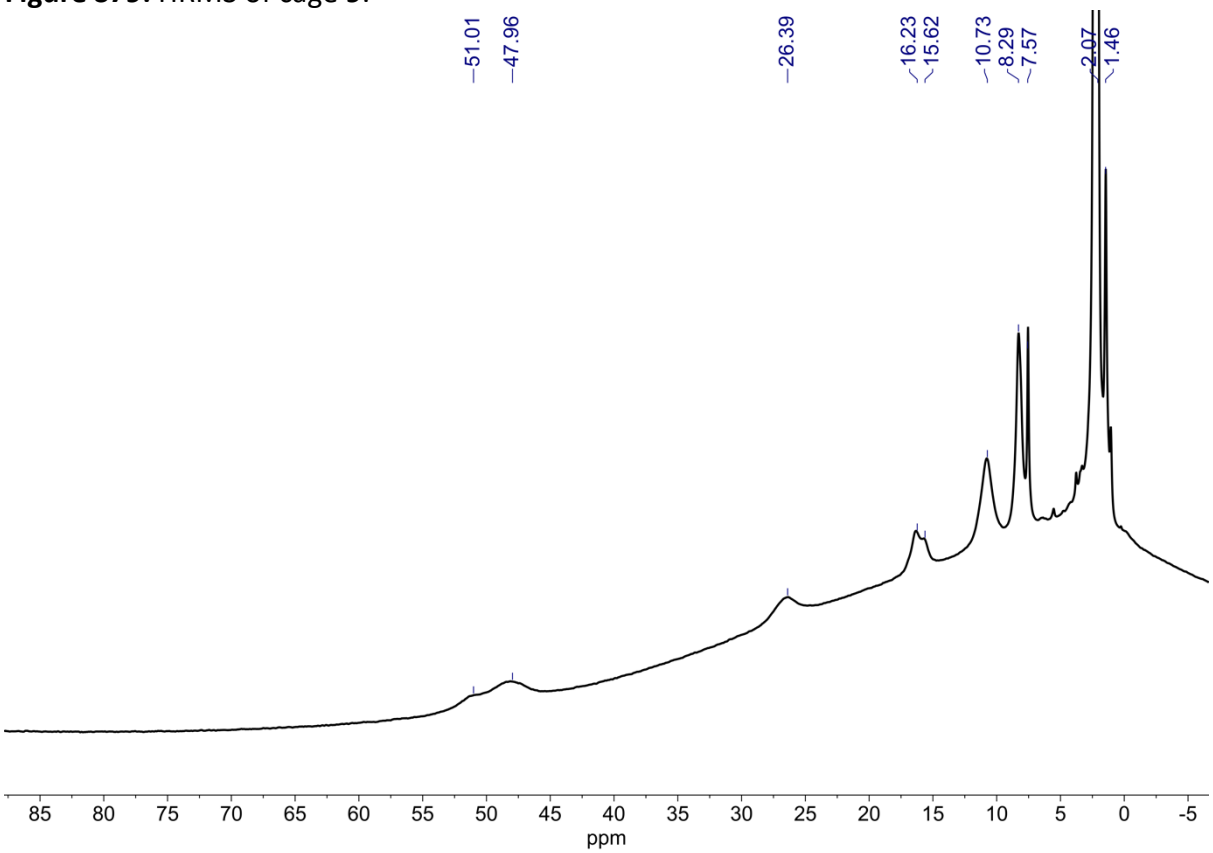

Figure S80: ^{1}H NMR (CD_3CN, 500 MHz, 298 K) of sandwich complex **8** and cage **9**.

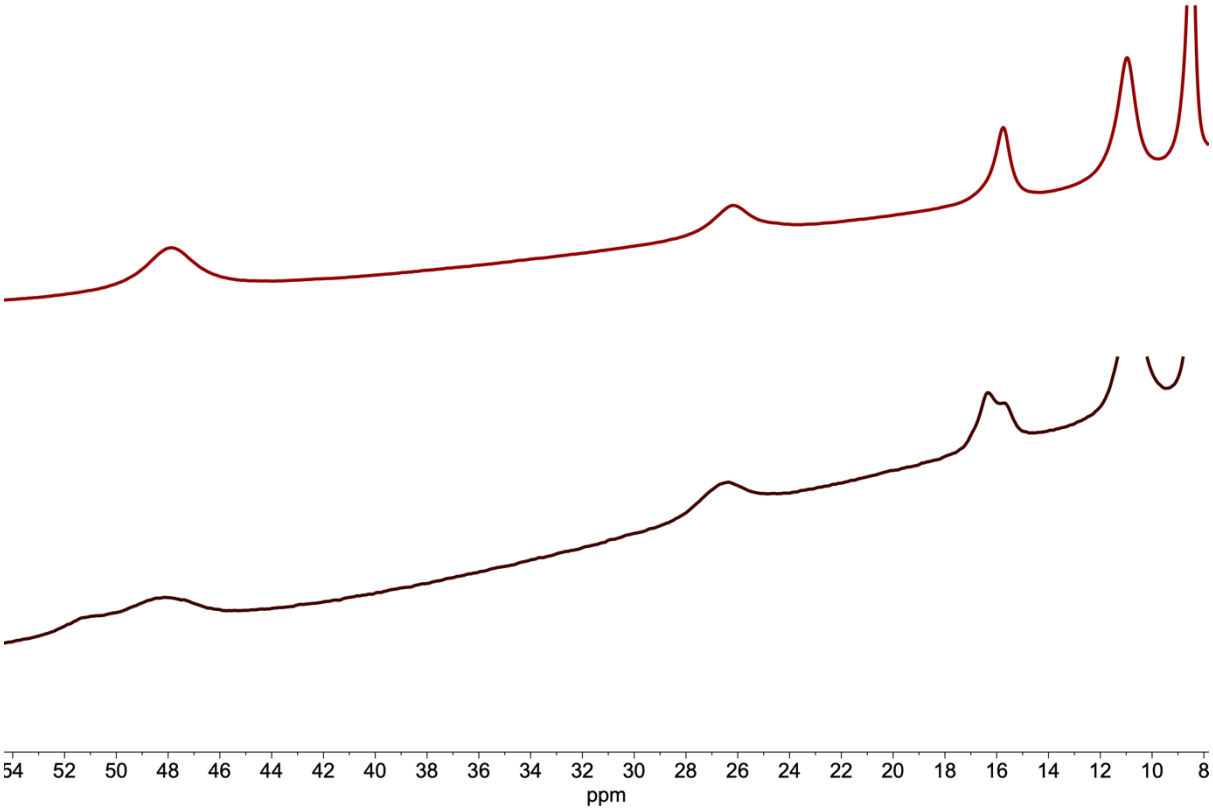

Figure S81: ^{1}H NMR (CD_3CN, 500 MHz, 298 K) stack of sandwich complex **8** and cage **9** (bottom) and phosphine oxide cage **10**. Note the splitting of peaks around 16 ppm and 48 ppm, lending support the MS evidence for two architectures being present.

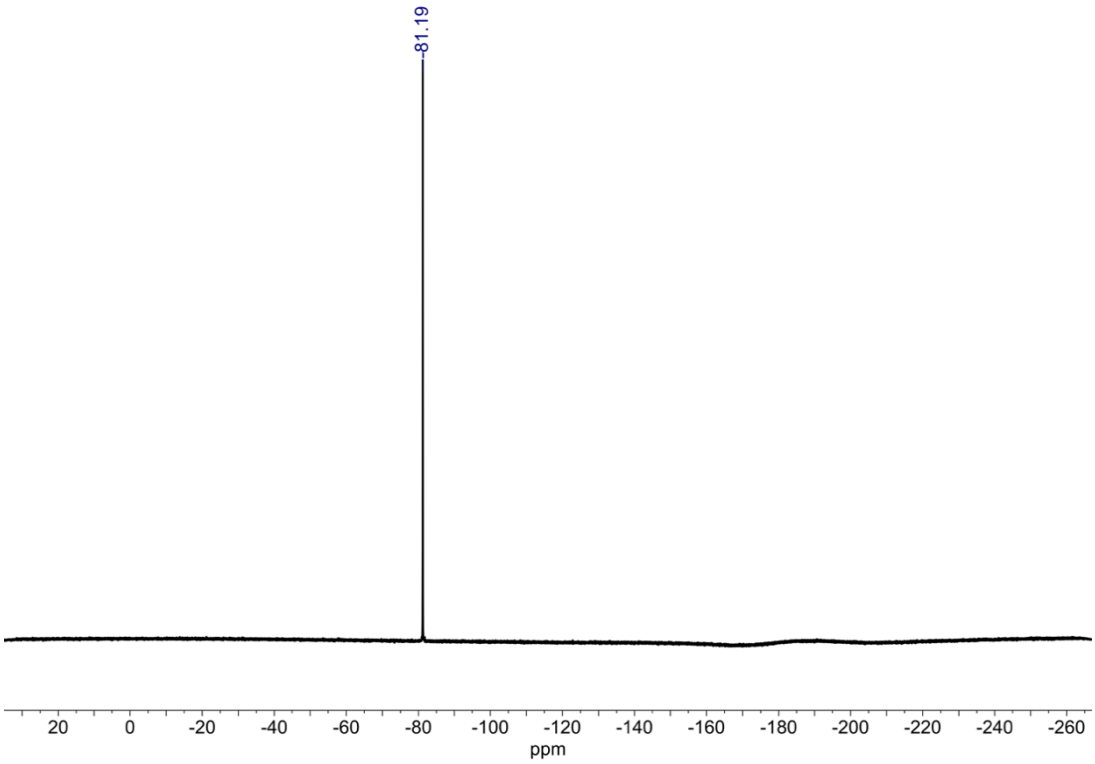

Figure S82: ^{19}F NMR (CD_3CN, 376 MHz, 298 K) of sandwich complex **8** and cage **9**.

Phosphine Oxide Cage formed from $Ni(NTf_2)_2$ **10**

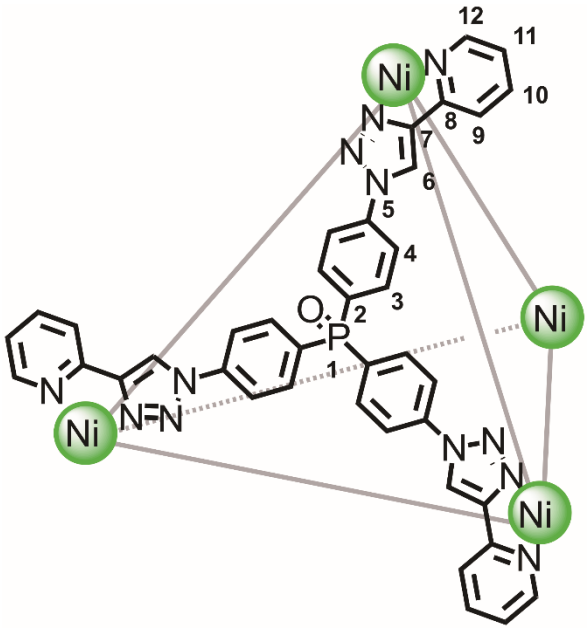

Phosphine oxide ligand **S1** (2.0 mg, 2.82 µmol) was dissolved in MeCN-d_3 (0.5 mL). $Ni(NTf_2)_2$ (1.75 mg, 2.82 µmol) was added and the reaction heated to 70 °C for 1 hour. The formed cage was used as synthesised.

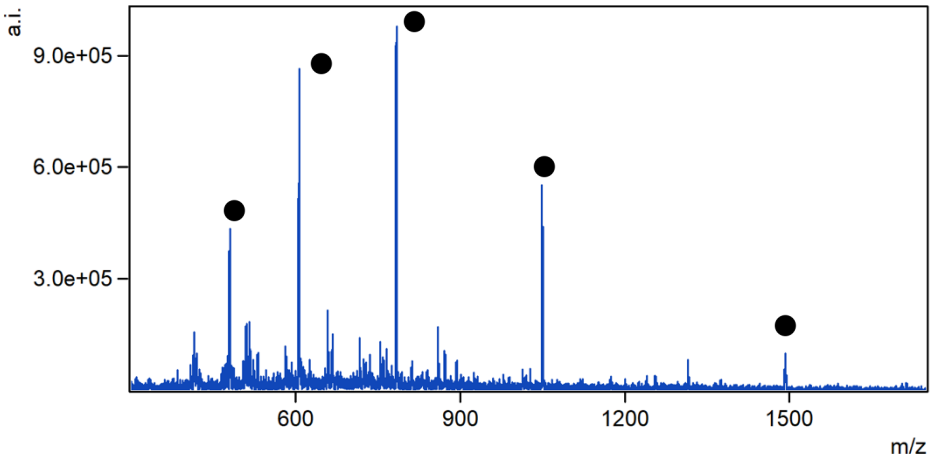

Figure S83: LRMS spectrum of **10**.

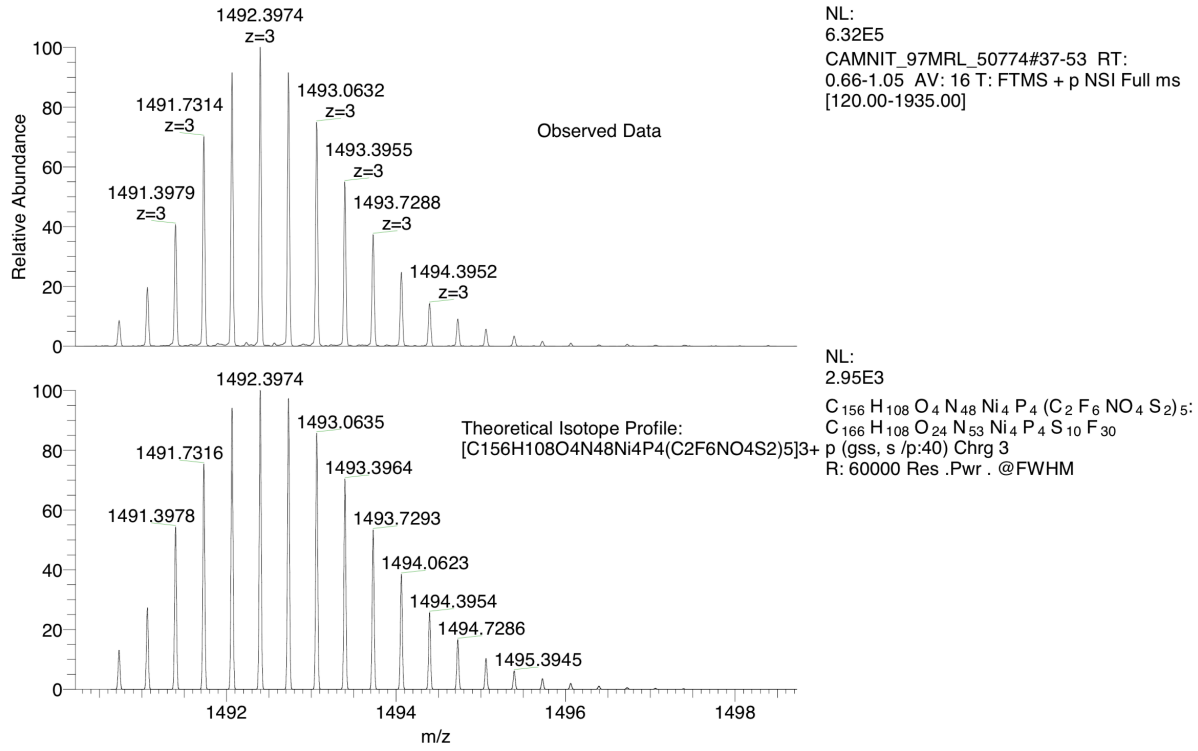

Figure S84: HRMS spectrum of **10**.

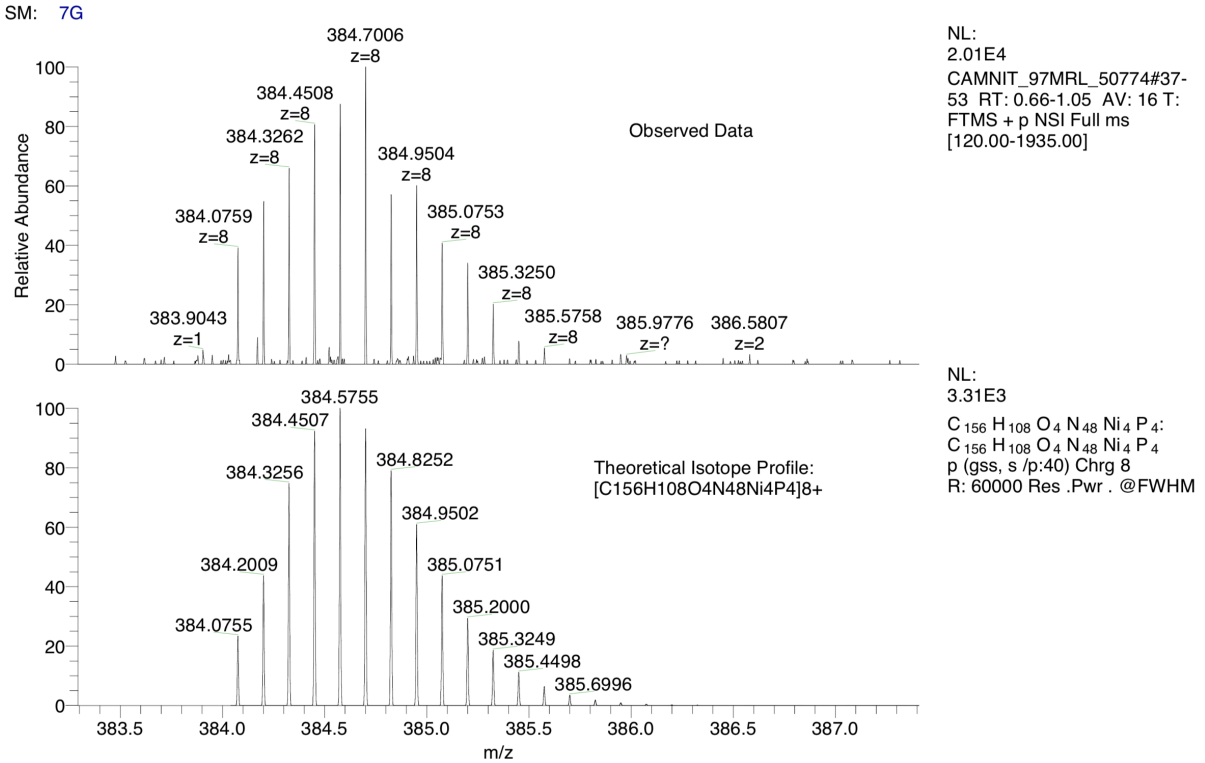

Figure S85: HRMS spectrum of **10**.

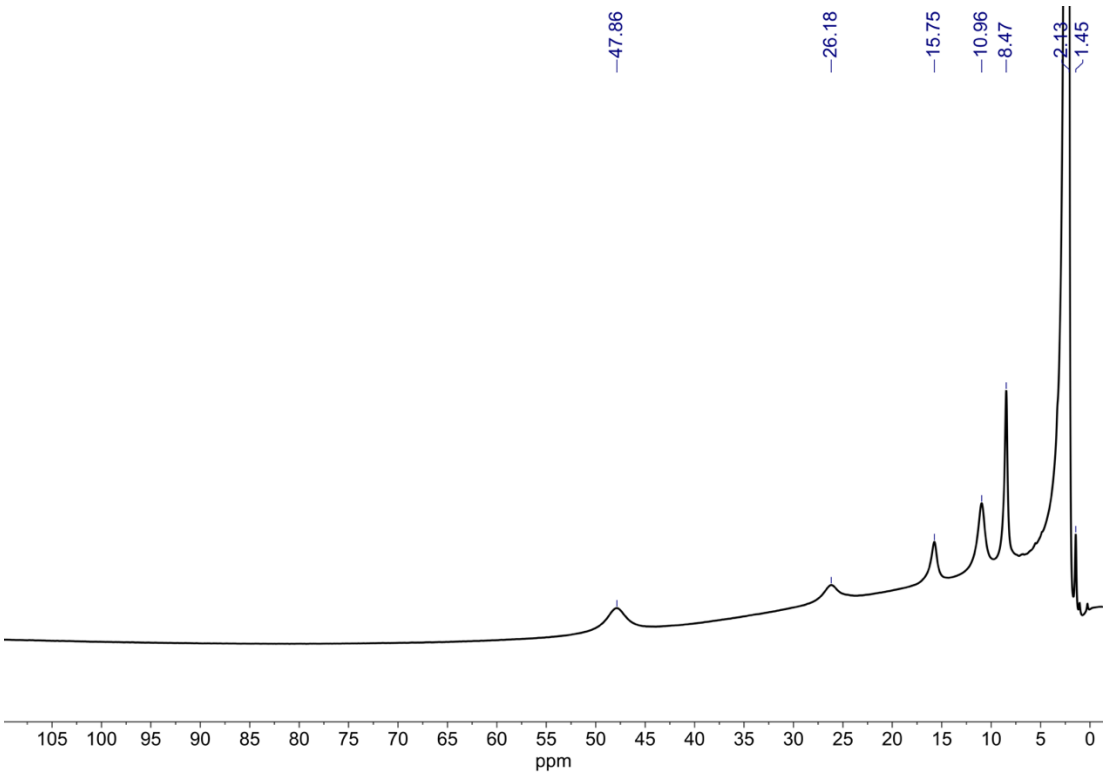

Figure S86: ^{1}H NMR (CD_3CN, 500 MHz, 298 K) of Cage **10**.

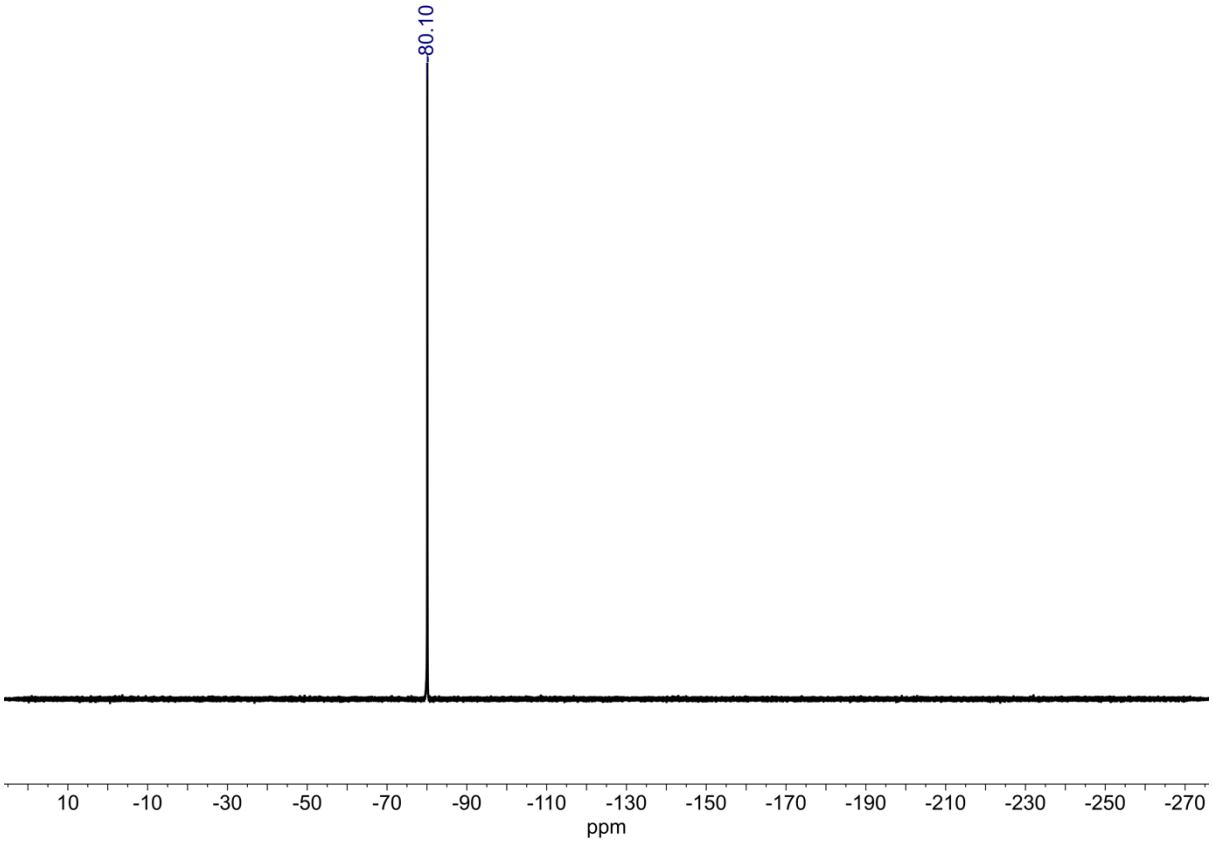

Figure S87: ^{19}F NMR (CD_3CN, 376 MHz, 298 K) of Cage **10**.

Phosphonium Salt Cage formed from $Ni(NTf_2)_2$ **12**

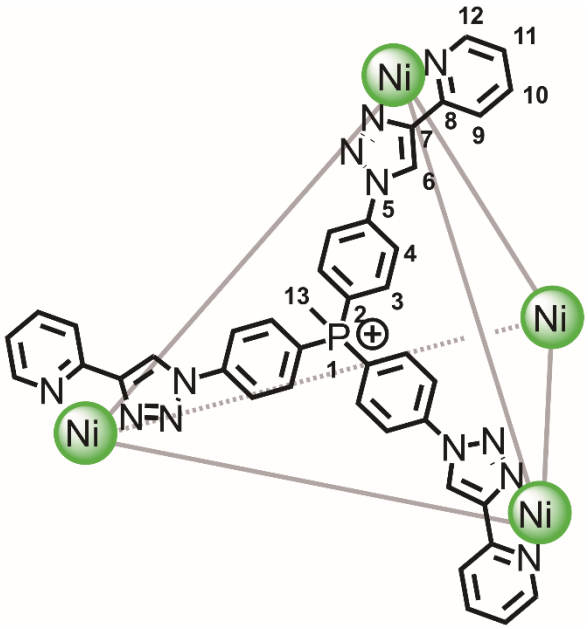

Phosphonium salt ligand **S4** (2.0 mg, 2.02 µmol) was dissolved in MeCN-d_3 (0.5 mL). $Ni(NTf_2)_2$ (1.25 mg, 2.02 µmol) was added and the reaction heated to 70 °C for 1 hour. The formed cage was used as synthesised.

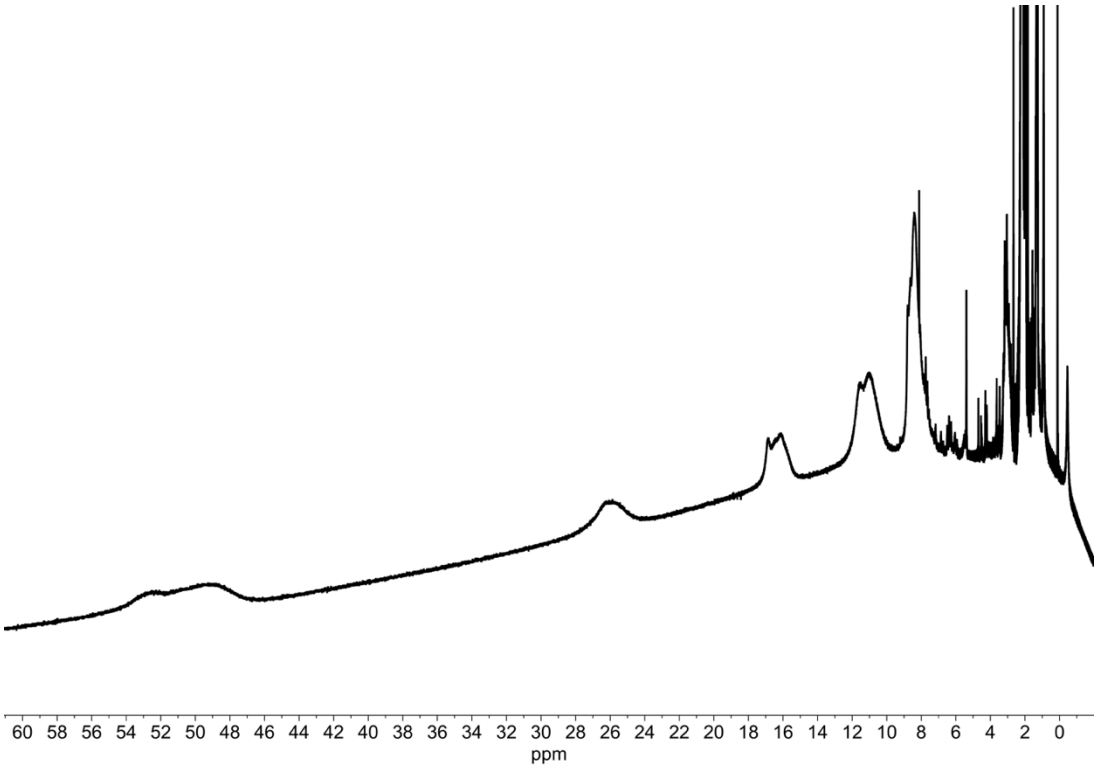

Figure S88: ^1H (CD_3CN, 500 MHz, 298 K) spectrum of **12**.

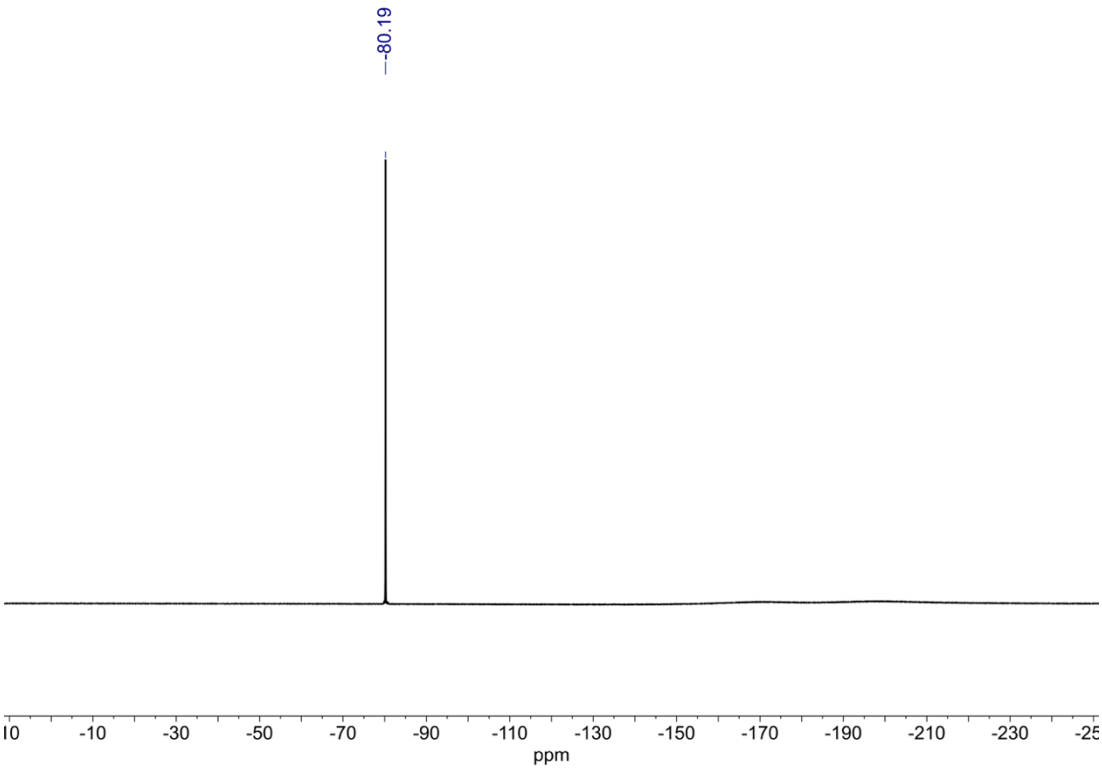

Figure S89: ^{19}F NMR (CD_3CN, 376 MHz, 298 K) spectrum of **12**.

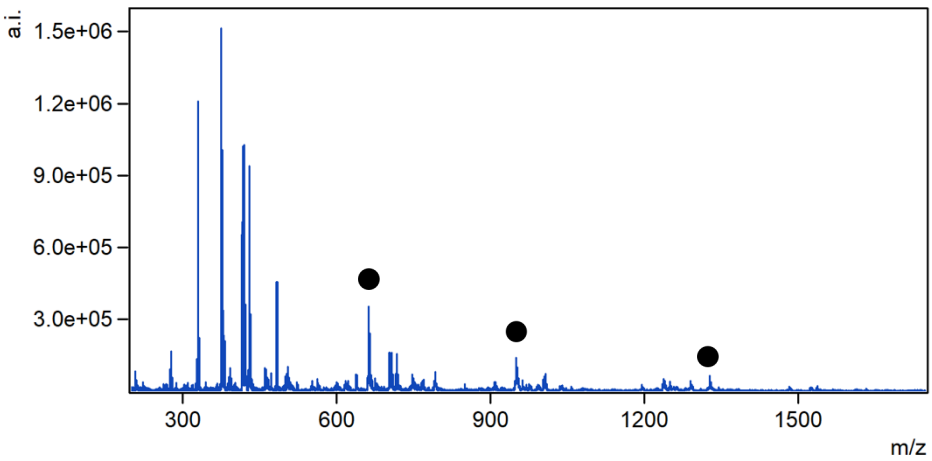

Figure S90: LRMS spectrum of **12**. Black dots denote relevant peaks. Soft ionisation conditions were required with all phosphonium salt cages, and extensive decomposition was still observed under the best conditions found. Presumably this is due to increased repulsion between phosphonium salts decreasing stability.

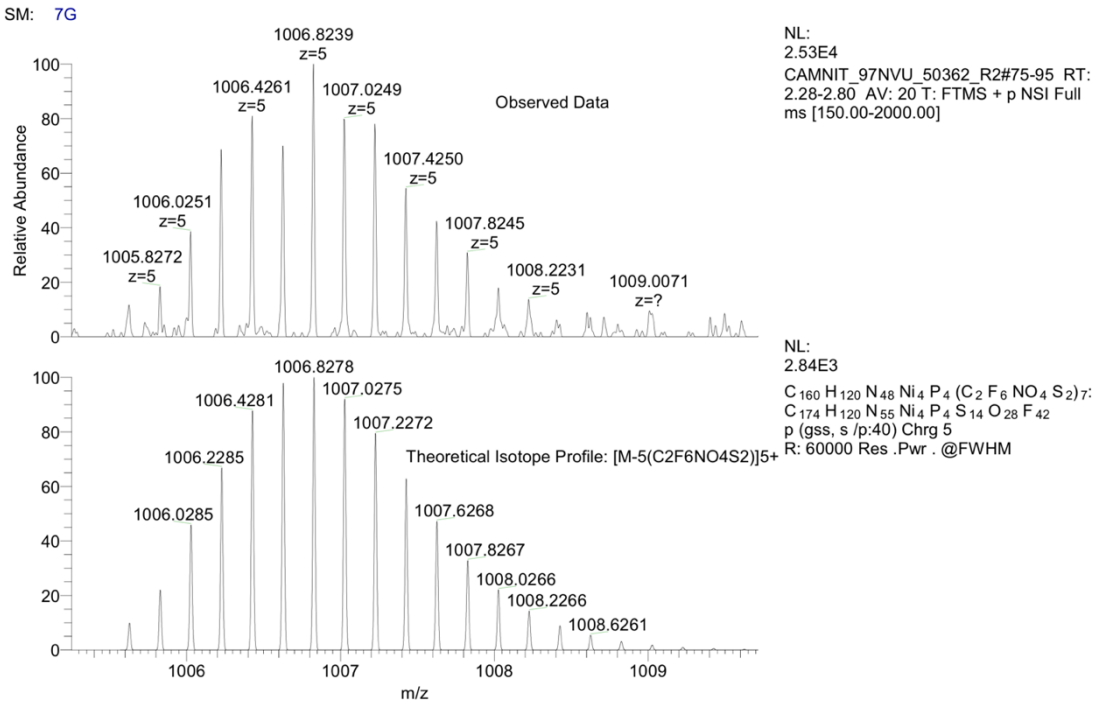

Figure S91: HRMS spectrum of **12**.

Further evidence for this structure was provided by the crystal structure obtained (*vide infra*).

Phosphine Cage formed from $Fe(NTf_2)_2$ **6**

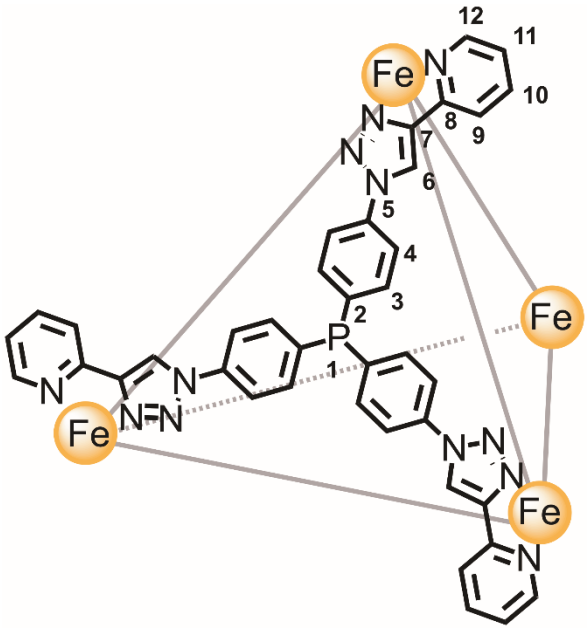

Phosphine ligand **2** (2.0 mg, 2.88 µmol) was dissolved in thoroughly sparged MeCN-d_3 (0.5 mL). $Fe(NTf_2)_2$ (1.78 mg, 2.88 µmol) was added and the reaction heated to 70 °C for 1 hour, under N_2. The formed cage was used as synthesised.

^{1}H NMR (500 MHz, CD_3CN) δ: 9.23 (s, 3H, H_6), 8.16 (t, J = 7.4 Hz, 3H, H_{11}), 8.10 (d, J = 7.3 Hz, 3H, H_9), 7.73–7.67 (9H, m, H_{12} + H_4), 7.43–7.38 (9H, m, H_{10} + H_3). **^{13}C NMR:** Line broadening prevented acquisition of a ^{13}C NMR spectrum for this compound. **^{31}P NMR** (162 MHz, CD_3CN) δ: − 5.65. **^{19}F NMR** (376 MHz, CD_3CN) δ: − 81.2.

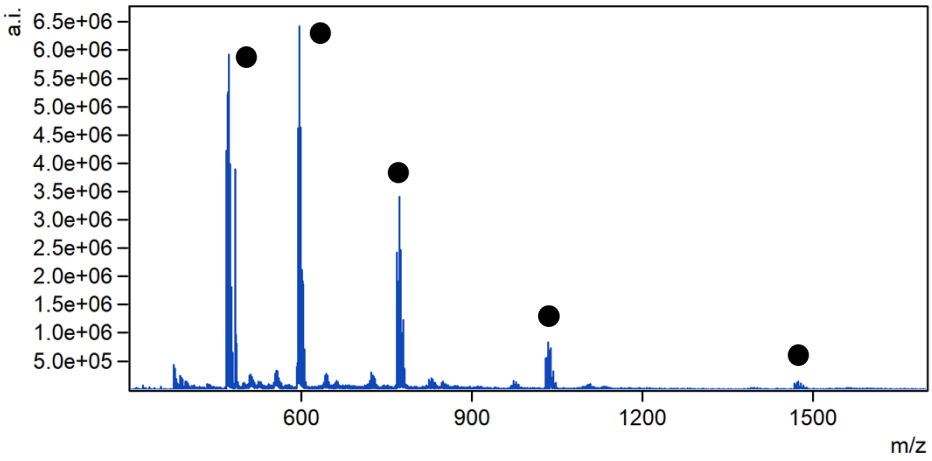

Figure S92: LRMS spectrum of **6** (showing *in situ* oxidation within the MS - cage with 0-4 oxygen atoms).

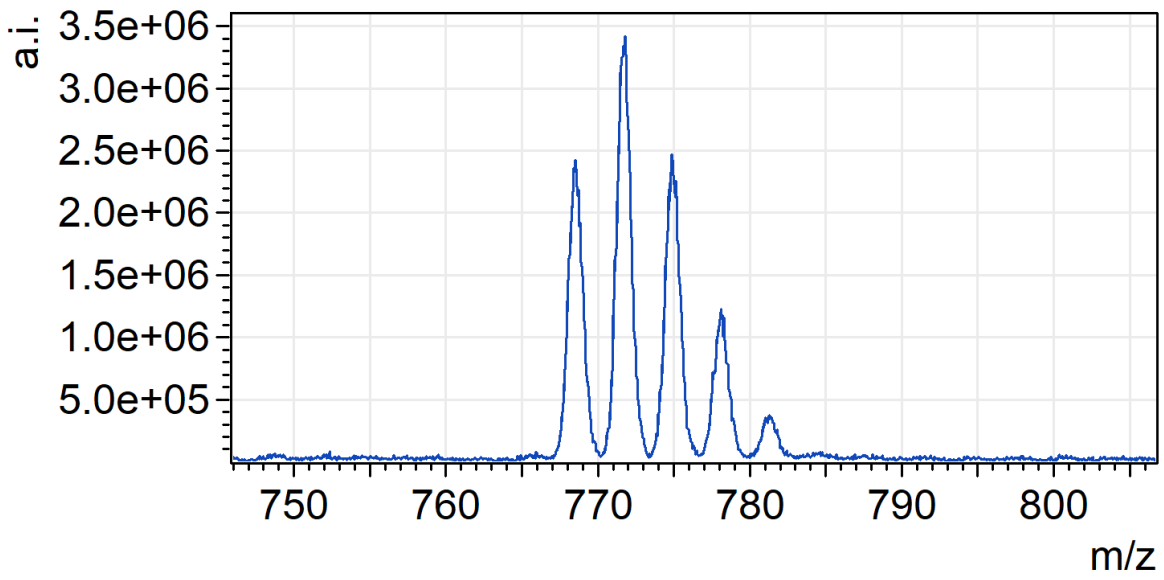

Figure S93: Expansion of LRMS spectrum of **6** showing *in situ* oxidation within the MS (cage + 0-4 oxygen atoms).

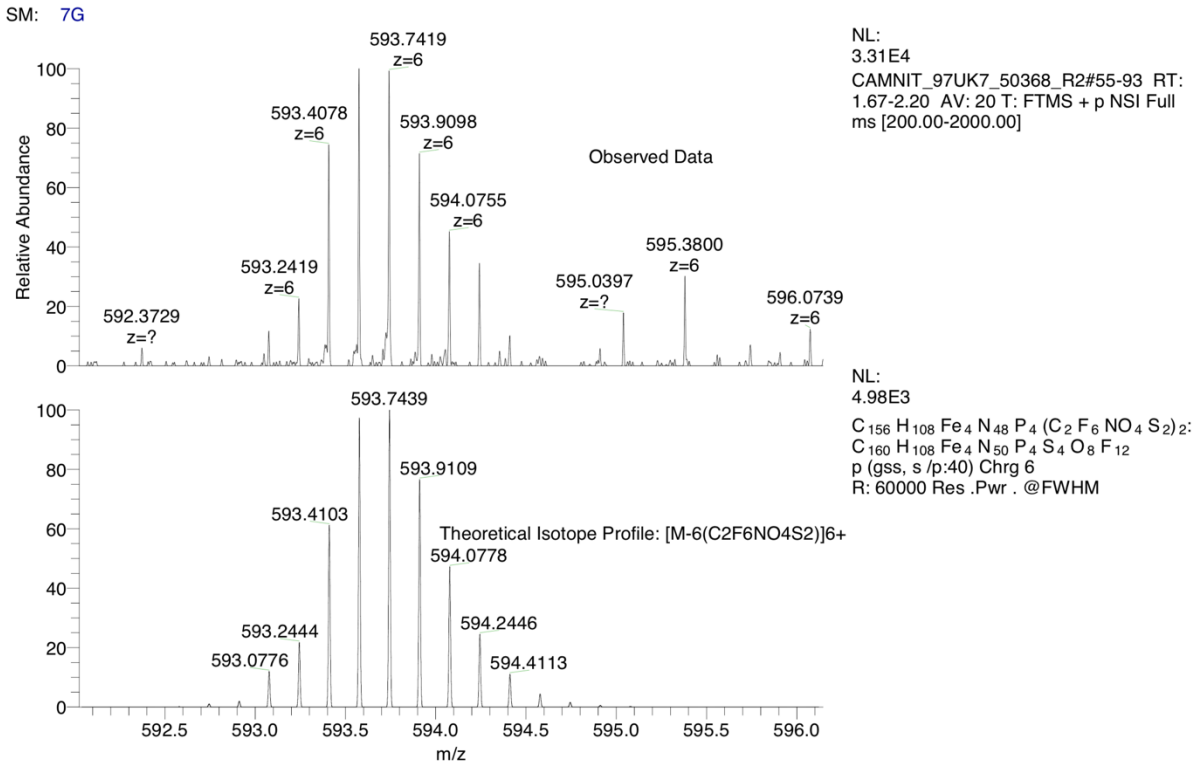

Figure S94: HRMS spectrum of **6**.

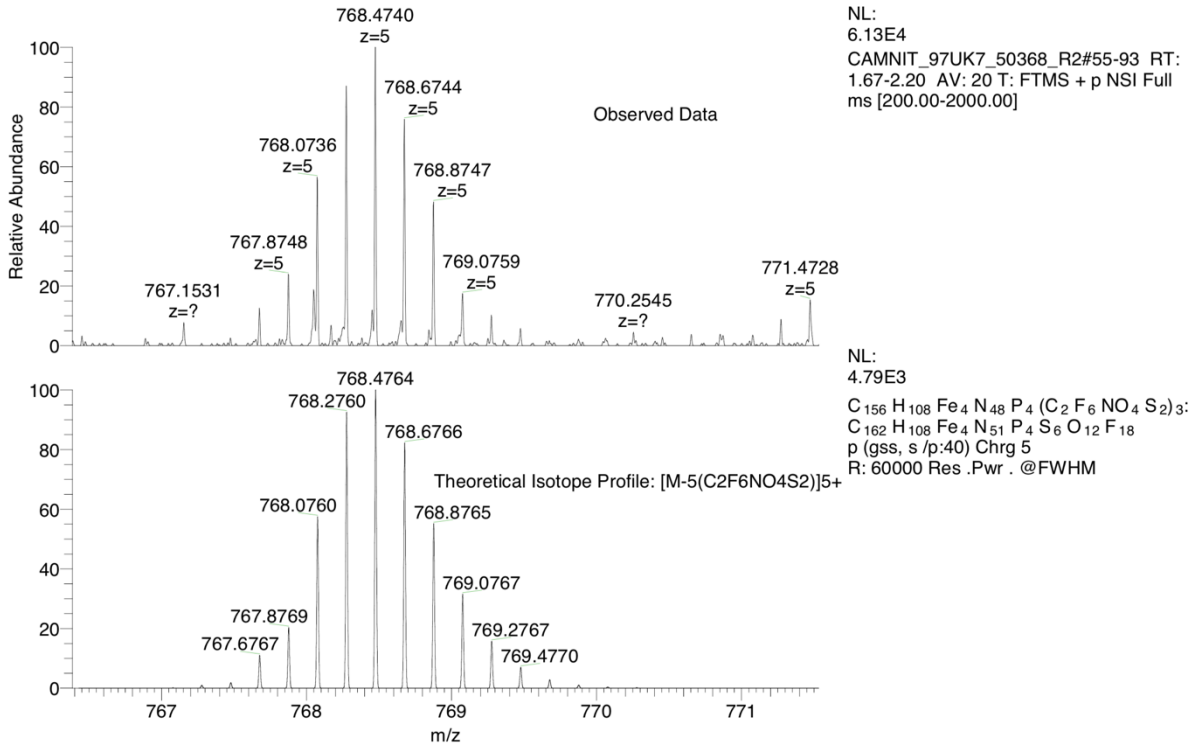

Figure S95: HRMS spectrum of **6**.

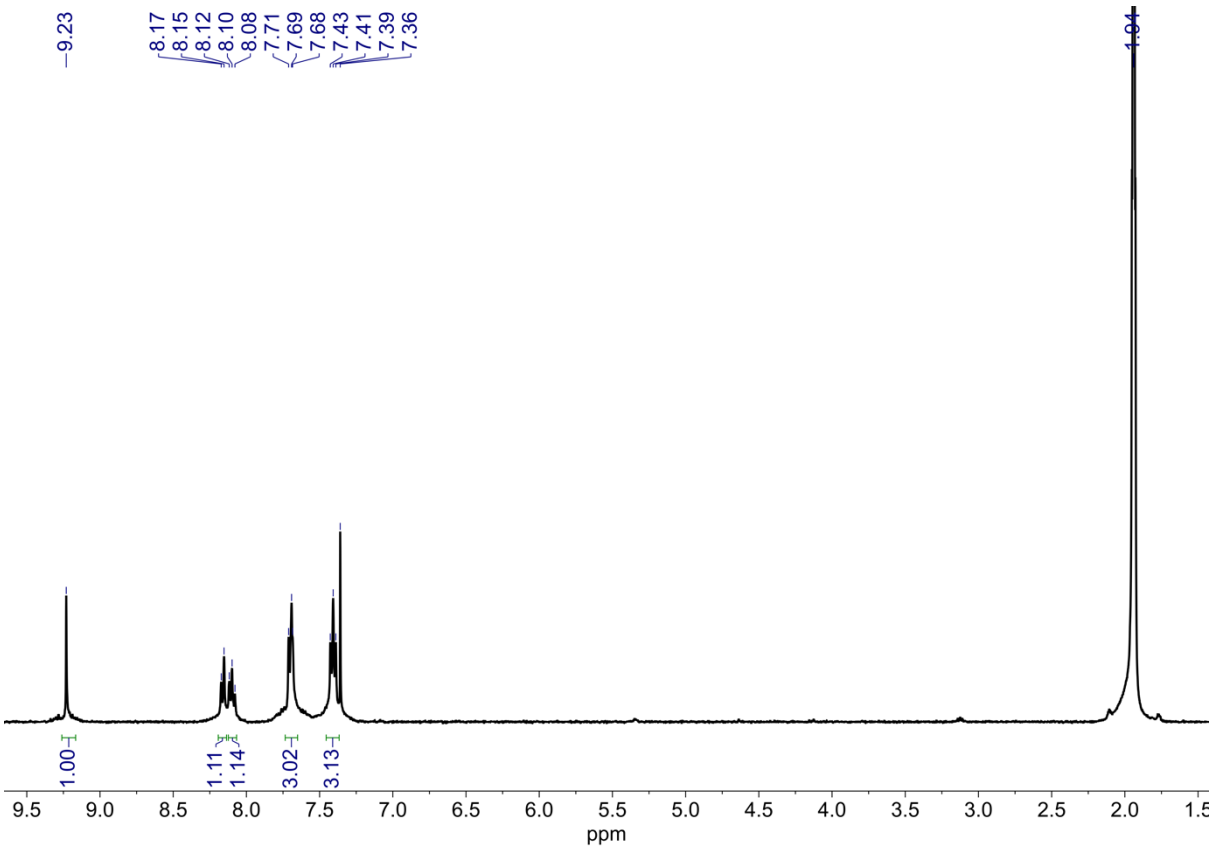

Figure S96: ^{1}H NMR (CD_3CN, 500 MHz, 298 K) spectrum of **6**.

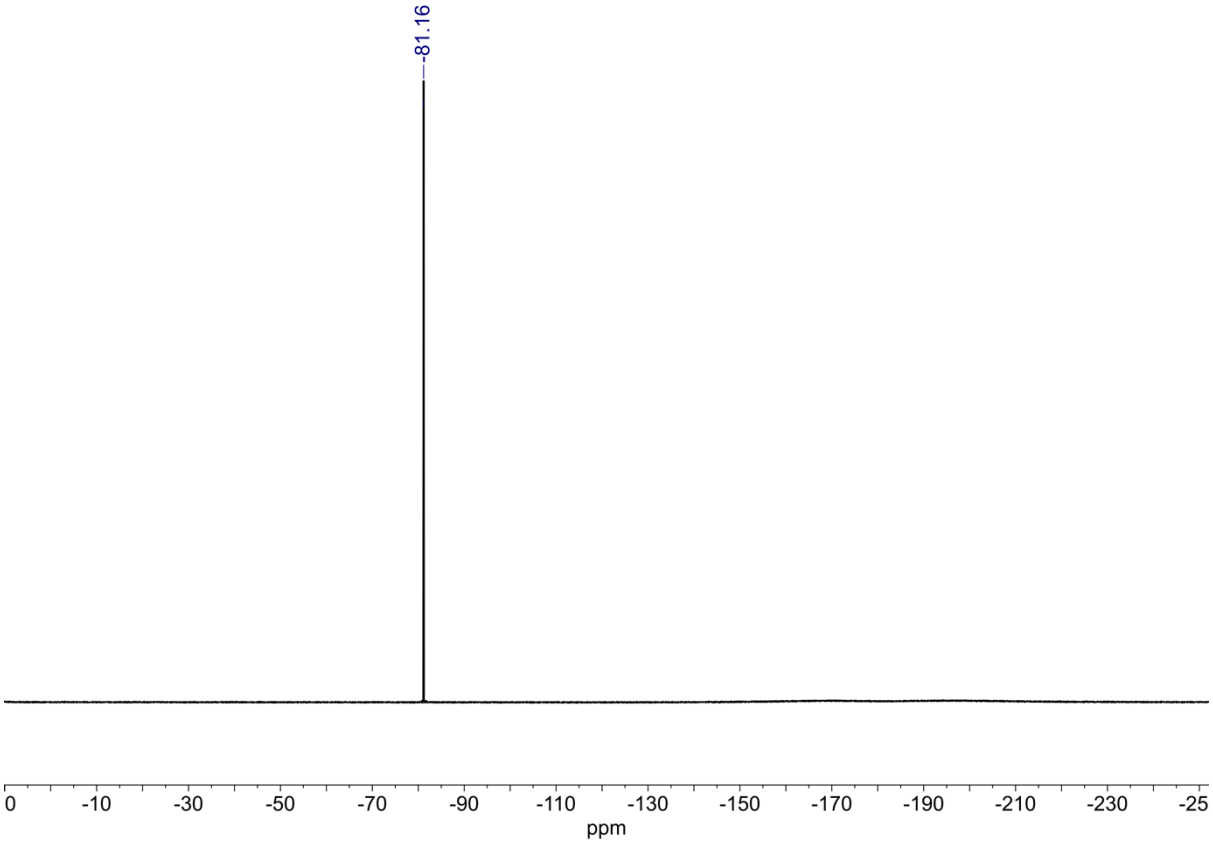

Figure S97: ^{19}F NMR (CD_3CN, 376 MHz, 298 K) spectrum of **6**.

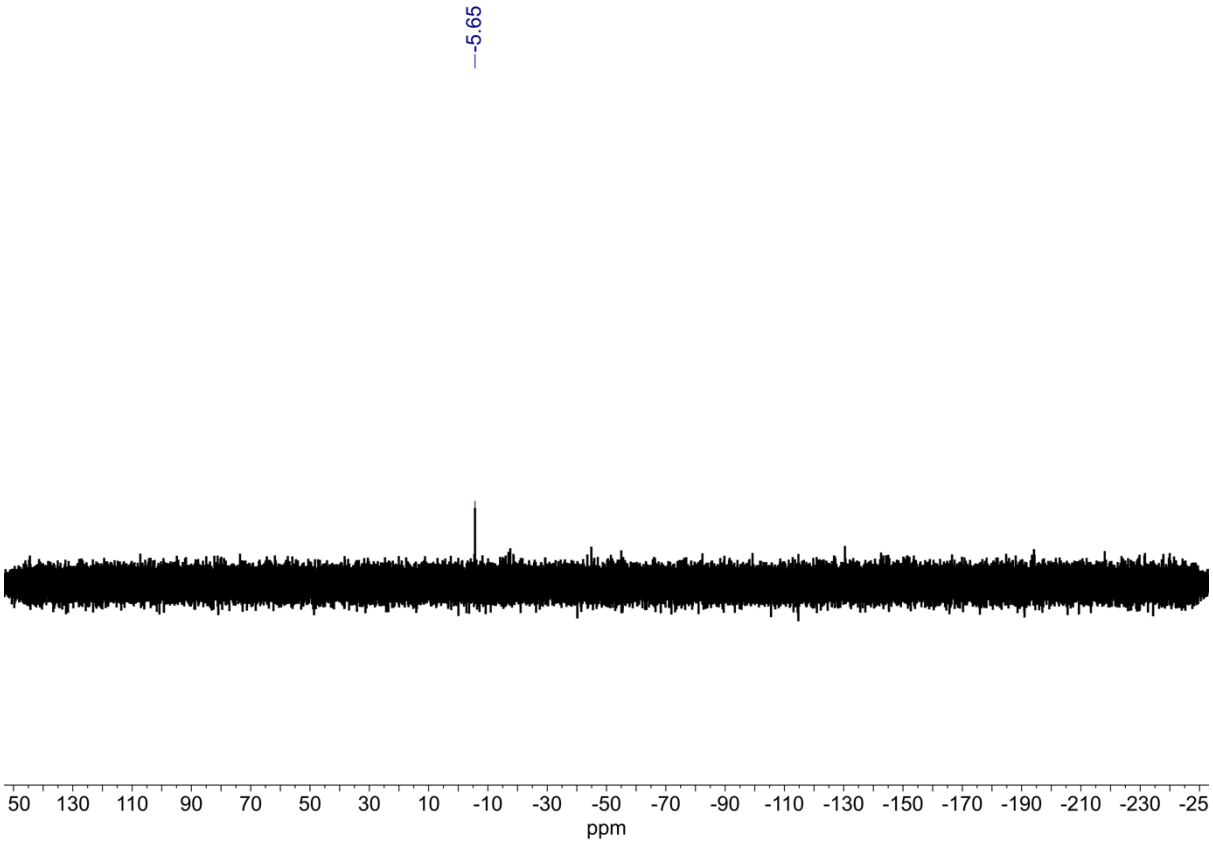

Figure S98: ^{31}P NMR (CD_3CN, 162 MHz, 298 K) spectrum of **6**.

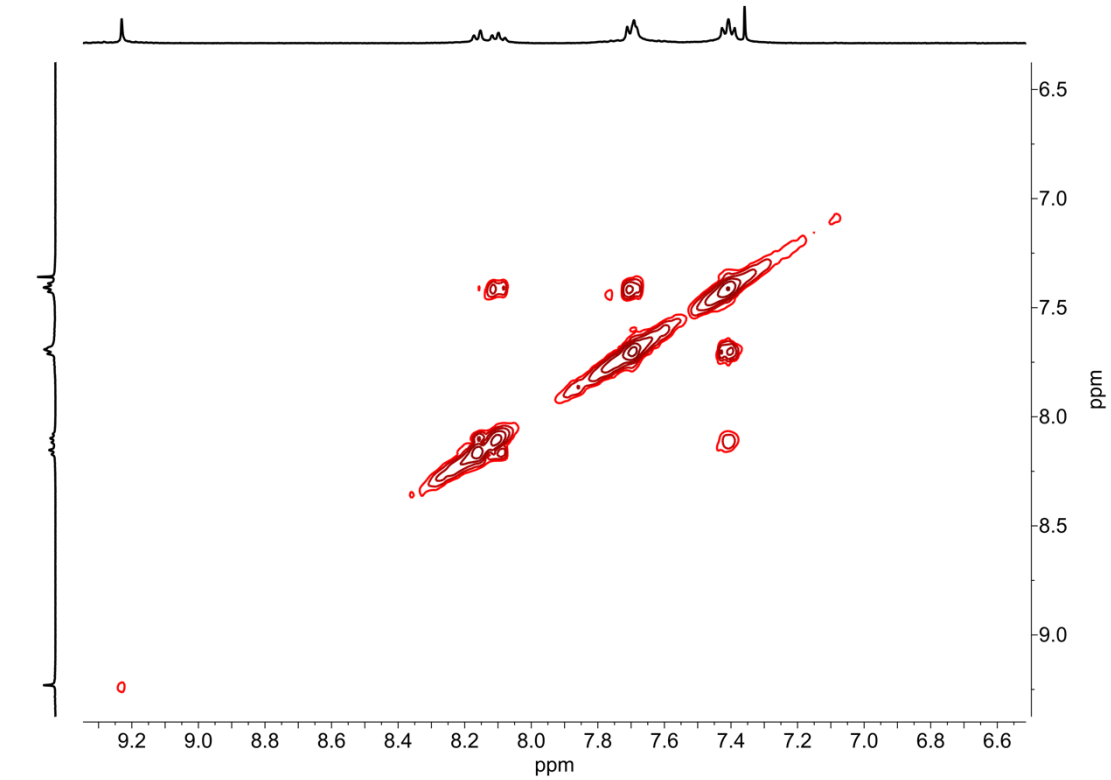

Figure S99: Partial COSY spectrum of **6**.

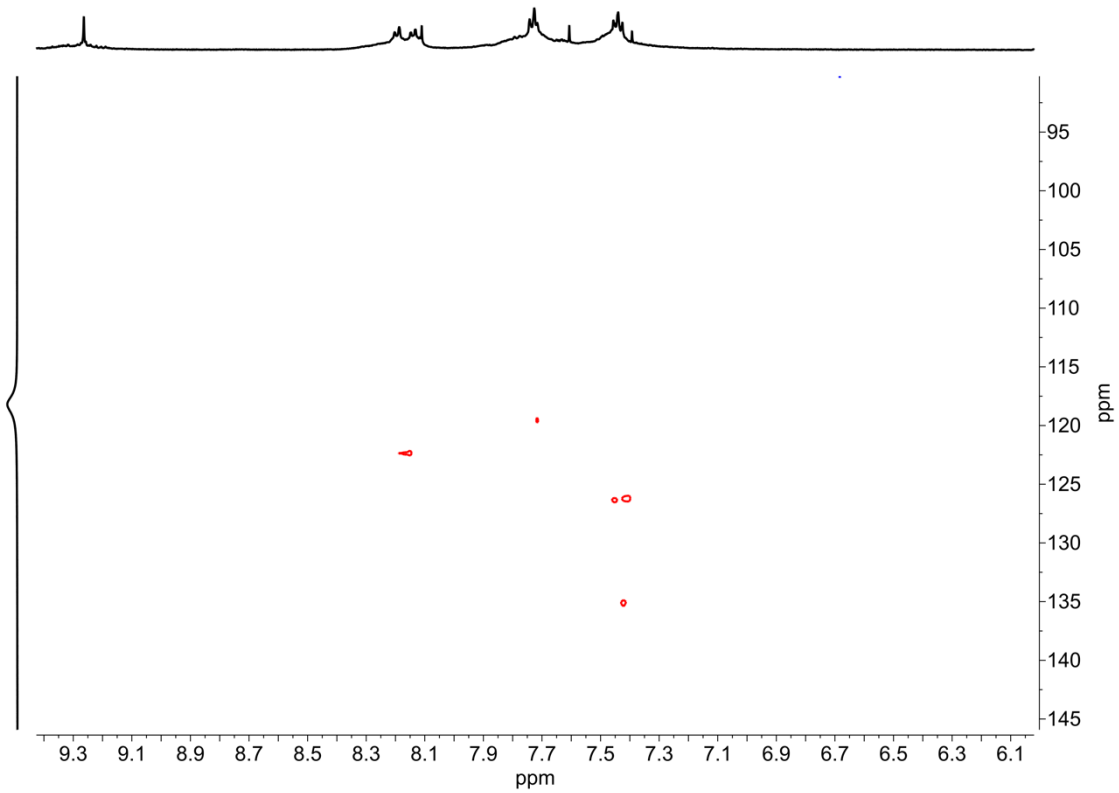

Figure S100: Partial HSQC spectrum of **6**.

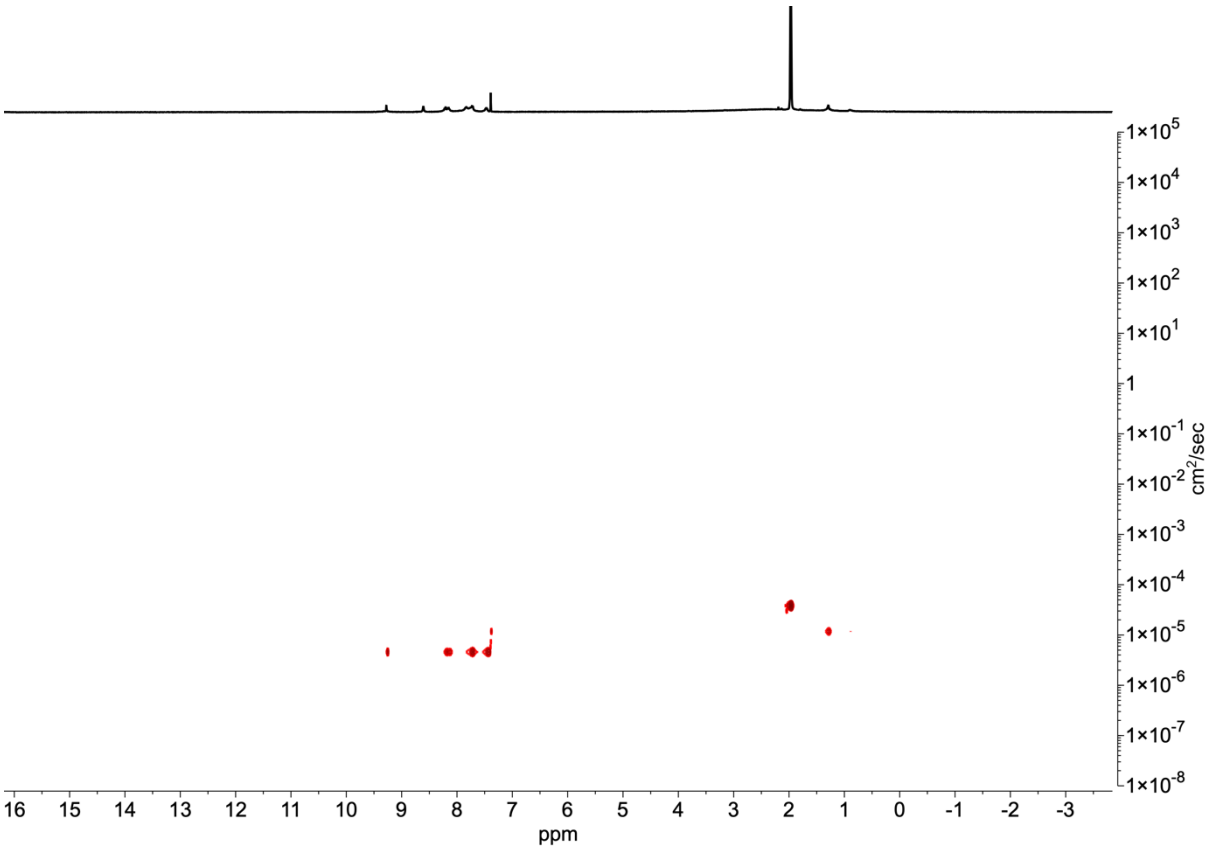

Figure S101: DOSY spectrum of **6**. Diffusion coefficient: 4.61×10^{-10} m^2s^{-1}. R_H from DOSY: 13.8 Å. Calculated R_H: 12.1 Å.

Phosphine Oxide Paneled Cage formed from $FeSO_4$ **11**

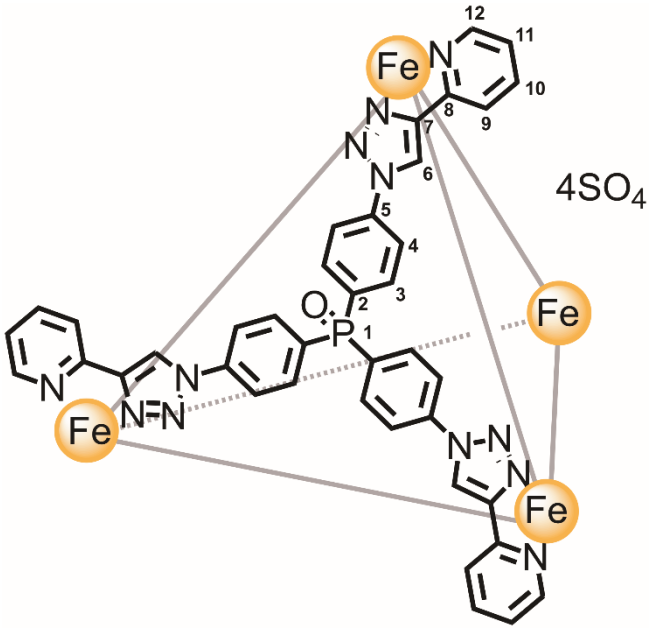

Phosphine oxide ligand **S1** (2.0 mg, 2.82 µmol) was added to MeCN-d_3 (0.25 mL) and D_2O (0.25 mL). $FeSO_4.7H_2O$ (0.78 mg, 2.82 µmol) was added and the reaction heated to 70 °C for 1 hour. The formed cage was used as synthesised.

^{1}H NMR (500 MHz, CD_3CN) δ: 9.58 (s, 3H, H_6), 8.26 (d, J = 7.4 Hz, 3H, H_{11}), 8.12 (d, J = 7.3 Hz, 3H, H_9), 7.89 (t, J = 7.4 Hz, 6H, H_4), 7.71–7.62 (m, 12H, H_3 + H_{12}), 7.43 (t, J = 6.6 Hz, 3H, H_{11}). **^{13}C NMR** (126 MHz, CD_3CN) δ: 155.5, 152.8, 151.9, 140.7, 139.9, 134.8 (d, J = 10.5 Hz), 131.0 (d, J = 106.1 Hz), 127.5, 123.7, 121.3 (d, J = 12.0 Hz), 121.2. **^{31}P NMR** (162 MHz, CD_3CN) δ: 28.1.

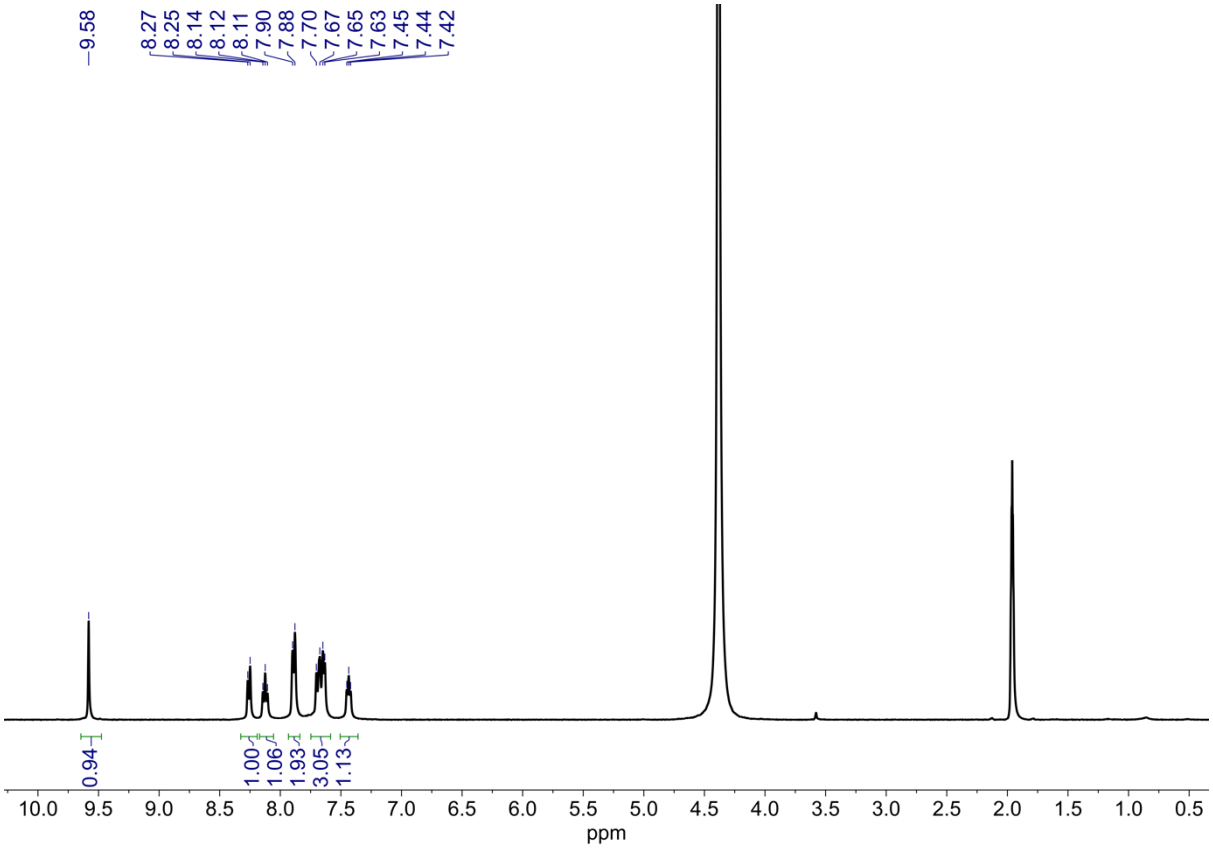

Figure S102: ^{1}H NMR (CD_3CN, 500 MHz, 298 K) spectrum of **11**.

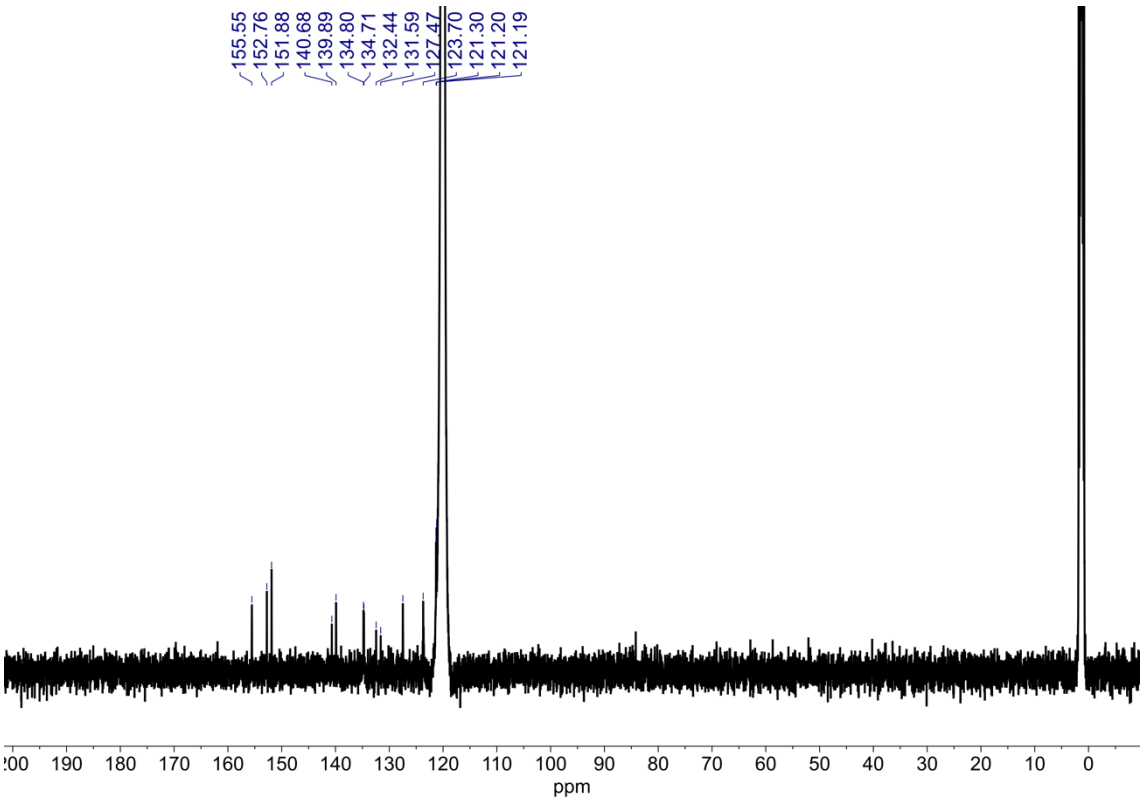

Figure S103: ^{13}C NMR (CD_3CN, 126 MHz, 298 K) spectrum of **11**.

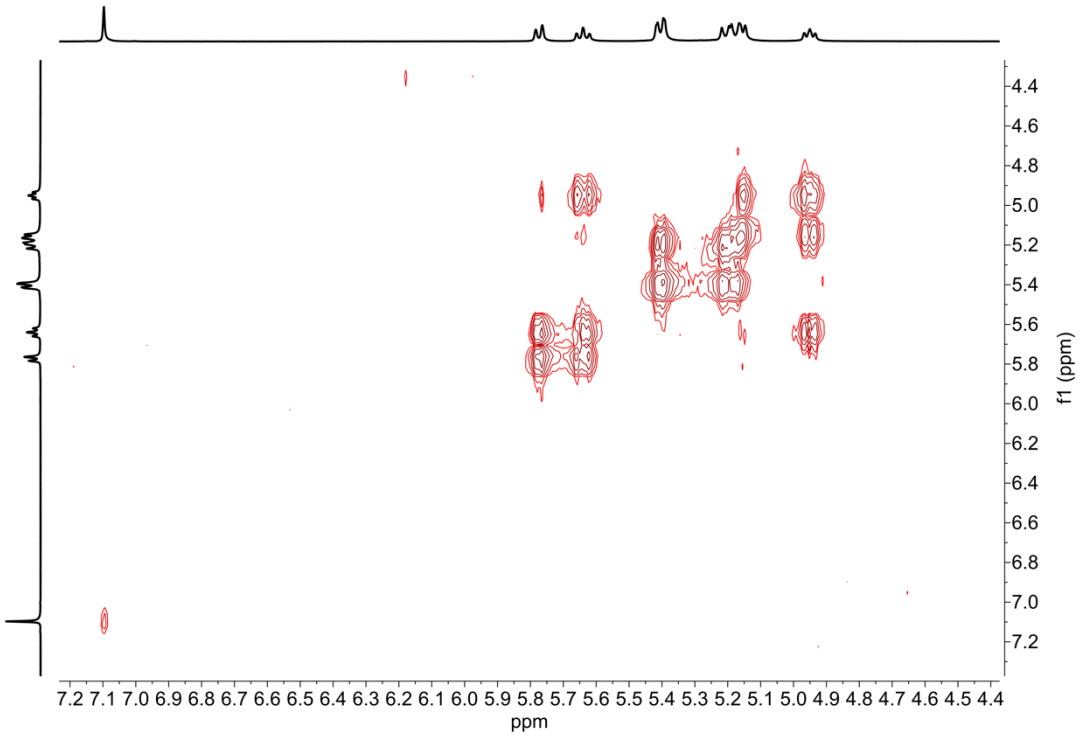

Figure S104: Partial COSY NMR spectrum of **11**.

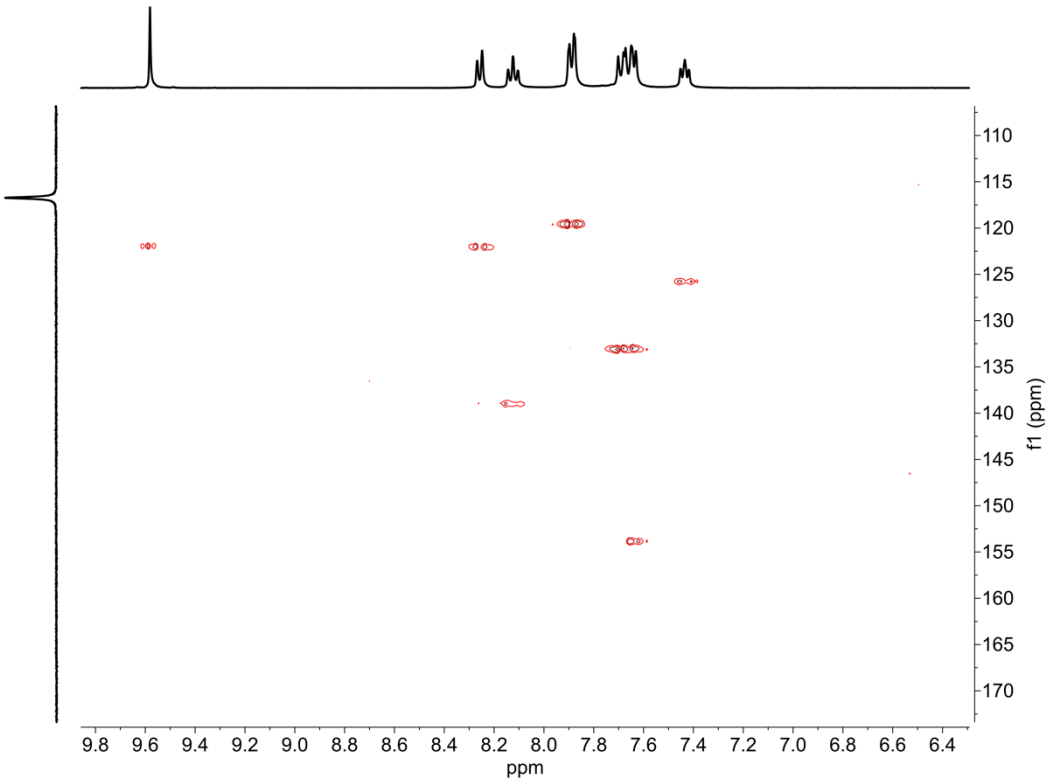

Figure S105: Partial HSQC NMR spectrum of **11**.

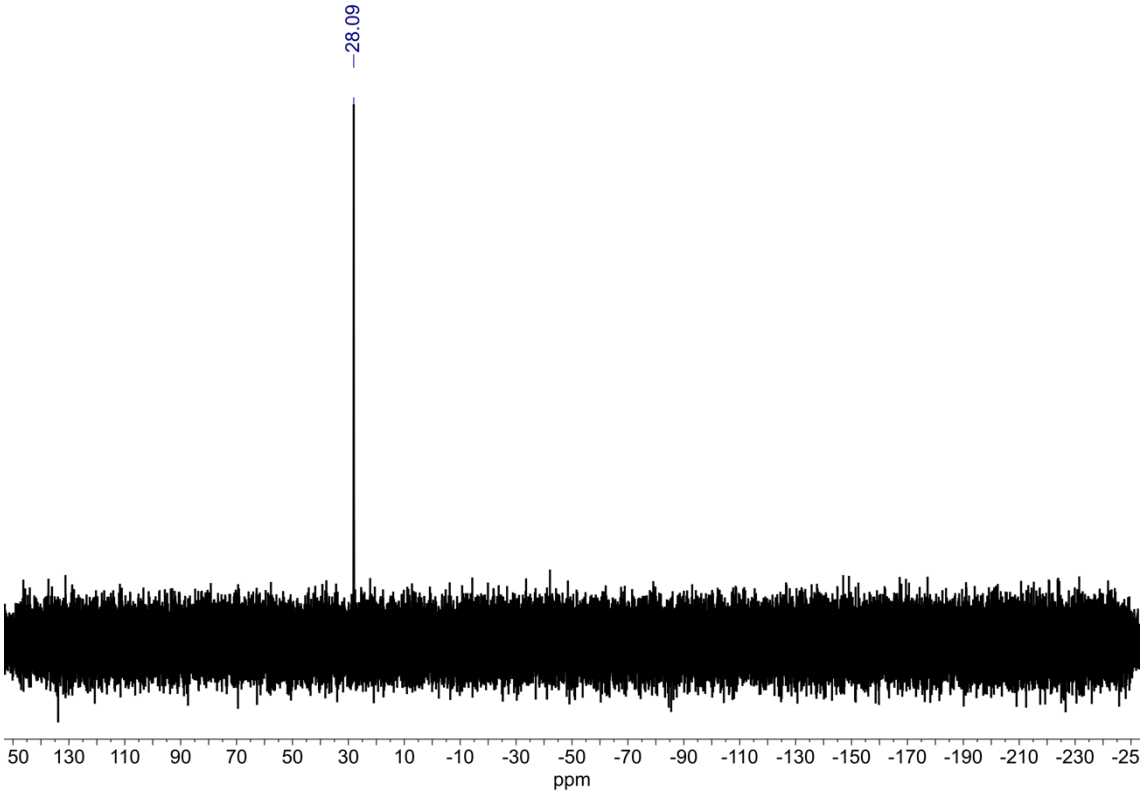

Figure S106: ^{31}P NMR (CD_3CN, 162 MHz, 298 K) spectrum of **11**.

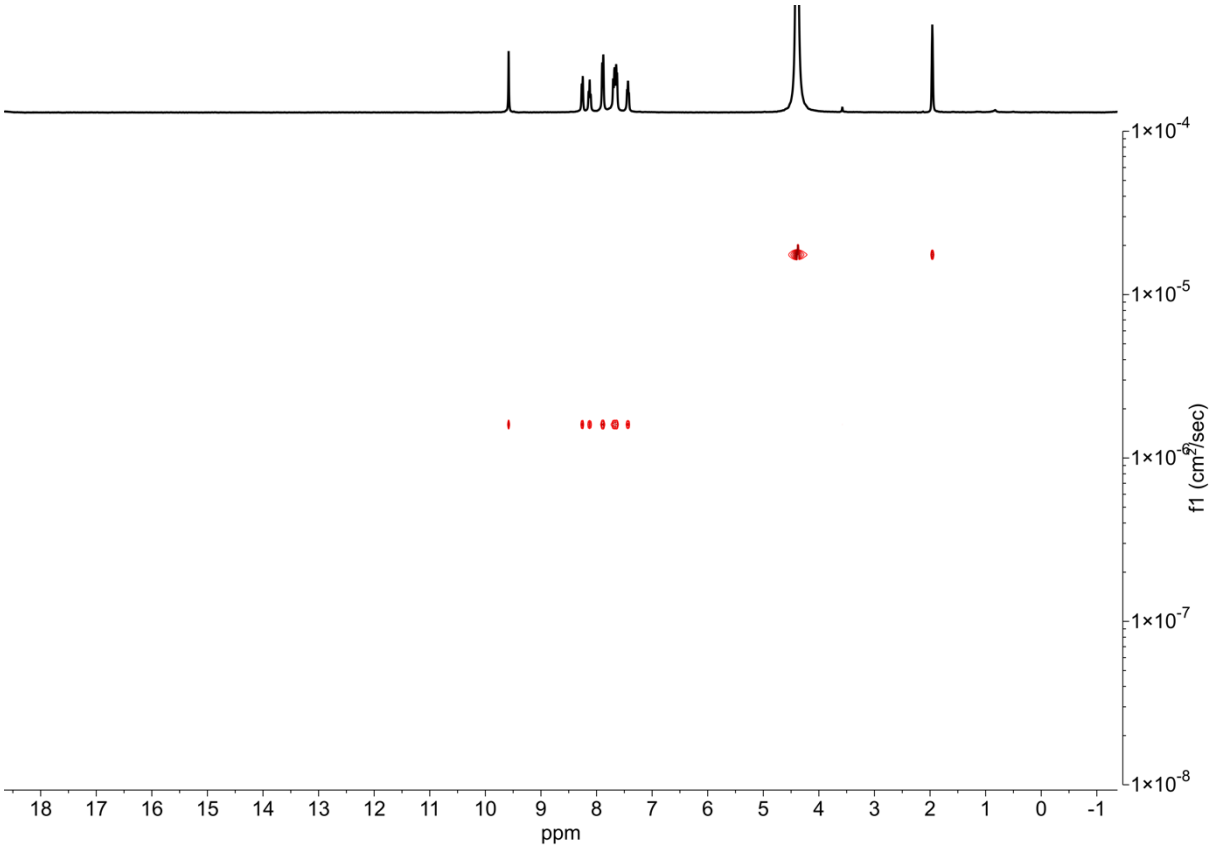

Figure S107: DOSY NMR spectrum of **11**. Diffusion coefficient: 1.61 × 10^{-10} m^2s^{-1}. R_H from DOSY: 15.2 Å. Calculated R_H: 12.1 Å.

No mass spectrometry data could be recorded for cage **11**. To confirm the identity of the cage anion exchange was performed.

Anion exchange to form Iron Phosphine Oxide Cage **7** as Triflimide salt

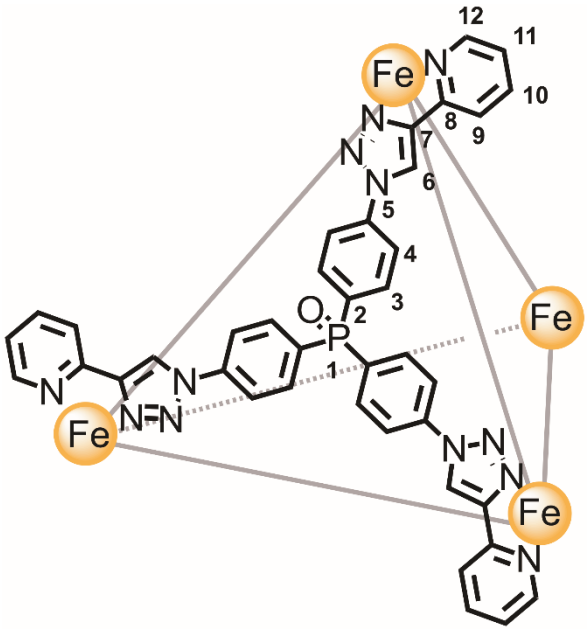

To Cage **11** in H_2O:MeCN (0.5 mL, as synthesised, assumed 2.82 µmol) was added $LiNTf_2$ (13.1 mg, 45.1 µmol). A precipitate was formed and collected by centrifugation. The precipitate was washed three times with H_2O (1 mL) and dried under a flow of nitrogen. The precipitate was dissolved in MeCN-d_3 (0.5 mL) and characterised without further purification (assumed quantitative). This compound could also be formed from direct assembly with $Fe(NTf_2)_2$.

^{1}H NMR (500 MHz, CD_3CN) δ: 9.28 (s, 3H, H_6), 8.21 (d, *J* = 7.7 Hz, 3H, H_{11}), 8.15 (5, *J* = 7.7 Hz, 3H, H_{10}), 7.84 (d, *J* = 7.7 Hz, 6H, H_4), 7.76 (dd, *J* = 11.6, 9.0 Hz, 6H, H_3), 7.72 (d, *J* = 5.5 Hz, 6H, H_{12}), 7.46 (t, *J* = 6.5 Hz, 3H, H_{11}). **^{13}C NMR** (126 MHz, CD_3CN) δ: 155.9, 153.3, 151.6, 140.6, 139.8, 134.7 (d, *J* = 11.7 Hz), 143.2 (d, *J* = 106.1 Hz), 127.4, 123.7, 123.5, 121.4 (d, *J* = 12.7 Hz), 120.8 (q, *J* = 320.7 Hz). **^{31}P NMR** (162 MHz, CD_3CN) *δ*: 25.2. **^{19}F NMR** (376 MHz, CD_3CN) *δ*: −80.2.

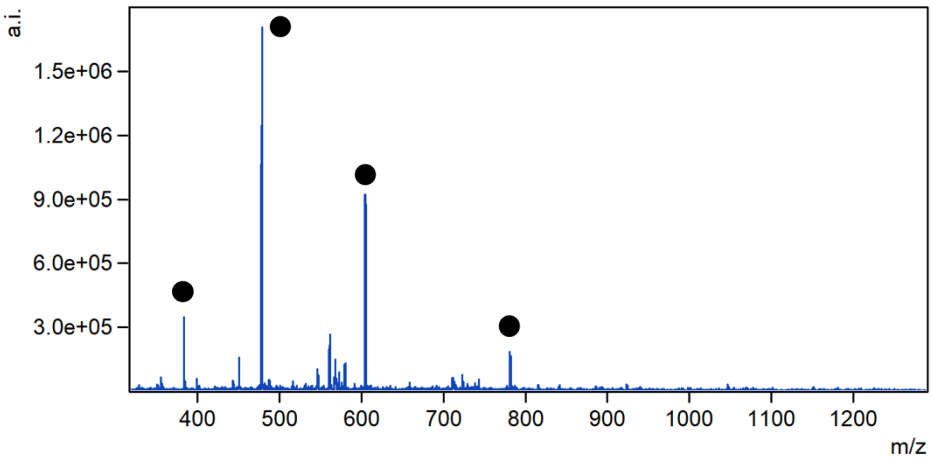

Figure S108: LRMS spectrum of **7**.

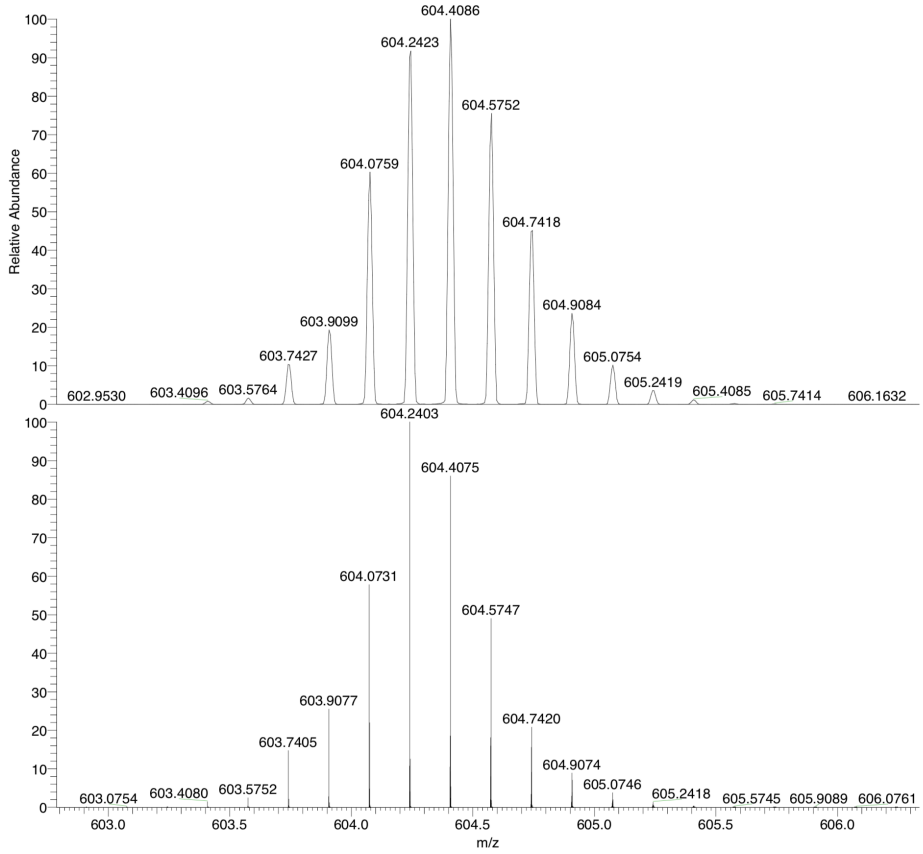

Figure S109: HRMS spectrum of **7**.

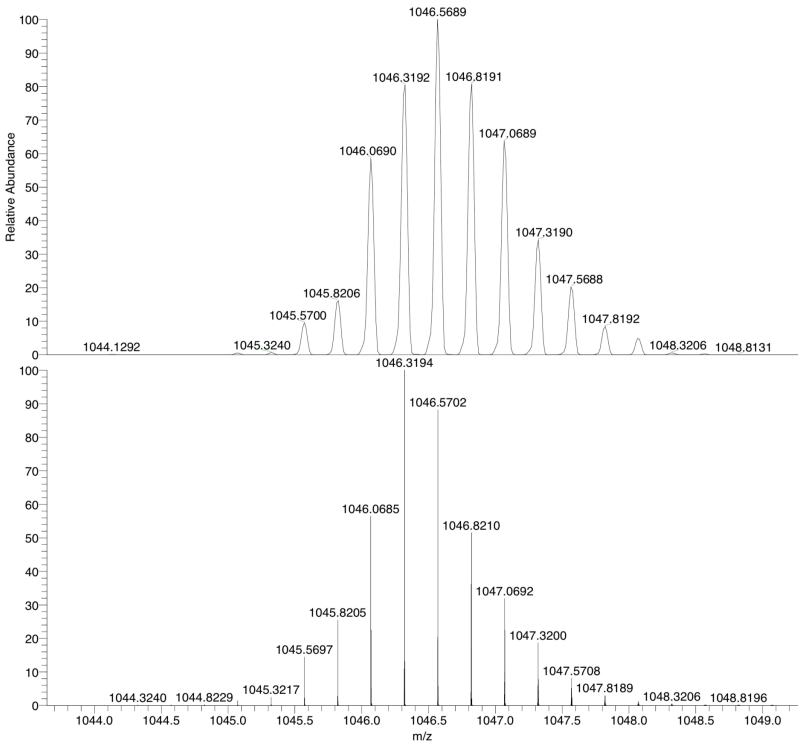

Figure S110: HRMS spectrum of **7**.

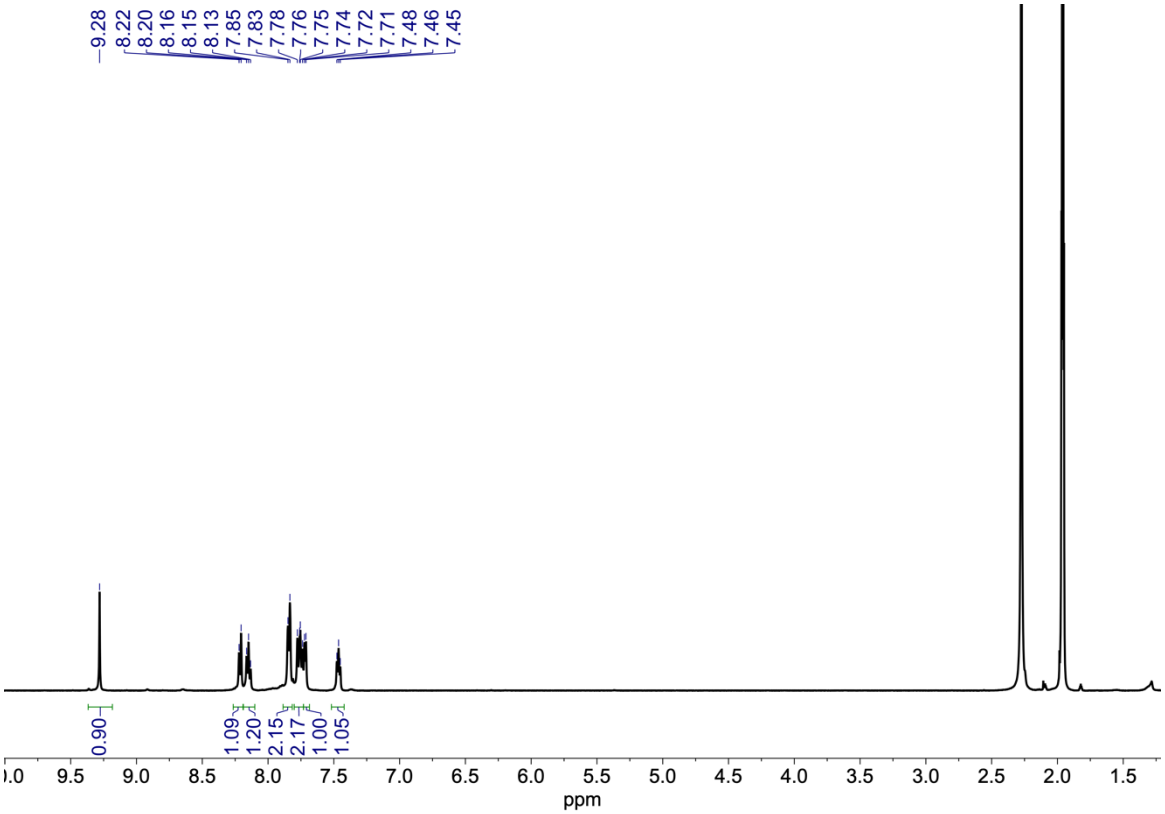

Figure S111: ^{1}H NMR (CD_3CN, 500 MHz, 298 K) spectrum of **7**.

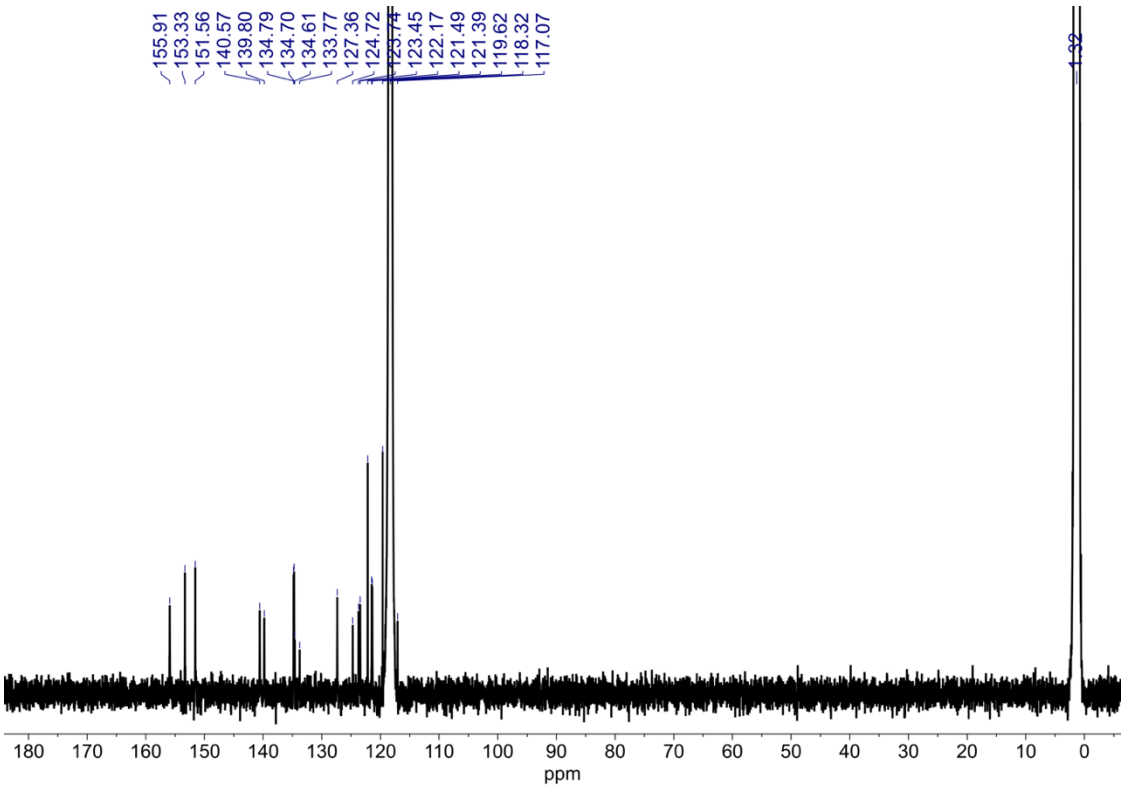

Figure S112: ^{13}C NMR (CD_3CN, 126 MHz, 298 K) spectrum of **7**.

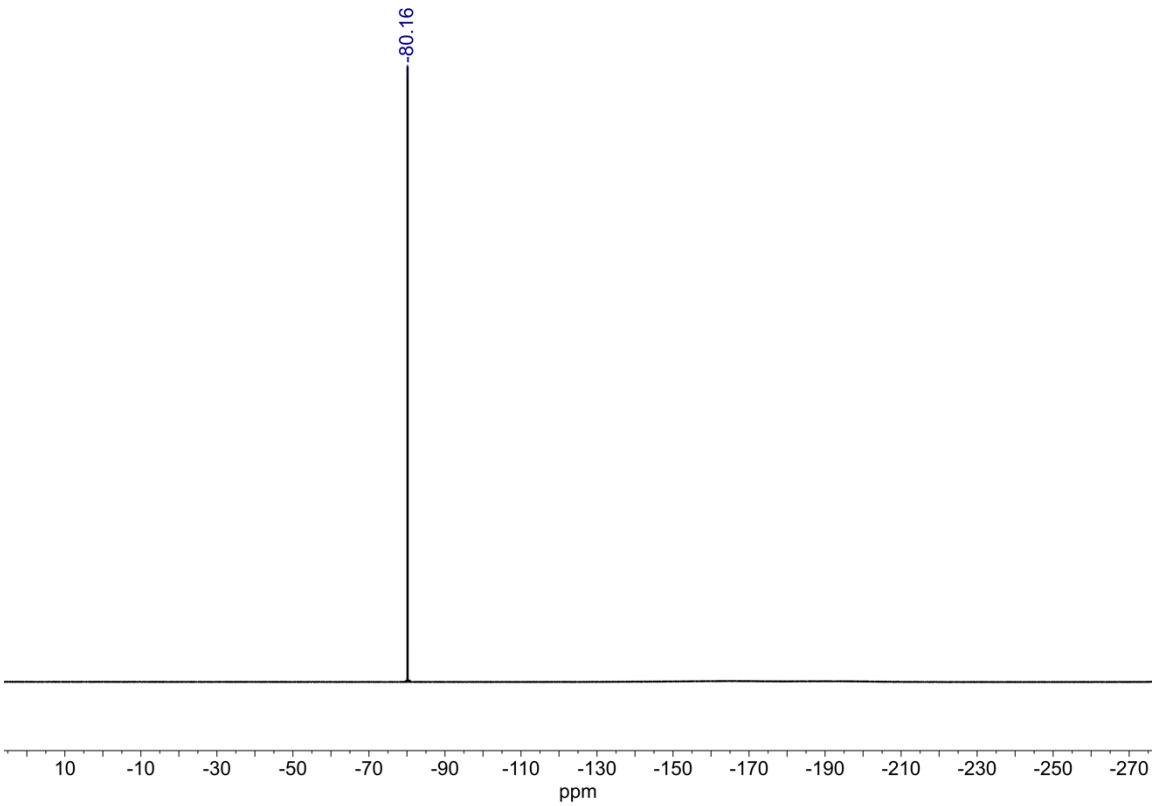

Figure S113: ^{19}F NMR (CD_3CN, 376 MHz, 298 K) spectrum of **7**.

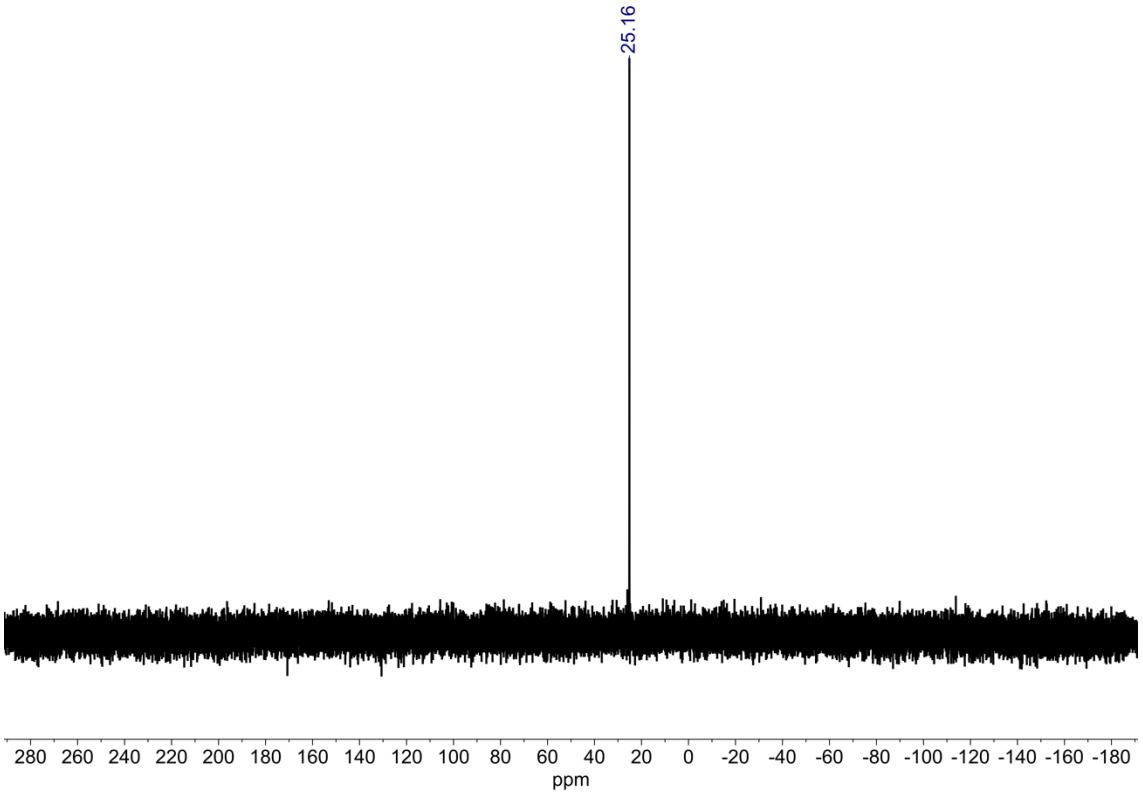

Figure S114: ^{31}P NMR (CD_3CN, 162 MHz, 298 K) spectrum of **7**.

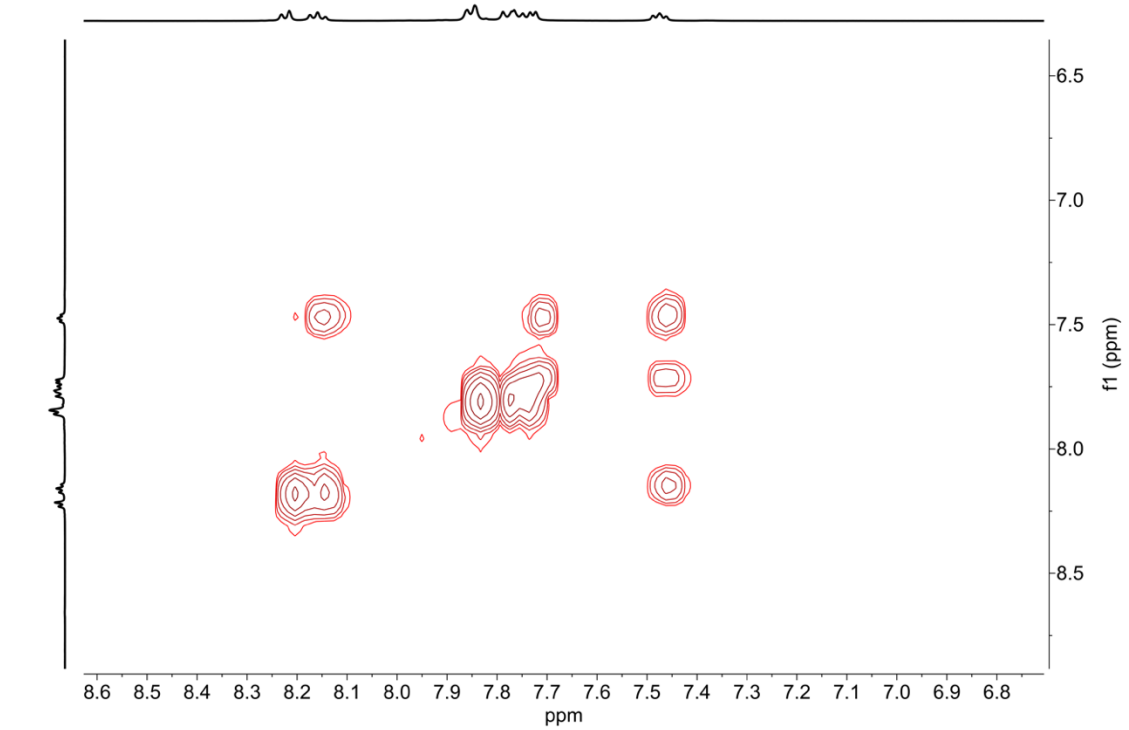

Figure S115: Partial COSY NMR spectrum of **7**.

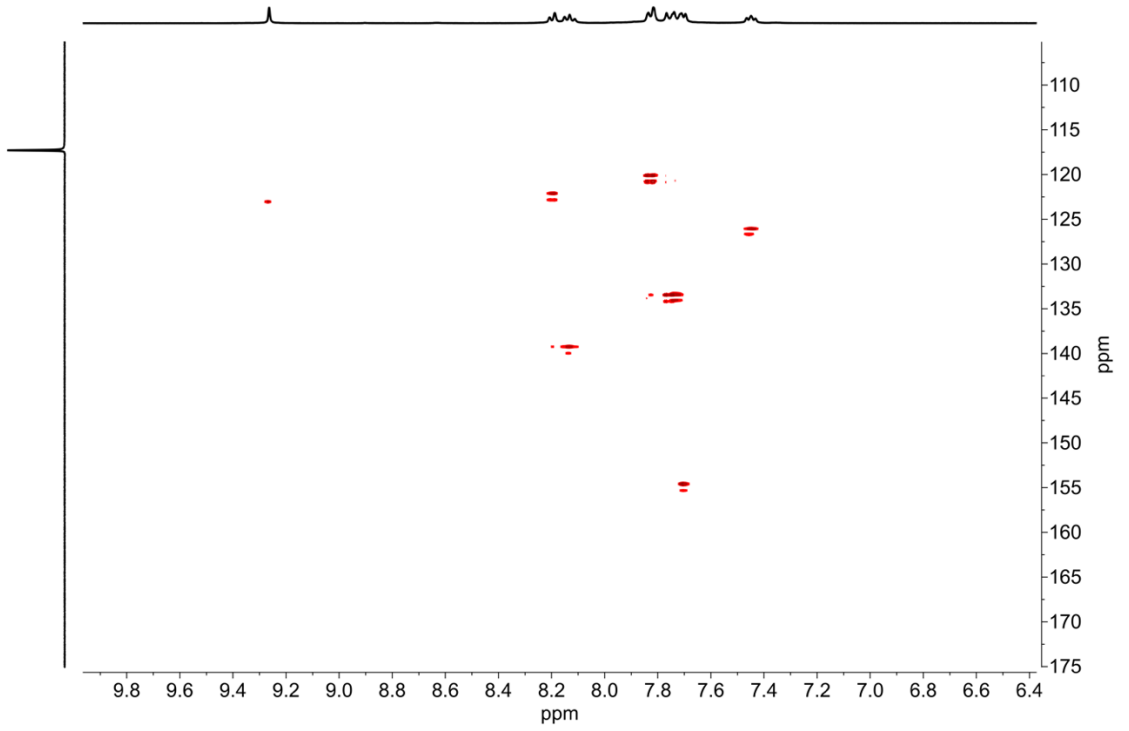

Figure S116: Partial HSQC NMR spectrum of **7**.

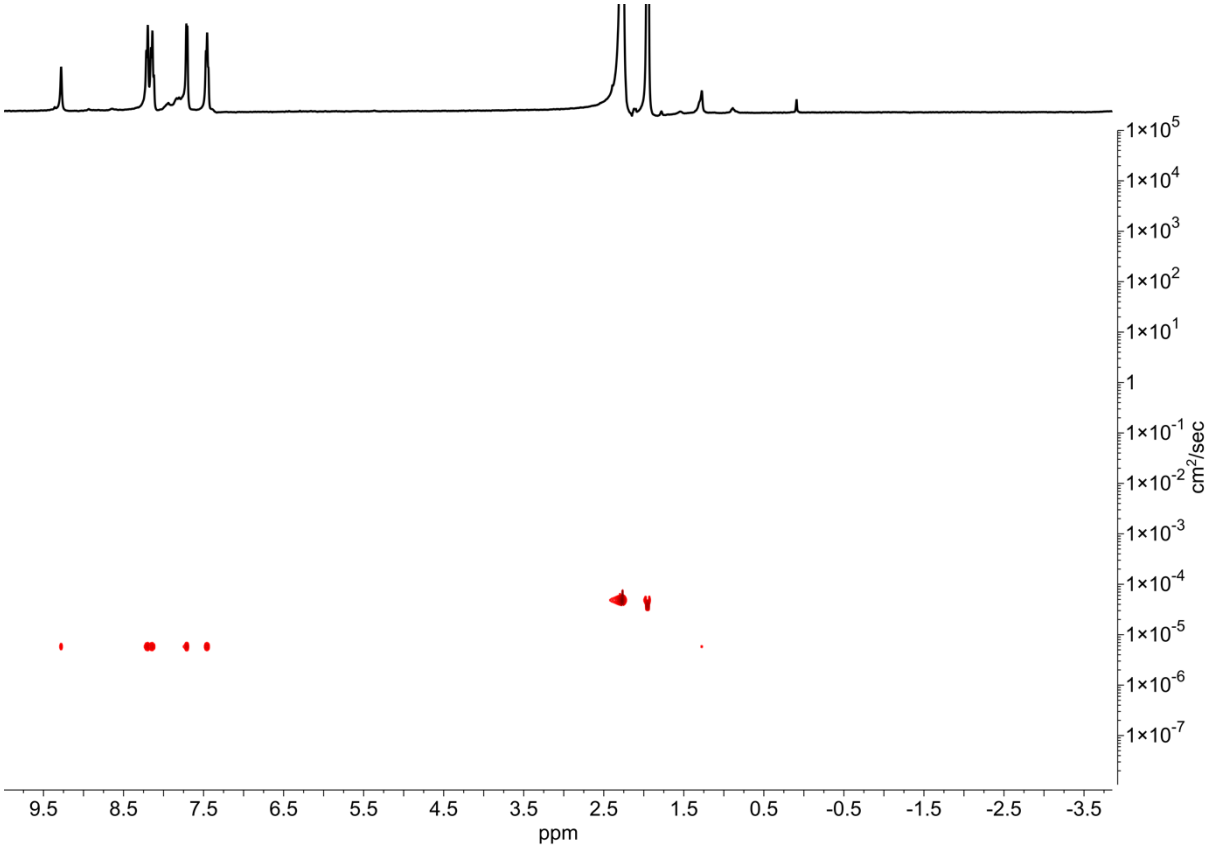

Figure S117: DOSY NMR spectrum of **7**. Diffusion coefficient: 5.82×10^{-10} m^2s^{-1}. R_H from DOSY: 10.9 Å. Calculated R_H: 12.1 Å.

7. X-Ray Crystallography

Data were collected at Beamline I19 of Diamond Light Source employing silicon double crystal monochromated synchrotron radiation (0.6889 Å) with ω and ψ scans at 100(2) K.[4] Data integration and reduction were undertaken with Xia2.[5-7] Subsequent computations were carried out using the WinGX-32 graphical user interface.[8] Multi-scan empirical absorption corrections were applied to the data using the AIMLESS[9] tool in the CCP4 suite.[10] The structures were solved by direct methods using SHELXT[11] then refined and extended with SHELXL.[12] In general, non-hydrogen atoms with occupancies greater than 0.5 were refined anisotropically. Carbon-bound hydrogen atoms were included in idealized positions and refined using a riding model. Disorder was modelled using standard crystallographic methods including constraints, restraints and rigid bodies where necessary. Crystallographic data along with specific details pertaining to the refinement follow. Crystallographic data have been deposited with the CCDC (1900370-1900372).

11 - $[Fe_4L_6]\cdot 0.667(L)\cdot 4SO_4\cdot 7MeCN\cdot 16.5H_2O$ [+ solvent]

Formula $C_{196}H_{180}Fe_4N_{63}O_{37.17}P_{4.67}S_4$, *M* 4508.85, Trigonal, space group R -3 c (#167), *a* 42.04600(10), *b* 42.04600(10), *c* 107.4786(4) Å, *γ*120°, *V* 164551.5(10) $Å^3$, D_c 0.819 g cm^{-3}, *Z* 18, crystal size 0.020 by 0.020 by 0.015 mm, colour orange, habit block, temperature 100(2) Kelvin, *λ*(Synchrotron) 0.6889 Å, *μ*(Synchrotron) 0.228 mm^{-1}, $T(\text{Analytical})_{min,max}$ 0.965032575515, 1.0, $2\theta_{max}$ 42.52, *hkl* range -44 44, -44 44, -113 113, *N* 201649, N_{ind} 22355(R_{merge} 0.0377), N_{obs} 15823(I > 2σ(I)), N_{var} 1422, residuals* *R*1(*F*) 0.1045, *wR*2(F^2) 0.3396, GoF(all) 1.306, $\Delta\rho_{min,max}$ -0.539, 0.830 e^- $Å^{-3}$.

* $R1 = \Sigma||F_o| - |F_c||/\Sigma|F_o|$ for $F_o > 2\sigma(F_o)$; $wR2 = (\Sigma w(F_o^2 - F_c^2)^2/\Sigma(wF_c^2)^2)^{1/2}$ all reflections

$w=1/[\sigma^2(F_o^2)+(0.2000P)^2+100.0000P]$ where $P=(F_o^2+2F_c^2)/3$

Specific refinement details:

The crystals of $[Fe_4L_4]\cdot 0.667(L)\cdot 4SO_4\cdot 7MeCN\cdot 16.5H_2O$ were grown by diffusion of acetonitrile into an aqueous solution of $[Fe_4L_4]\cdot 4SO_4$. The observation of additional free ligand in the sample was an artefact of crystallisation and was not observed in the bulk sample. The crystals employed immediately lost solvent after removal from the mother liquor and rapid handling prior to flash cooling in the cryostream was required to collect data. Despite these measures and the use of synchrotron radiation few reflections at greater than 0.95 Å resolution were observed. Nevertheless, the quality of the data is far more than sufficient to establish the connectivity of the structure. The asymmetric unit was found to contain one half of a Fe_4L_4 assembly, one third of an uncoordinated ligand molecule and associated counterions and solvent molecules.

Due to the less than ideal resolution, bond lengths and angles within the two chemically identical organic ligands were restrained to be similar to each other. One phenyl ring was modelled as disordered over two locations; the disordered atoms were modelled with isotropic thermal parameters and bond length and angle restraints were employed to ensure a reasonable refinement. Several solvent molecules were also modelled as disordered over two locations. The hydrogen atoms of the water molecules and some disordered acetonitrile

solvent molecules could not be located in the electron density map and were not included in the model.
Only one sulfate anion (per asymmetric unit) could be located in the electron density map. The remaining anion (included as sulfate in the formula) was highly disordered and no satisfactory model for it could be obtained despite numerous attempts at modelling, including with rigid bodies. Therefore the SQUEEZE[13] function of PLATON[14] was employed to account for this highly disordered anion and further disordered solvent molecules, which gave a potential solvent accessible void of 74186 Å^3 per unit cell (a total of approximately 13720 electrons). Since the diffuse solvent molecules could not be assigned conclusively to acetonitrile or water they were not included in the formula. Consequently, the molecular weight and density given above are likely to be underestimated.
CheckCIF gives two A and twenty three B level alerts. These alerts (both A and B level) result from the limited data resolution, water molecules for which hydrogens were not modelled and thermal motion and/or unresolved disorder of some anions and solvent molecules as described above.

12 - $[Ni_4L_4]\cdot 2.25(NTf_2)\cdot 1.1(NiI_4)\cdot 4.1(I)\cdot 2.75MeCN\cdot 9.75C_6H_6$ [+ 3.45 anions + solvent]
Formula $C_{228.50}H_{186.75}F_{13.50}I_{8.50}N_{53}Ni_{5.10}O_9P_4S_{4.50}$, *M* 5721.77, Triclinic, space group P -1 (#2), *a* 21.1855(2), *b* 24.1723(2), *c* 33.8253(3) Å, α 89.9610(10), β 84.2150(10), γ 65.8950(10)°, *V* 15715.3(3) Å^3, D_c 1.209 g cm^{-3}, *Z* 2, crystal size 0.02 by 0.02 by 0.01 mm, colour green brown, habit block, temperature 100(2) Kelvin, λ(Synchrotron) 0.6889 Å, μ(Synchrotron) 1.133 mm^{-1}, $T(\text{Analytical})_{min,max}$ 0.97710440761, 1.0, $2\theta_{max}$ 48.42, *hkl* range -25 25, -28 28, -40 40, *N* 148944, N_{ind} 53682(R_{merge} 0.0479), N_{obs} 35894(I > 2σ(I)), N_{var} 3084, residuals* *R*1(*F*) 0.0901, *wR*2(F^2) 0.3003, GoF(all) 1.004, $\Delta\rho_{min,max}$ -1.032, 1.573 e$^-$ Å^{-3}.
* $R1 = \Sigma||F_o| - |F_c||/\Sigma|F_o|$ for $F_o > 2\sigma(F_o)$; $wR2 = (\Sigma w(F_o^2 - F_c^2)^2/\Sigma(wF_c^2)^2)^{1/2}$ all reflections $w=1/[\sigma^2(F_o^2)+(0.2000P)^2+10.0000P]$ where $P=(F_o^2+2F_c^2)/3$
Specific refinement details:
The crystals of $[Ni_4L_4]\cdot 2.25(NTf_2)\cdot 1.1(NiI_4)\cdot 4.1(I)\cdot 2.75MeCN\cdot 9.75C_6H_6$ were grown by diffusion of benzene into an acetonitrile solution of $[Ni_4L_4]\cdot 8NTf_2$. The observation of NiI_4^{2-} and iodide and was not observed in the bulk sample and is assumed to be an artefact of crystallisation, caused by the used of crude reaction material in the crystallisation. The crystals employed immediately lost solvent after removal from the mother liquor and rapid handling prior to flash cooling in the cryostream was required to collect data. Data were obtained to 0.84 Å resolution. The asymmetric unit was found to contain one complete Ni_4L_4 assembly and associated counterions and solvent molecules. Bond lengths and angles within pairs of chemically identical organic ligands were restrained to be similar to each other and thermal parameter restraints (SIMU, RIGU) were applied to all atoms except for nickel and iodine.
The anions and solvent molecules within the structure show evidence of substantial disorder. Two of the triflimide anions were modelled as disordered over two locations with bond length and thermal parameter restraints applied to facilitate a reasonable refinement. The disordered atoms were modelled with isotropic thermal parameters with the exception of

the sulfur atoms. Bond length restraints were also applied to some solvent molecules and the benzene solvent molecules were modelled as rigid groups (AFIX 66).
The occupancies of all anions were freely refined and then fixed at the obtained values. A further 3.45 anions per Ni_4L_4 assembly remain unaccounted for and no satisfactory model for these anions could be obtained despite numerous attempts at modelling, including with rigid bodies. Therefore the SQUEEZE[13] function of PLATON[14] was employed to account for the highly disordered anions and further disordered solvent molecules, which gave a potential solvent accessible void of 2711 $Å^3$ per unit cell (a total of approximately 864 electrons). Since the identity of the diffuse anions and solvent molecules could not be assigned conclusively they were not included in the formula. Consequently, the molecular weight and density given above are underestimated.
CheckCIF gives three A and ten B level alerts. These alerts (both A and B level) all result from thermal motion and/or unresolved disorder of some anions and solvent molecules as described above.

4 - $[Zn_4L_4]\cdot 0.75(NTf_2)\cdot 1.25(ZnI_4)\cdot 0.75(ZnI_3H_2O)\cdot 1.75(I)\cdot 0.5MeCN\cdot 2.5C_6H_6\cdot 0.5H_2O$ [+ 6.25 anions + solvent]

Formula $C_{177.50}H_{139.50}F_{4.50}I_9N_{49.25}O_{4.50}P_4S_{1.50}Zn_6$, *M* 4826.17, Triclinic, space group P -1 (#2), *a* 21.1660(4), *b* 21.8072(4), *c* 35.8636(7) Å, σ 90.804(2), β 102.438(2), γ 104.311(2)°, *V* 15623.8(5) $Å^3$, D_c 1.026 g cm^{-3}, *Z* 2, crystal size 0.05 by 0.04 by 0.03 mm, colour pale yellow, habit block, temperature 100(2) Kelvin, λ(Synchrotron) 0.6889 Å, μ(Synchrotron) 1.291 mm^{-1}, *T*(Analytical)$_{min,max}$ 0.97067650853, 1.0, $2\theta_{max}$ 36.50, *hkl* range -19 19, -19 19, -32 32, *N* 40437, N_{ind} 23203(R_{merge} 0.0511), N_{obs} 14475(I > 2σ(I)), N_{var} 2523, residuals* *R*1(*F*) 0.1265, *wR*2(F^2) 0.3638, GoF(all) 1.031, $\Delta\rho_{min,max}$ -0.665, 0.881 $e^- Å^{-3}$.

* $R1 = \Sigma||F_o| - |F_c||/\Sigma|F_o|$ for $F_o > 2\sigma(F_o)$; $wR2 = (\Sigma w(F_o^2 - F_c^2)^2/\Sigma(wF_c^2)^2)^{1/2}$ all reflections $w=1/[\sigma^2(F_o^2)+(0.2000P)^2+75.0000P]$ where $P=(F_o^2+2F_c^2)/3$

Specific refinement details:
The crystals of $[Zn_4L_4]\cdot 0.75(NTf_2)\cdot 1.25(ZnI_4)\cdot 0.75(ZnI_3H_2O)\cdot 1.75(I)\cdot 0.5MeCN\cdot 2.5C_6H_6\cdot 0.5H_2O$ were grown by diffusion of benzene into an acetonitrile solution of $[Zn_4L_4]\cdot 8NTf_2$. The observation of zinc iodides and iodide was not consistent with the bulk sample and is assumed to be an artefact of crystallisation, caused by the used of crude reaction material in the crystallisation. The crystals employed immediately lost solvent after removal from the mother liquor and rapid handling prior to flash cooling in the cryostream was required to collect data. Despite these measures and the use of synchrotron radiation few reflections at greater than 1.1 Å resolution were observed. The crystals were subject to rapid beam damage during data collection using synchrotron radiation; consequently only 94 % data completeness could be achieved and the quality of the integration was lower than ideal. Nevertheless, the quality of the data is far more than sufficient to establish the connectivity of the structure. The asymmetric unit was found to contain one complete Zn_4L_4 assembly and associated counterions and solvent molecules.
Due to the limited resolution, bond lengths and angles within pairs of chemically identical organic ligands were restrained to be similar to each other and thermal parameter restraints

(SIMU, RIGU) were applied to all atoms except for zinc and iodine. The occupancies of all anions and solvent molecules were freely refined and then fixed at the obtained values. A further 6.25 anions per Zn_4L_4 assembly remain unaccounted for and no satisfactory model for them could be obtained despite numerous attempts at modelling, including with rigid bodies. Therefore the SQUEEZE[13] function of PLATON[14] was employed to account for the highly disordered anions and further disordered solvent molecules, which gave a potential solvent accessible void of 5725 $Å^3$ per unit cell (a total of approximately 1368 electrons). Since the identity of the diffuse anions and solvent molecules could not be assigned conclusively they were not included in the formula. Consequently, the molecular weight and density given above are underestimated. The hydrogen atoms of the water molecules could not be located in the electron density map and were not included in the model.
CheckCIF gives eight A and thirteen B level alerts. These alerts (both A and B level) all result from the limited data resolution, beam damage and thermal motion and/or unresolved disorder of some anions and solvent molecules as described above.

S8. Organic Guests Screened for Host Guest Binding

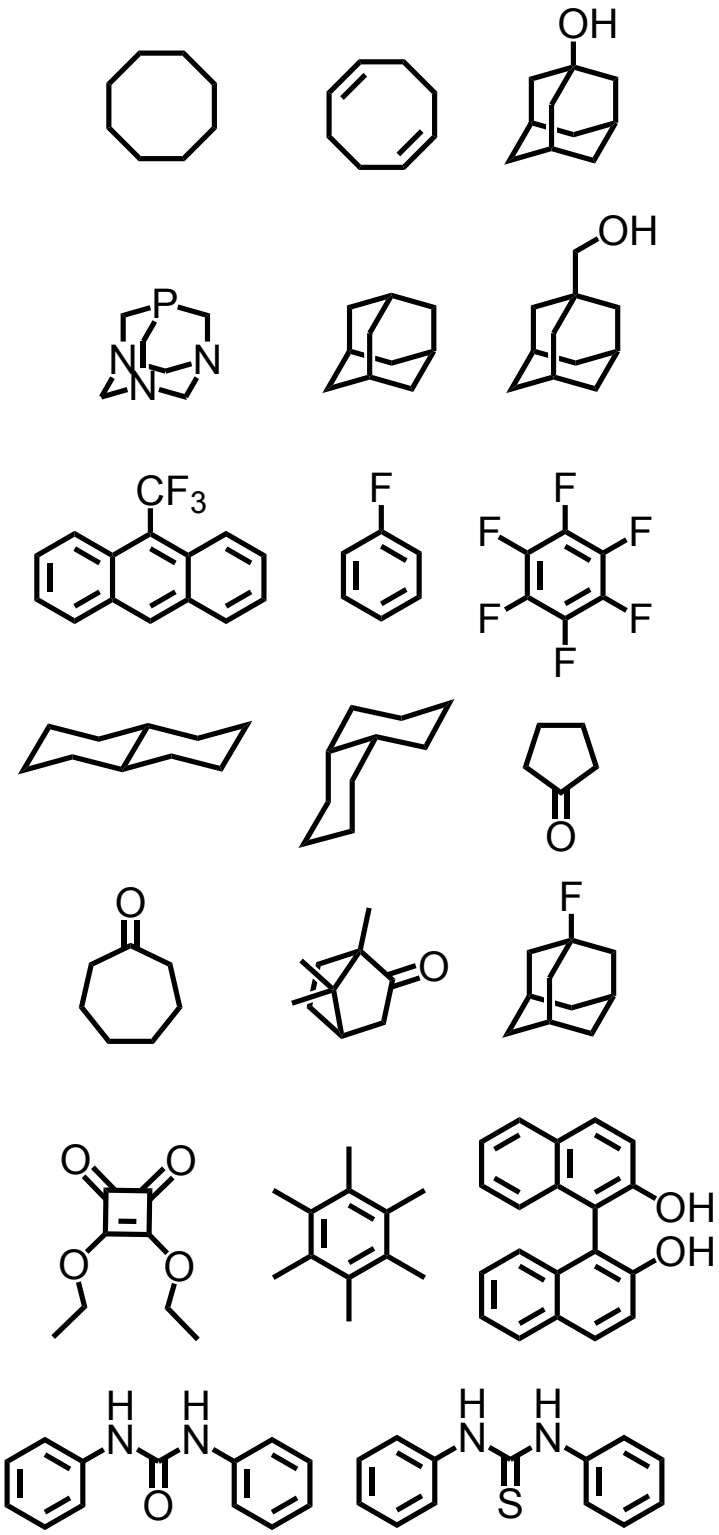

An excess of organic guest was added to each cages **3**, **4**, and **5**, and the solution heated at 70 °C overnight prior to NMR. No evidence of guest binding was observed for any of the above molecules.

S9. Metal Salts Screened for Binding to Cage 2

Metal Salt	Binding Observed?
Chloro(dimethylsulfide) gold	Yes
Triruthenium dodecacarbonyl	No
Tris(dibenzylideneacetone)dipalladium	No
Bis(dibenzylideneacetone)palladium	No
Bis(acetonitrile)dichloropalladium	No
Tetrakis(acetonitrile) palladium terafluoroborate	No
Tetrakis(acetonitrile) copper triflate	No

Table S2: Metal salts screened for binding to cage **2**.

S10. Effect of Et_3NHCl on Assembly of Cage 2

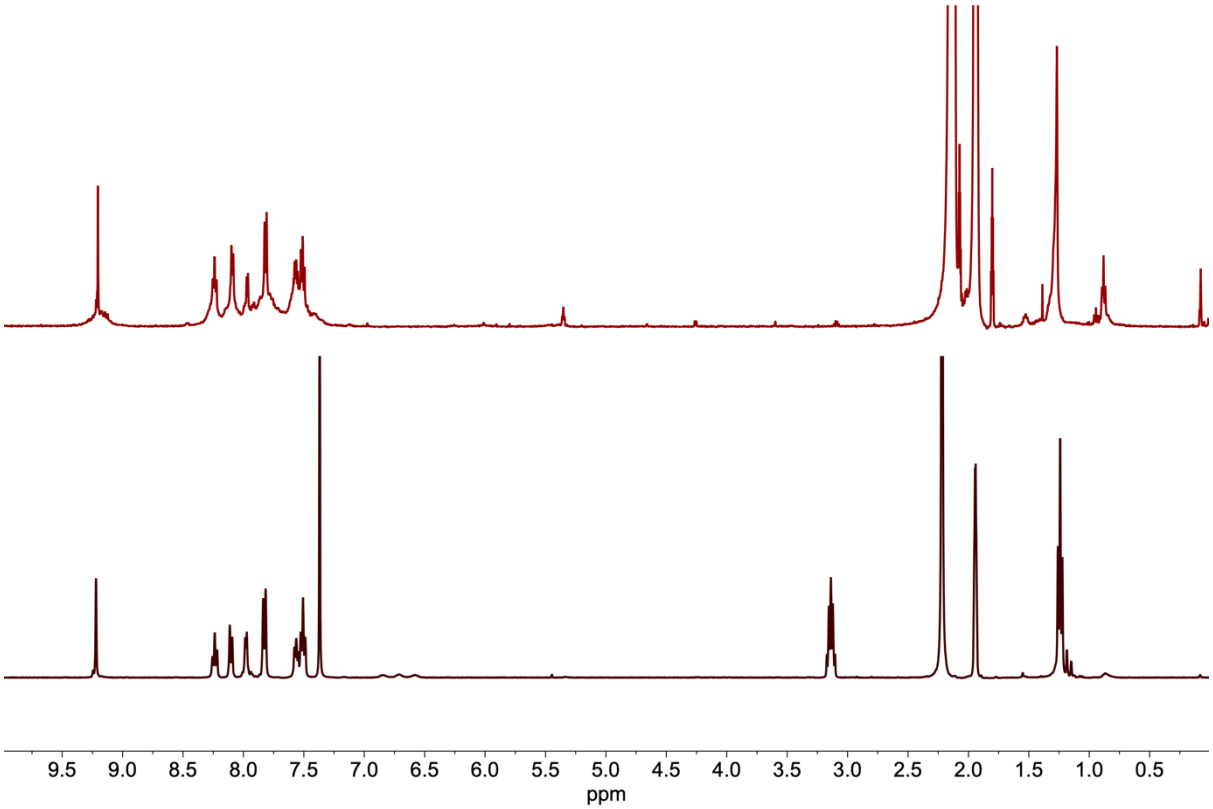

Figure S118: ^1H NMR (CD_3CN, 500 MHz, 298 K) spectrum of **7**. Top: Assembly (4 equiv $Zn(NTf_2)_2$, 70 °C, 1 hour) after removal of Et_3NHCl from phosphine **1**. Bottom: Assembly (4 equiv $Zn(NTf_2)_2$, 70 °C, 1 hour) in the presence of Et_3NHCl. Note the assembly in the presence of Et_3NHCl is significantly cleaner.

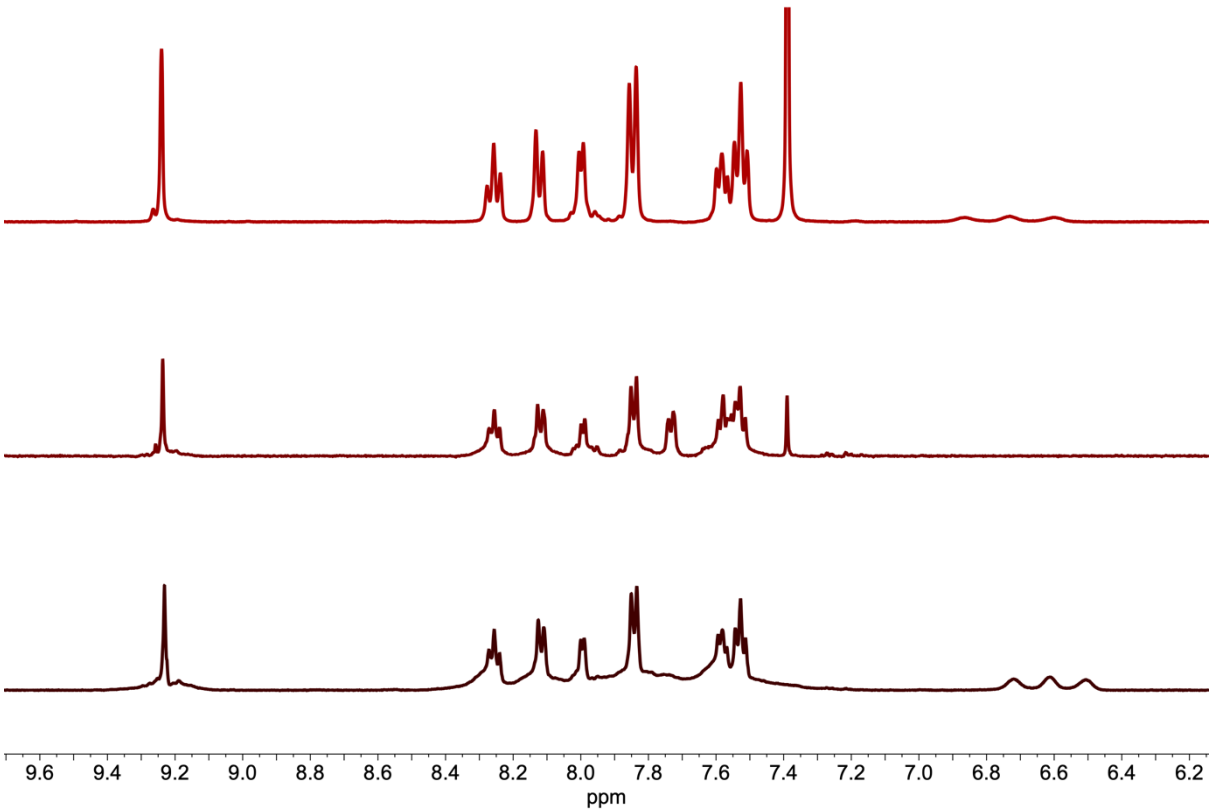

Figure S119: Investigation into the effect of Et_3NHCl on cage assembly. Top: Cage **2** assembled from phosphine **1** containing Et_3NHCl from the reduction of phosphine oxide **S1**. Middle: Cage **2** assembled from phosphine **1** with the addition of 4 equiv. TBACl. Bottom: Cage **2** assembled from phosphine **1** with post-assembly addition of Et_3NHCl. Cleanest assembly was found when Et_3NHCl was present during cage synthesis.

S11. References

1. a. Smith, J. N.; Hook, J. M.; Lucas, N. T. Superphenylphosphines: Nanographene-based ligands that control coordination geometry and drive supramolecular assembly. *J. Am. Chem. Soc.* **2018**, *140*, 1131–1141. b. Albrecht, M.; Song, Y. Synthesis of phosphane oxide bridged bis- and triscatechol derivatives. *Synthesis* **2006**, *18*, 3037–3042.
2. Riddell, I. A.; Hristova, Y. R.; Clegg, J. K.; Wood, C. S.; Breiner, B.; Nitschke, J. R. Five discrete multinuclear metal-organic assemblies from one ligand: deciphering the effects of different templates. *J. Am. Chem. Soc.* **2013**, *135*, 2723–2733
3. Thordarson, K., Bindfit, http://app.supramolecular.org/bindfit/.
4. Allan, D.; Nowell, H.; Barnett, S.; Warren, M.; Wilcox, A.; Christensen, J.; Saunders, L.; Peach, A.; Hooper, M.; Zaja, L.; Patel, S.; Cahill, L.; Marshall, R.; Trimnell, S.; Foster, A.; Bates, T.; Lay, S.; Williams, M.; Hathaway, P.; Winter, G.; Gerstel, M.; Wooley, R. A novel dual air-bearing fixed-X diffractometer for small-molecule single-crystal X-ray diffraction on beamline I19 at Diamond Light Source. *Crystals* **2017**, *7*, 336–359.
5. Collaborative Computational Project, Number 4. *Acta Cryst.* **1994**, *D50*, 760–763.
6. Evans, P. Scaling and assessment of data quality. *Acta Cryst.* **2006**, *D62*, 72–82.
7. Winter, G. *xia2*: An expert system for macromolecular crystallography data reduction. *J. Appl. Crystallogr.* **2010**, *43*, 186–190.
8. Farrugia, L. WinGX and ORTEP for windows: an update. *J. Appl. Crystallogr.* **2012**, *45*, 849–854.
9. Evans, P. R.; Murshudov, G. N. How good are my data and what is the resolution? *Acta Cryst.* **2013**, *D69*, 1204–1214.
10. Winn, M. D.; Ballard, C. C.; Cowtan, K. D.; Dodson, E. J.; Emsley, P.; Evans, P. R.; Keegan, R. M.; Krissinel, E. B.; Leslie, A. G. W.; McCoy, A.; McNicholas, S. J.; Murshudov, G. N.; Pannu, N. S.; Potterton, E. A.; Powell, H. R.; Read, R. J.; Vagin, A.; Wilson, K. S. Overview of the *CCP4* suite and current developments. *Acta Cryst.* **2011**, *D67,* 235–242.
11. Sheldrick, G. M. *SHELXT* - Integrated space-group and crystal-structure determination. *Acta. Cryst.* **2015**, *A71*, 3–8.
12. Sheldrick, G. M. Crystal structure refinement with *SHELXL*. *Acta. Cryst.* **2015**, *C71*, 3–8.
13. van der Sluis, P.; Spek, A. L. BYPASS: An effective method for the refinement of crystal structures containing disordered solvent regions. *Acta Cryst.* **1990**, *A46*, 194–201.
14. Spek, A. L., PLATON: A Multipurpose Crystallographic Tool. Utrecht University: Utrecht, The Netherlands, **2008**.